M-6 Design Implementation

USSF 2k Rocket Launch Black Team

Sponsor: United States Space Force (USSF)

Submitted:

Prepared by:

Dahl, Calvin (Aerospace)

Giegler, Cameron (Mechanical)

Mann, Zachary (Mechanical)

Sayles, Joshua (Aerospace)

Shinault, Nicholas (Aerospace)

Williams, Jon (Aerospace)

Faculty Advisor: **Kurt Stresau**

Executive Summary

Our team has been challenged to design, construct and launch a high powered rocket with the mission to carry as many eggs as possible to an altitude of 2000 feet and safely return them to Earth unscathed. This venture was proposed by the United States Space Force (USSF) with the goal of using low orbit rockets to deliver goods and supplies around the world in less than one hour. Through its journey, the rocket will be subject to many forces that could damage or destroy a sensitive payload. In this application the sensitive payload is simulated by eggs, if the eggs are returned from the flight unharmed it will lay the groundwork for larger scale missions.

This project is not only important to the USSF but to the entire world. The ability to quickly deliver medical supplies, food and water to areas impacted by natural disasters or conflict is critical to saving lives. Soldiers in need of equipment could receive aid when aircrafts or other modes of transportation are not an option. The desired outcome of this project and others like it, on a grand scale, is that it will benefit the USSF and eventually lead to the creation of a world rocket delivery system.

Table of Contents

List Of Figures

List Of Tables

Glossary

Acronyms/Technical Terms	
USSF	United States Space Force
CFD	Computational Fluid Dynamics
FEA	Finite Element Analysis
RIN	Requirement Identification Number
LRS	Launch Recovery System
AGL	Above Ground Level
PDR	Preliminary Design Review
Apogee	Max height rocket will reach
COM	Center of Mass
FOS	Factor of Safety
FMEA	Failure Modes and Effects Analysis
FDM	Fused Deposition Modeling
PLA	Polylactic Acid
ABS	Acrylonitrile Butadiene Styrene
HPR	High Powered Rocket

1 Introduction

This project will play an integral role in the U.S.S.F quest to design, build and operate a rocket based delivery system that will provide much needed cargo and supplies to remote areas around the world, in less than an hour. To simulate this on a much smaller scale, a project has been implemented to launch a high powered rocket loaded with eggs to an altitude of 2000 feet and safely return them to Earth unharmed. In order for this to be achieved a team effort has been put in place to research, design and engineer a rocket that can perform this task. The purpose of this report is to illustrate the design and decision making process that goes into creating, testing, launching and recovering a rocket and its payload carrying multiple eggs. It is no easy feat to successfully perform this task. Many of the obstacles encountered during this project will be the same obstacles encountered by the U.S.S.F during their journey to create the world's first rocket powered delivery system. This report will highlight the needs of such a service, including all those who would benefit. It will break down the different components that will be utilized to pull off such a challenge.

The history of logistics can be traced back to ancient civilizations where the organization and the coordination of resources were essential for military campaigns, trade and construction. As troops conquered parts of the world, logistical concepts were evident in the Roman, Greek and Egyptian armies. They learned to coordinate the movement of supplies and equipment over vast distances. During the Middle Ages, there was a rise of merchant guilds and trade

routes. The Silk Road for example, became a complex logistical network, connecting the East and West. During the Industrial Revolution of the 18th and 19th centuries, mass production and the rise of factories, the demand for more sophisticated logistics were required to manage raw materials, production processes and distribution. Both World War I and World War II were characterized as massive logistical efforts. The scale and magnitude of these conflicts required huge supply chains to sustain armies and coordinate global movements of troops and materials. After World War II, logistics became a distinct field, leading to the establishment of supply chain management principles. The development of the cargo aircraft was a major game changer for logistics, moving goods around the globe faster than boats, trains or vehicles could. During the latter half of the 20th century, there was a widespread adoption of technology in logistics. Computers and advanced software revolutionized inventory management and order fulfillment. With the rise of e-commerce, logistics has further been transformed, utilizing sophisticated technologies, data analytics and automation to optimize supply chains and meet the demands of a rapidly changing global market. Today, logistics continues to adapt to new challenges and opportunities in our interconnected world.

The problem that has always plagued logistics is time. In order for logistics operations to be efficient, timing is everything. Logistics is a fundamental component of the broader supply chain. This involves the coordination and movement of goods and resources to ensure a timely delivery and minimize delays. If something takes too long to get delivered, stock runs out, costing money and in some cases, lives. Delays in any aspect of logistics can lead to

customer dissatisfaction and impact the overall success of a business. In an interconnected global economy, timing becomes even more critical because of factors like varying time zones and international regulations. In summary, effective timing is a linchpin for efficient logistics. Whether it's synchronizing a supply chain, managing inventory, resupplying a military or providing humanitarian aid, timing is essential for logistics to thrive in today's interconnected world.

Time is the nemesis of logistics. The only way to deal with that nemesis, is to create a system that can remove time, completely from the equation. What is the motivation to do that? Because every second that ticks by, is costing someone either their money or their life. Trains, trucks and cargo planes take too long to get to their destination. By implementing a rocket based delivery system, a huge chunk of time has been removed from the actual delivery. Today's world has an insatiable demand for faster, more efficient delivery solutions and the prospect of a one hour delivery service to anywhere in the world, is a force to be reckoned with. A rocket based delivery service is a concept that has the potential to redefine the boundaries of what's possible and what is not. With the integration of this program, the efficiency of the supply chain will be enhanced, and economic growth will be fostered by the increased accessibility to goods and services worldwide. Life Saving medical supplies and humanitarian aid will save lives everywhere. As we embark on this exploration, envision a future where low orbit space is the gateway to a more connected and accessible global community.

2 Project Objectives and Scope

Over the course of the semester we were tasked to complete the following list of objectives separated into current semester and long term.

Current Semester:

- Design and build a payload housing unit that will be installed into a high powered rocket.
    - This will include testing of different version to ensure the most practical and efficient design is selected
- Develop a practical, yet effective recovery system that will ensure the safety of the rocket and the sensitive payload during descent and landing.
    - Research different parachute sizes and their respective drag coefficients to determine the most efficient recovery system for a sensitive payload.
    - Perform shock cord testing to determine the optimum length for parachute inflation and performance.

- Print and assemble housing group for avionics bay and nose cone
- Build fully functional rocket ready for test and final launch dates
    - To include data gathering from simulation testing in CFD and FEA software.
    - Determine the most effective methods of manufacturing
    - Testing of all subcomponents

- Have a full understanding of how to utilize Finite Element Analysis (FEA) and Computational Fluid Dynamics (CFD) using software that pertains to these subjects.
    - To be able to confidently perform these analyses using multiple types of software.
    - To know everything there is to know about the software to be able to analyze efficiently and correctly.

Long Term

- Increase the scale of the mission
- Provide feedback that can realistically be used in determining better materials and documenting all possible errors encountered while going through the design process.
- The development of commercialized low earth orbit delivery service. A delivery service that can bring goods from one side of the Earth to the other, without relying on a government agency.
- The improvement of communication and tracking facilities around the world to be able to track the cargo from launch to recovery.

3 Assessment of Relevant Existing Technologies and Standards

3.1 Avionics

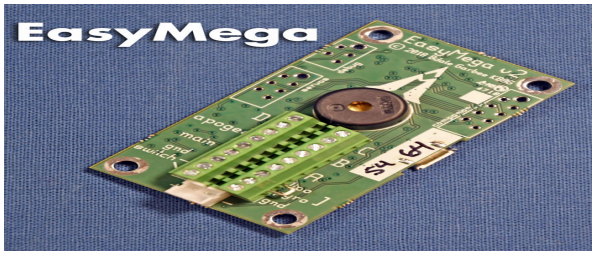

Figure 3.1.1 - Photo of an avionics board

The avionics compartment for this rocket consists of a flight computer, a master on/off switch and a nine volt battery. As referenced in Milestone 3, section 3.1, the flight computer records altitude through a barometric pressure sensor and gives data on the time to apogee. It also records maximum velocity and acceleration, flight time, rocket location and controls the deployment of the parachute. This data is acquired through a ground control station which is connected to a smartphone, where the information is displayed. When the rocket achieves a predetermined apogee, the flight computer will send an electric current through an e-match which is connected to a black powder charge. If the rocket fails to reach its predetermined apogee, a preset rate of descent will trigger a second impulse, igniting a second black powder charge, ultimately ejecting the nose cone and deploying the parachute. The GPS locator within the flight computer gives an accurate location of where the rocket landed by displaying a map of the area, via the ground station, on the smartphone. Armed

with this information, the hunt to find the rocket should be minimal. The flight computer and master control switch are all powered by one nine-volt battery. For the mission, there are two black powder charges and two e-matches on board the rocket. The black powder is contained in a small rubber pouch. The e-match is a single wire that has been dipped in pyrogen on one end. One end of the wire is connected to the flight computer, while the pyrogen dipped end is embedded into the black powder charge. As stated previously, there are two charges, one for apogee and a secondary in case the primary charge fails. When the black powder ignites, there is a large amount of pressure build up, ultimately ejecting the nose cone off of the rocket.

3.2 Additive Manufacturing

Figure 3.2.1 - Prusa MINI+ 3D Printer

3-D printing has multiple categories that can be utilized in manufacturing. For more information on these methods, please refer to section 3.2 in Milestone 3.

For this project, Fused Deposition Modeling (FDM) was used to manufacture the rocket's nose cone, avionics compartment and separation ring. FDM is a method of 3-D printing in which filaments, made from various polymer materials, are melted into a paste. The paste is deposited linewise to make a layer. Subsequently, many layers are then made to form a product. FDM is a great choice for this project because it is highly accessible, easy to use and inexpensive. There are many different types of filaments that can be used with FDM printing (see section 3.2, Milestone 3 for more information), this project focused mainly on using Polylactic Acid (PLA) and Polycarbonate Filament (PC). Polycarbonate filament is much tougher than PLA, but also heavier, which made it a great material to use for the manufacturing of the rocket's nose cone. The added weight pushed the aerodynamic center forward on the rocket, giving it more stability. The nose cone can be subjected to many intense, external forces during flight, and needs to be strong enough to sustain composure. With its high resistance to heat, PC was also used for the separation plate between the payload bay and the motor housing unit. The PC provides ample strength and protection to keep heat and blast forces, created by the motor, away from the sensitive payload that lies inches away. PLA is a material that is much lighter, inexpensive and easier to work with, than PC. PLA was used to print the avionics compartment for the rocket. During the initial planning phase of this project, PLA was used to make prototypes of the nose cone, until a perfect fit could be made. It was at this point that the final nose cone was printed using the more expensive Polycarbonate Filament. The Polycarbonate Filament showed its toughness

during the rocket's first launch. There was a malfunction during descent, where the parachute failed to deploy. The rocket impacted the ground, at terminal velocity, nose first. The nose cone survived the impact and was recovered, undamaged .

3.3 Rocket Chassis, Fins and Materials

Figure 3.3.1 - Unpainted Rocket Chassis using Blue Tube Material.

The rocket chassis used for this project is 58.3” long with a 4” diameter. The chassis serves as the backbone of the rocket and provides structural support, stability and functionality for a safe and successful mission. The material that makes up the chassis must be one that provides structural integrity that ensures the rocket, and its payload, can withstand the intense forces experienced during launch, flight, and recovery. Chassis failure will have catastrophic consequences. There are many different materials that can be used for the body of a rocket. For a broader list, please refer to section 3.3 in Milestone 3. Of all the available materials that could be used, Blue Tube stood out above the rest. Blue Tube, also known as phenolic resin impregnated fiberglass, boasts a high compression strength while being extremely lightweight. Its strength and durability are capable of withstanding the extreme stresses of high powered flight, while also having extreme resistance to

impact forces. This was highlighted during the first launch for this project. As the rocket was in free-fall, the parachute failed and the rocket impacted the ground at a high rate of speed. Upon recovery, the rocket body was completely intact and unfractured. Aside from being extremely tough, Blue tube is easy to work with. It can be cut, drilled and customized to fit components such as fins and nose cones. Compared to other materials, such as carbon fiber, Blue Tube is relatively inexpensive.

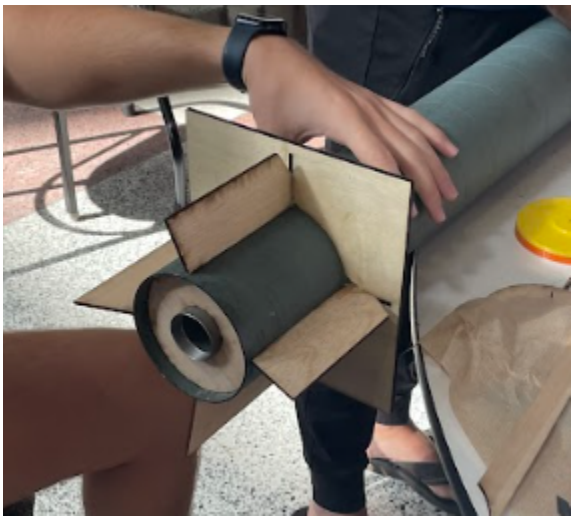

Figure 3.3.2 - Trapezoidal fin design with fin guard

The main function of the fins is to act as a stabilizer for the rocket during launch. This is done via the Bernoulli effect and the forces caused by pressure differentials on either side of the fin. The fin design, geometry and weight play a significant factor in determining the location of the aerodynamic center of the rocket. Because of the fins' large importance on stability the material chosen in return plays an equally large part. Section 3.3 in Milestone 3, many different materials for fins are discussed, including G-10 fiberglass and birch plywood. For

this rocket design, the team decided to go use four fins as opposed to three. Four fins provide greater stability, with four points of contact with the airflow. This adds redundancy to the rocket's stability, making it less likely to wobble or veer off course during flight, especially in windy conditions.

After researching materials and cost, it was decided the best option for this project was to use Balsa wood for the fins. For aerodynamic purposes, it is important to keep the weight of the rocket more towards the nose. Balsa wood is exceptionally lightweight, which is crucial when the fins are located at the bottom of the rocket. Despite its lightweight nature, balsa wood has a favorable strength to weight ratio. This means that it provides sufficient structural strength to withstand the aerodynamic forces and stresses experienced during launch and flight, while keeping weight to a minimum. Another contributing factor is that balsa wood is easy to work with. It cuts, shapes and sands comfortably, making it ideal for crafting custom fins. Balsa wood has some inherent flexibility which allows it to absorb and dampen vibrations and shocks experienced during launch and flight. This helps reduce the risk of fin damage or failure due to high-G maneuvers or rough landings.This was evident during the first launch when the parachute failed to inflate. The rocket impacted the ground at a high rate of speed, resulting in the loss of only one fin. Balsa wood is also relatively inexpensive and widely available compared to other materials commonly used for fins, such as fiberglass or carbon fiber.

3.4 Nose Cone

Figure 3.4.1 Parabolic nose cone made from poly-carbonate

The nose cone may be the most critical component on a rocket. Its design is important because it optimizes aerodynamics, protects the payload and maintains structural integrity throughout the flight. The nose cone minimizes drag and enhances performance. Its streamlined shape helps to guide the airflow around the chassis, improving efficiency. The nose cone for this project consisted of a 3-D printed, parabolic shaped unit, made from poly-carbonate. The parabolic shape is important in the fact that it improves stability while providing added protection to the payload bay. Since this mission will be a subsonic flight, the parabolic shape is optimum. The rounded shape of the parabolic nose provides effective shielding from turbulent aerodynamic forces. This protection is crucial for ensuring safety and integrity of the sensitive payload on board. The parabolic nose also allows for more space inside the capsule. The rounded tip provides an

excellent nook to place black powder charges and the parachute. For a complete list of other nose cone options, please refer to Milestone 3, section 5.3.

3.5 Rocket/Payload Recovery System

Figure 3.5.1 - Unfolded 36” parachute

Initially, when this project began, it was decided that the rocket would have a dual deployment parachute recovery system. Research had revealed that the dual deployment system was ideal for softer, gentler landings, which is required for recovering a rocket carrying a sensitive payload. However, this idea came with its fair share of disadvantages. The dual deployment design adds extra moving parts, which makes the system much more complex. It requires additional mechanisms such as a multi-deployment altimeter, multiple black powder charges and e-matches, multiple parts separating from the rocket and extra space to house two parachutes. This added complexity not only reduces our

payload mass, but increases the likelihood of system failures and malfunctions. Other disadvantages include increased cost, parachute entanglement and deployment timing challenges. After careful consideration, it was decided to go with a single parachute to recover the rocket and the sensitive payload.

Figure 3.5.2 - 36" inflated parachute with exposed apex vent

Initial research had shown that an acceptable landing speed for a rocket carrying a sensitive payload, would be around 25 ft./sec. Using the modeling software 'OpenRocket', it was discovered that with the total weight of the rocket, and using a single parachute, a 58" canopy would be required to ensure a landing at, or less than 25 ft./sec. A major issue with a 58" parachute, is the amount of space required to house it. The deployment design for this project is to house the parachute in the nose cone. As the black powder charge expels the nose cone, the parachute will be ejected into the open environment and inflate. Test photos show that this process works when deployed on the ground and in stagnant wind conditions.

Figure 3.5.3 - Nose cone ejection and parachute deployment testing.

What the team failed to realize is that the parachute must be packed in a specific way for it to successfully inflate in the turbulent environment of flight. The proper manner of packing a high powered rocket parachute includes folding it in half, width wise, until all shroud lines are lined up together in one uniform line. Then, fold the parachute lengthwise twice, and wrap the shroud lines around the folded parachute twice. When doing this procedure on the 58” parachute, there was no room to fit it into the nose cone. So modified packing techniques were performed, and this proved catastrophic on the first launch, as the parachute failed to inflate. The clear path forward was to go with a smaller parachute. The next step was to test the sensitive payload and find a maximum descent rate that would afford the rocket to land and not destroy the payload. Testing was performed with the payload, in a test rocket chassis and dropped from a height of 60 feet. It was determined that the payload could withstand a landing speed of over 50 ft./sec. Armed with this tidbit of data, the team went back to OpenRocket and simulated

the flight using a smaller parachute. A 36” parachute showed that the rocket would land at a rate of around 30 ft./sec which fell well within the parameters of a safe landing. For the final launch, the rocket will be equipped with a 36” vented parachute. The apex vent at the top of the canopy will offer much needed stability on the descent back to Earth. The parachute will be made of ripstop nylon and connected to the rocket by a single kevlar shock cord.

3.6 Payload

Figure 3.6.1 - EVA foam egg holders or ‘pucks’.

The main objective for this project is to launch as many chicken eggs as possible, to an altitude of 2000 feet, and recover them fully intact and unbroken. To achieve this, the payload bay must be designed in a way that the sensitive eggs are completely protected from the violent forces associated with a high

powered rocket flight. The payload design must also efficiently use every available square inch of space to carry as many eggs as possible. Ideas, such as packing peanuts, popcorn, gel, feathers and foam were tossed around as possible materials that could be used to protect the eggs. In the end, Expanded Polyethylene Vinyl Acetate (EVA) foam was found to be the most logical material to be used in the payload bay. EVA foam is what

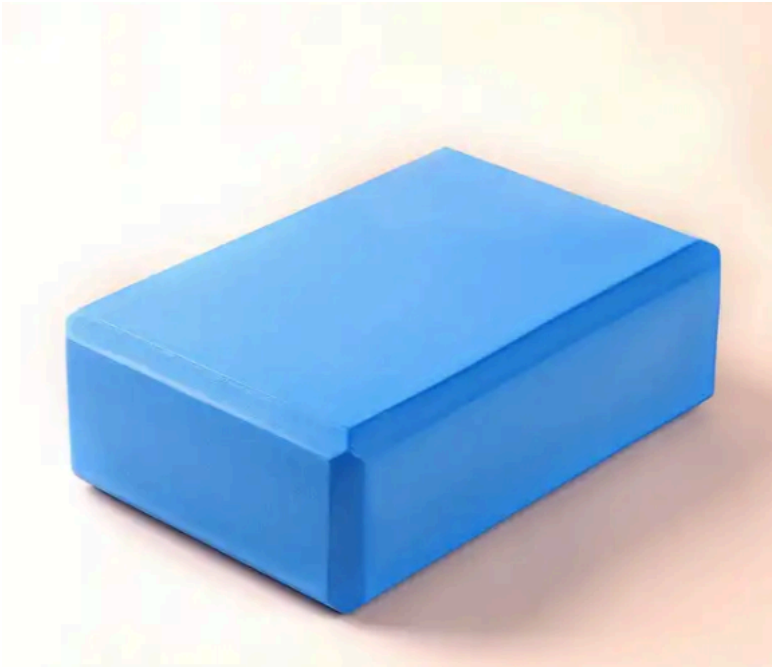

Figure 3.6.2 - EVA foam yoga block

Yoga blocks are made out of. EVA foam offers several advantages. It has excellent cushioning properties that can absorb impacts and shocks, making it ideal protective padding for sports equipment, footwear and packing material. It is also extremely lightweight, and easy to work with. EVA foam is flexible and resilient allowing it to conform to irregular shapes and absorb dynamic forces. It also has thermal insulating properties, which helps regulate temperatures and prevent heat loss or gain. This is extremely valuable for this project, as the payload bay

lies inches away from the rocket motor. EVA foam also has great versatility. It can be molded, cut, and shaped to fit specific requirements. Above all, it is inexpensive and readily available.

With a payload length of 24” and a diameter of 4”, it became evident that in order to get as many eggs onboard as possible, creativity would have to be front and center. With an average egg height of 2.25” and width of 1.75”, it was decided to make a series of EVA foam pucks that were 3” tall and 3.9” in diameter. The layout would be such that each puck would house one half of four eggs.

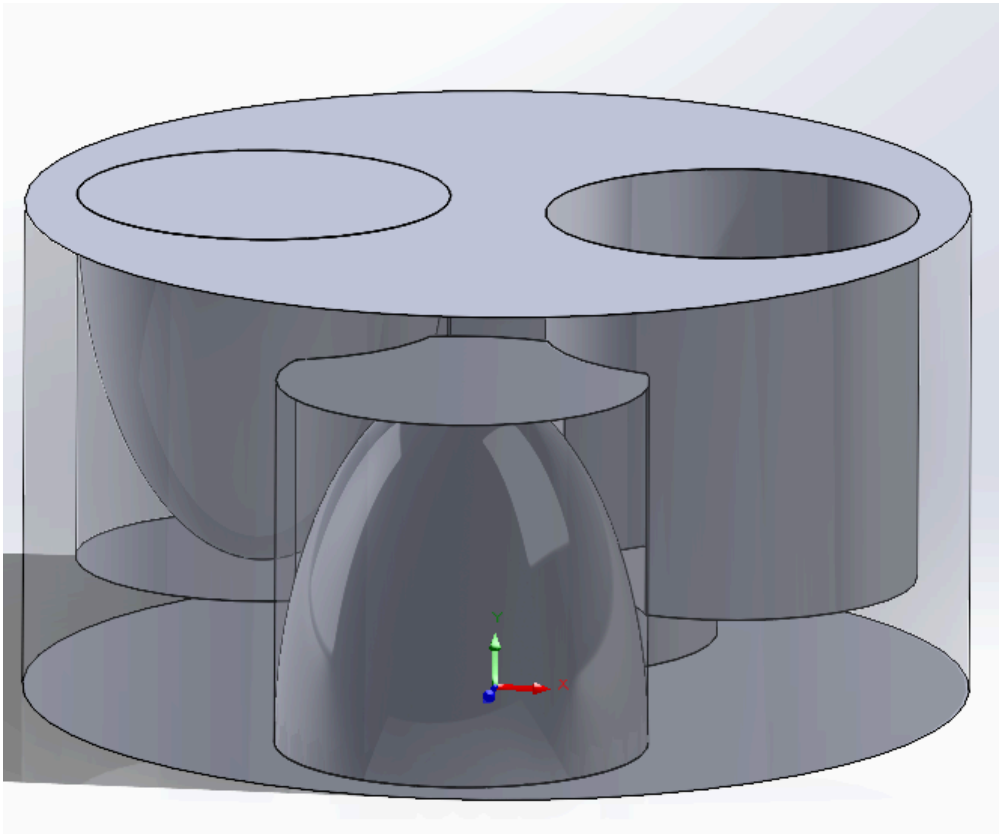

Figure 3.6.3 - SolidWorks design of egg layout within the foam ‘pucks’.

This would allow the maximum amount of eggs to be used in the space allotted, while still leaving enough foam to protect them. The foam pucks would be stacked in series, with 1.5” end caps to protect the eggs at the top and bottom of the stack. With the eggs nested inside of the foam, the stack would then be wrapped in saran wrap to make it all one unit, allowing the full stack to absorb the turbulent forces being applied to it.

Figure 3.6.4 - Egg carrying pucks stacked in series and wrapped in cellophane.

3.7 Rocket Motor and Centering Rings

Figure 3.7.1 - Cesaroni I-216 motor with igniter.

To achieve any of the goals set by the team, the prerequisite requirement of reaching an altitude of 2000ft needed to be met. While other components are important to achieve this requirement; the rocket motor is the only component that can generate the force required to meet that need. The main criteria examined when picking a rocket motor was naturally the impulse provided by the

motor. If a motor was not capable of reaching the target altitude given preliminary mass and drag characteristics - that motor received an overall unsatisfactory rating, and more powerful motors were analyzed.

Cost of the motor was the second main criteria examined, to determine in future cost analysis if that motor was too expensive and a less powerful but cheaper alternative was necessary for the project. Initial thrust and weight were also examined for stability purposes of the rocket during launch and flight conditions respectively. Certain rocket motors are reusable and after a flight a new motor can be reloaded easily; because the team is planning test launches this criterion was also examined. Finally, max acceleration is an important factor when protecting the payload: in this case a low maximum acceleration received a higher grade.

The motor with the best overall features needed to fulfill all requirements for competition is the Cesaroni I-216 motor. This motor has the highest total impulse of all the alternatives discussed and is at the cusp of the classification of an I motor. Given the amount of force generated (85.4 lbs) the rocket is simulated to achieve an altitude of over 2400 ft AGL while carrying a payload of 24 eggs. This motor provides a high initial thrust alongside a high weight - which would face similar challenges to the AeroTech I-280 motor (Milestone 3, section 5.3.6). Additionally, the Cesaroni I-216 also has a lower max acceleration and is also reusable. While the Cesaroni I-216 outperforms the rest of the motors discussed it comes at a cost – as the most expensive motor analyzed yet.

As displayed in the chart below, the Cesaroni I-216 motor performs impressively. It provides an initial thrust that gives the rocket the momentum needed to achieve altitude, while following up with a lighter thrust to achieve optimal flight characteristics. This is important when carrying a sensitive payload because it cuts down on the turbulent aerodynamic forces of flight.

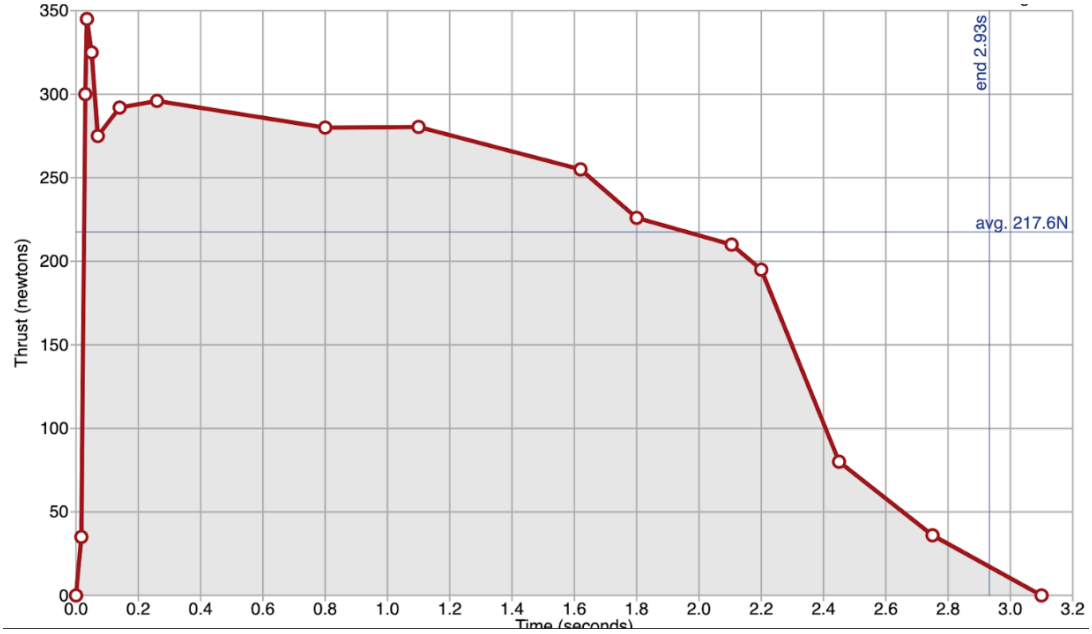

Figure 3.7.2 - Cesaroni I-216 motor, Thrust vs. Burn Time plot

Figure 3.7.3 - Balsa centering rings being cut out with a laser cutter.

Initially, the centering rings (motor mounts) for this project were constructed out of ⅛” Balsa wood. Finite Element Analysis was conducted using Ansys Mechanical software. The FEA concluded that the balsa wood would be able to withstand the thrust force from the motor during launch. However, the analysis was flawed in the fact that there are many different types of Balsa wood. The material characteristics entered into the analysis were different from the balsa being used for the actual rocket motor mounts. This proved fatal during a test launch in March, 2024, when the centering rings failed and the Cesaroni I-216 punched its way into the payload bay and buried itself within the EVA foam. To correct this, another FEA was performed analyzing ¼” pine plywood as a new material for the motor mounts. During the final launch on April 20, 2024, this

system appeared to not fail, however, the rocket was lost and unrecoverable, therefore a complete final analysis was never performed.

Figure 3.7.4 - ¼" pine plywood centering rings.

4 Professional and Societal Considerations

To date the fastest modes of supply transportation rely on airplanes which still can take hours to arrive. Aircraft transportation also comes with limited flying conditions, airspace issues, and cargo is limited by the weight and size of the aircraft itself. If a successful suborbital launch system is designed the time of delivery can be drastically decreased, avoid hazardous environments and minimize traveling through multiple airspaces. All while allowing transportation of more supplies to be delivered directly to the most valuable locations. This can greatly improve our military's ability to respond in a moment's notice to any conflict with overwhelming force. Reliving some responsibilities from current aircraft carriers.

There are many users and scenarios where a low orbit delivery service would be beneficial. For instance, people living in remote or isolated areas facing natural disasters, or conflict zones, or places with a lack of infrastructure. These groups could receive rapid assistance that would improve the quality of life in their area and potentially save lives. U.S. soldiers and their allies fighting in war torn regions, facing logistical challenges, could receive quick and direct support. During medical emergencies where supplies like vaccines, medications, and medical equipment are urgently needed, a rocket based delivery system could be a swift and efficient solution. To aid their relief efforts, humanitarian organizations such as the Red Cross, Doctors Without Borders and the United Nations could greatly appreciate receiving their supplies within the hour of making a call. Research and development teams would benefit greatly by attracting scientists who are developing cutting edge

technologies to enhance global advancement. Finally, a low orbit rapid delivery system would greatly help with global supply chain issues, such as what the world saw following the Covid-19 pandemic. These are just a few of the users that would benefit from this concept, although there are many more.

Another benefit this product will have is an increase in economic power and production. Throughout human history, whenever a new method of transportation is created an economical bomb quickly follows. This is because one of the key pillars in the world economy is the ability to trade. Quicker access to resources and goods usually means faster consumption and therefore bigger economies. The speed and accuracy of deliveries can also impact fields such as health and safety and greatly improved with the ability to respond quicker to deadly disasters whether man made or natural.

There are many stakeholders who would love to see a new, rapid delivery service become available. Some of these stakeholders include global logistics and shipping companies, giving them options for time sensitive or high-value cargo delivery. These companies could revolutionize their services by offering incredibly fast and efficient global delivery options, reducing transit times and operational costs. This would help retail companies by allowing ultra-fast delivery capabilities, rapid order fulfillment and enhancing customer satisfaction. Manufacturers and suppliers, especially those with time sensitive or perishable goods could leverage this system to ensure quick and reliable distribution of their product. Stakeholders involved in global supply chain networks, including raw material suppliers, could optimize their operations by reducing lead times and improving overall supply chain efficiency. Overall, consumers would experience the direct benefits of high speed deliveries,

with the convenience of receiving their goods in a timely fashion. Other stakeholders involved in this project include Aerospace and Technology companies such as NASA, SpaceX, and Microsoft to name a few. These companies involved in the development and manufacturing of a rocket based delivery system, would directly benefit from the creation, deployment, services and maintenance of such systems. Professionals in these industries, including engineers and scientists would be involved in the designing, developing and maintaining this delivery system. Investors and financial institutions would be key stakeholders as they would benefit greatly from the growth and profitability of companies involved in this sector. Telecommunication companies involved in providing communications services and real time tracking capabilities for all involved, would also see profit and growth as these services become more available.

In conclusion, the 2K Egg Launch project is just the beginning of a new era for logistics, technology and economic growth. A Low Earth Orbit delivery system will literally touch every corner of the world and positively impact millions of people, for generations to come. And to think, it all started right here. The members of the Black Team should be proud to know that all of their hard work will have a significant impact on Earth and touch the lives of everyone who lives here.

5 System Requirements and Constraints

LRS - 08: Reduces velocity to less than 25 ft/s

The above requirement was determined to be unnecessary in our design. With the results of the payload after the test launch, it was shown the payload can withstand impact at terminal velocity. Meaning speeds of 60 + mph were possible for recovery of some eggs. Moving forward for the final launch it was decided to make the parachute a 36” in order to simplify packing and lessen the chance of parachute deployment failure.

LRS - 04: Stability Margin to be between 1.2 and 1.8

This requirement was determined to be too low. On final launch the rocket was unable to stabilize before reaching its designed altitude. This may have been too low of a stability margin and needed to be increased to a margin of 2. Some causes for this may have been since a majority of the weight was further aft of the rocket, causing it to naturally have a tendency to tip at lower speeds.

6 System Concept Development

6.1 Avionics

The objective for the avionics development was to design a simple circuit able to read and store flight data, allow control of pyro events to separate the rocket at apogee, and aid in recovery. To achieve these tasks the circuit needed to include an altimeter, black powder charges and a tracking device.

To start the process a simple circuit was created as shown in figure 6.1.1. The altimeter was connected to power through a switch and LEDs were connected to a power distribution board and the altimeter. These LEDs are place holders for future pyro

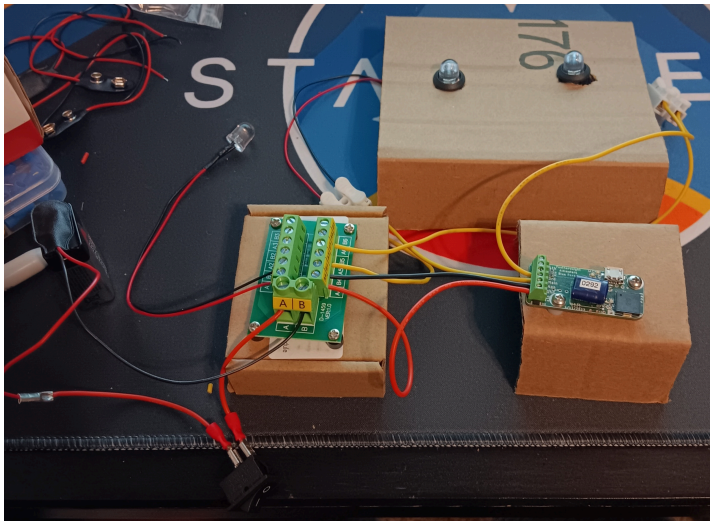

Figure 6.1.1 - Simple altimeter circuit

event connections. Using this circuit in conjunction with the FeatherWeight UI app a simple simulation was performed to test the settings in the altimeter and provide

a baseline for how the altimeter will react as settings change. Figures 6.1.2 and 6.1.3 show the simulation in action. Figure 6.1.2 shows the left LED illuminating representing

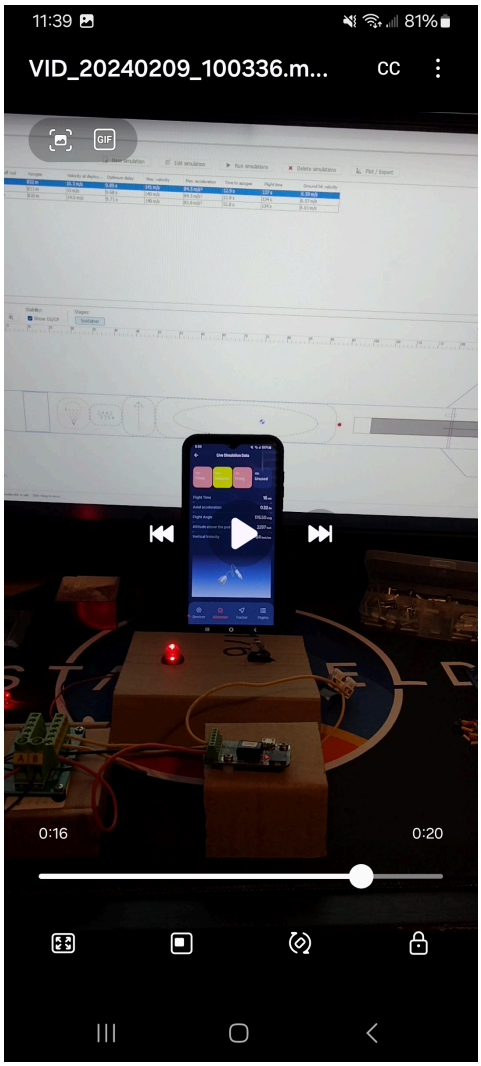

Figure 6.1.2 - Avionic simulation

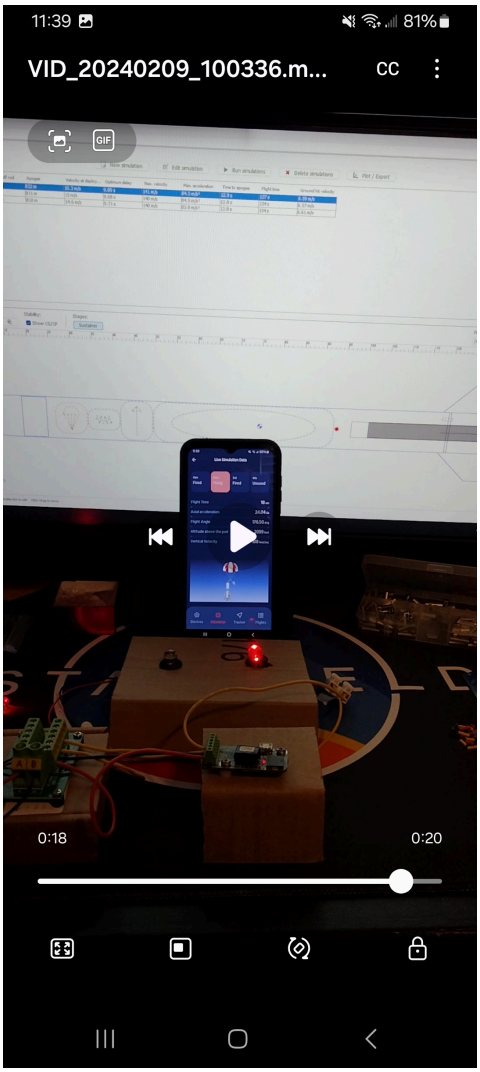

Figure 6.1.3 - Avionics Simulation

a pyro event occurring on the apogee channel of the altimeter. Figure 6.1.3 shows the right LED illuminating representing a pyro event on the main channel of the altimeter. Both channels are utilized to add a redundancy charge to the system. The next stage in developing the avionics was to create a board the units could be mounted to and a casing that protects the avionics circuit from any harmful

conditions it may experience during flight and recovery. The process to design these components began in SolidWorks generating 3D models. It took many iterations to find the most efficient geometries to maximize the space available. Figures 6.1.4 and 6.1.5 show the final models of the board and canister.

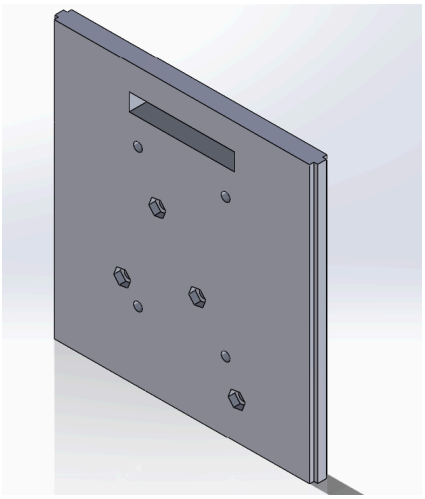

Figure 6.1.4 - Avionics board

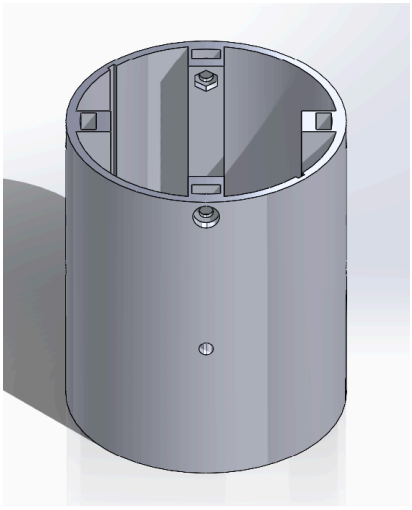

Figure 6.1.5 - Avionics canister

Manufacturing the board and the canister was the next phase. The board was to be 3D printed from PLA filament and the canister was to be 3D printed from polycarbonate filament. Once the board was printed M3 nuts were pressed into the designated holes. These newly pressed nuts allow the avionics components to be mounted to the board. The final result is shown in figure 6.1.6. After gluing the nuts into place to ensure they were secured the avionics components were mounted, this can be seen in figure 6.1.7. The channel of the canister was widened after printing to better accommodate the board. This was done using a combination of files and sandpaper until we achieved the desired fitment.

Figure 6.1.6 - Pressed M3 nuts

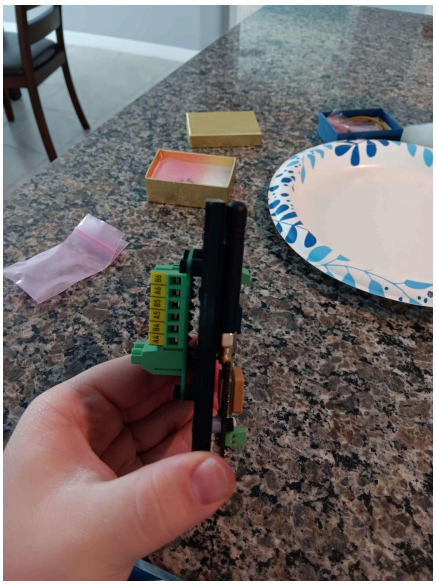

Figure 6.1.7 - Mounted avionics

With the board built and the canister printed the final circuit could be created. The final circuit did not change much from the original circuit used to conduct the simulation. Quick connection points were added to allow easy removal from the canister and the tracking unit was added to the circuit. Figure 6.1.8 shows a wiring diagram of the final circuit and figure 6.1.9 shows the avionics unit fully assembled.

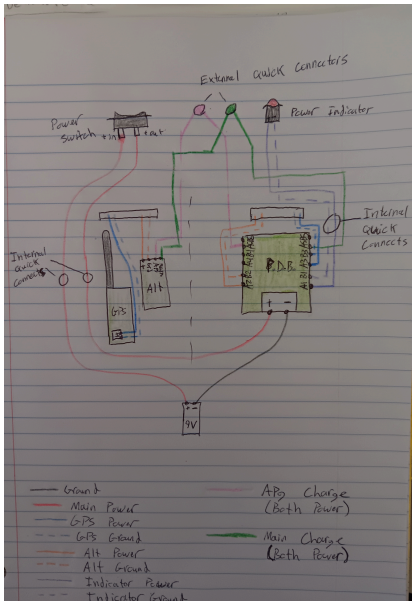

Figure 6.1.8 - Avionics wiring diagram *Figure 6.1.9 - Assembled avionics*

The next phase in the avionics development was moving away from the simple LED placeholders and designing black powder charges capable of producing enough energy to separate the rocket. The black powder charges are made up of a rubber glove finger tip, an e-match, and masking tape to hold them tight shown in figure 6.1.10. Through testing it was determined that the e-matches needed to be coated with a pyrogen solution to ignite and with that ignition medium approximately 2 grams of black powder is necessary to separate our nose cone from the rocket body. Figure 6.1.11 is a screenshot from black powder testing showing how energetic these charges can be.

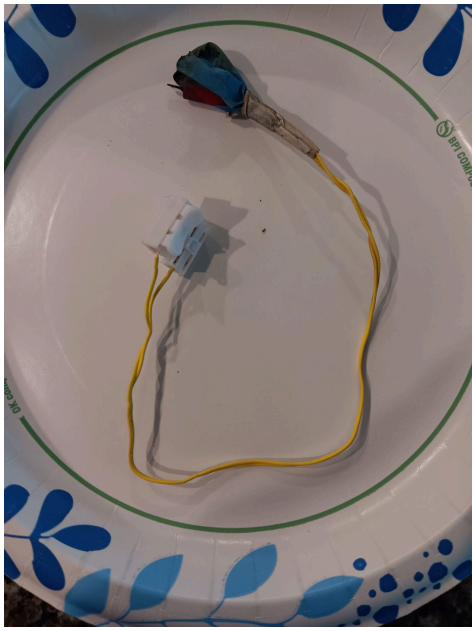

Figure 6.1.10 - placeholder

Figure 6.1.11 - Black powder test

The final stage in the avionics development was testing the GPS tracking unit. This was a quick test to see how the unit functioned and how accurate the output is. The tracking system utilizes the FeatherWeight UI and a handheld ground station, shown in figure 6.1.12, to triangulate the location during flight making it easy to find once it lands.

Figure 6.1.12 - Ground station

6.2 Coupler

The development of the coupler came later in the design phase, however it is one of the most critical components of our rocket. The coupler connects the nose cone to the rocket body while housing the avionics system and locking the payload in place. The development for the coupler began with 3D modeling in SolidWorks with the idea that the component had to be durable enough to protect the payload and rigid enough to lock the payload in place. Due to manufacturing limitations the coupler could not be 3D printed as a single piece therefore three separate pieces would need to be created and printed and joined together using bolts and adhesives. The parts are as shown in figures 6.2.1, 6.2.2, and 6.2.3. Figure 6.2.1 is the avionics canister as mentioned in section 6.1. This canister houses the avionics and acts as the lower sleeve that slots into the rocket body. The bolts will go through the rocket body securing the canister and locking the payload in place. This component will experience a large amount of load scenarios during flight and recovery thus requiring that the materials used are strong. The canister will be 3D printed in polycarbonate filament and the bolts are 10.2 steel alloy. Figure 6.2.3 shows the section of the coupler that increases the outer diameter of the coupler to match the outer diameter of the rocket body. This section also serves as the mounting point for the shock cord and therefore will experience a large load scenario when the parachute is deployed. The material selected for this part is also polycarbonate filament which provides a great

strength to mass ratio. This middle section will attach to the canister via 10.2 steel alloy bolts, allowing it to be removed easily to gain access to the avionics. Figure 6.2.3 is the upper section of the coupler and its job is to connect the nose cone to the coupler. This part does not experience a significant load scenario and therefore does not require a material with as much strength as polycarbonate. The upper section will be printed with PETG filament.

The next phase in development is to verify that the geometry modeled and the materials chosen can withstand the expected load scenarios. This verification will be done utilizing FEA simulations (discussed in section 7).

6.3 Recovery

Figure 6.3.1 - Fully inflated HPR parachute descending.

The recovery system for this rocket was developed and evolved over the entire planning, designing and manufacturing phases of this project. Research was conducted on the best way to recover a high powered rocket, from 2000 feet, carrying a sensitive payload. Many experts and veterans of high powered rocketry had recommended a dual deployment system that would require two parachutes to bring the rocket back to Earth safely. The reason a dual deployment recovery system is best for recovering sensitive payload, is that it provides redundancy in parachute deployment, reducing the risk of complete failure during descent. It also allows for more precise altitude control when the rocket is descending. A drogue parachute is deployed at apogee and slows the rocket and helps stabilize it. A main parachute is then deployed at a much lower altitude that will slow the descent even further, ensuring a gentle touchdown. Another benefit of having two parachutes is that the load can be distributed more

Figure 6.3.2 - Dual Deployment Illustration

evenly, alleviating stress on the rocket and the payload. The more the team thought about the positive aspects of a dual deployment system, problems began to arise with the overall plan. The first problem was the complexity of deploying two parachutes. With multiple moving parts, all in sequence with one another, the possibility of a failure occurring was high. With two parachutes, a coupler and a nose cone, all reacting with turbulent aerodynamic conditions, the risk of entanglement was high. Also, having two parachutes takes up precious space that could be used for payload. Finally, being on a tight budget, the extra cost incurred by a second system could be money invested elsewhere.

The next phase of recovery development came in January of 2024, when the team decided to go with a single parachute to recover the rocket and its sensitive payload. Initially, the team had the idea that ‘Bigger is Better’ It was agreed that a 58” parachute would be used for recovery. A 58” parachute would provide ample drag to safely recover the rocket and payload well within the 25 ft/sec descent rate needed for a successful flight. The problems that came with having a big parachute is housing it in the rocket, during flight. For this project, the parachute was to be housed in the nose cone. In order for a parachute to deploy properly, it must be folded correctly. When a 58” parachute is folded correctly, its volume is greater than the volume within the nose cone. In order to get the parachute to fit, extra folds had to be placed within the parachute and the shock cord had to be wrapped around the chute multiple times more than recommended. For the test launch on March 16, 2024, the 58” parachute was packed into the nose cone, improperly folded to fit. As

the rocket failed to reach apogee, the rocket began to descend back to Earth. When the rocket achieved a predetermined descent rate, the redundant deployment system kicked in, ejecting the nose cone and deploying the parachute. The parachute failed to unroll and unfold itself before impacting the ground.

After the test launch failure, the recovery development evolved into its final phase. After doing drop testing with eggs nested in EVA foam, from a height of forty-feet, it was discovered that the payload design was more resilient than previously thought. Testing revealed that the eggs could withstand an impact velocity of 50 ft/sec. Armed with this new knowledge, the team decided it would be best to go with a 36” parachute. A parachute of this size, easily fit into the nose cone and could be folded properly. It also allowed for a descent rate of 35 ft/sec which is well below the threshold of 50 ft/sec. Testing was done on the 36” parachute to see if the

Figure 6.3.3 - Inflation testing on the 36” parachute at apogee velocity.

Eyebolt connected to the coupler could withstand the jarring forces associated with a parachute inflating at high rates of speed. The velocity at apogee was acquired through OpenRocket simulation software. A team member sat in the bed of a truck, with the truck matching the speed at apogee, and deployed the parachute. The eyebolt, coupler and shroud lines all withstood the force. During the final launch on April 20, 2024, the rocket did not take the flight path intended. Due to unforeseen circumstances, the rocket flew into a parabolic arc and was traveling at speeds far higher than expected. When the parachute did deploy, the force of inflation was so great that the parachute separated from the rocket. Where the point of failure occurred, is unknown because the rocket was never found.

6.4 Payload Handling

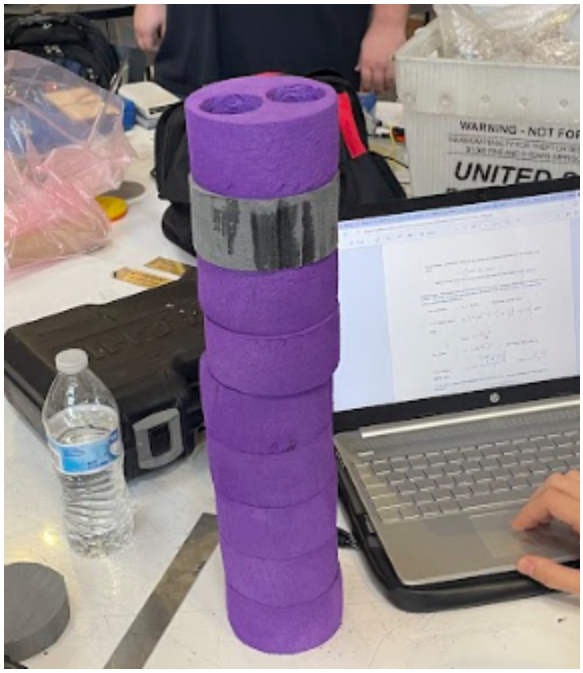

Figure 6.4.1 - EVA foam egg holders.

The payload may be the most critical component of this project. Carrying chicken eggs to 2000 feet and returning them safely to Earth, requires a cargo hold that can provide maximum protection against forces that will be placed on the rocket throughout the duration of the flight. There were many ideas that were kicked around, ranging from, 3D printing a cargo hold and filling it full of foam pieces, to using some form of gel for the eggs to suspend themselves in during flight. It became evident that the best way to protect the eggs from the harsh aerodynamic forces experienced in high powered rocketry, was to use foam. As the team started researching foam, it was abundantly clear that there are many different types of foam and each type has their own unique characteristics. The team was still on board with 3D printing a cargo hold that the foam would be placed inside of. Research was conducted on dampening springs and pucks to reduce the impact vibrations from turbulent flight and landing. However, when adding ⅛” PLA and ¼” dampening pucks to protect foam, the payload bay starts losing critical space. It wasn’t long and these ideas were scrapped.

The new vision for the payload soon evolved into using the actual rocket chassis to make up the payload bay walls, and have the eggs be nested inside of foam. Research was started on the best kinds of foam that can absorb a shock. EVA foam kept popping up on the radar. It was used in running shoes and yoga mats. It’s inexpensive and readily available. The team acquired some yoga blocks made out of EVA foam and cut them into 4” diameter circles that were 3” thick. Small egg shaped pockets were hollowed out in the foam for the eggs to

sit. Since the average egg is 2.25” tall and 1.75” wide, this gives ample foam on all sides of the egg, to provide protection. The foam puck was thrown into the air and the egg emerged unbroken. Soon, two eggs were placed side by side in the foam and thrown into the air, and they also emerged unbroken.

Figure 6.4.2 - Cardboard Test tube used to drop test eggs

A cardboard tube that had the same dimensions as the rocket, was purchased for the sole purpose of performing drop tests with the eggs nested inside of the EVA foam. The first test was conducted at a height of 10 feet, to simulate the rocket landing at a velocity of 25 ft/sec. The eggs survived that test. The next test was performed at 20 feet and they also survived. The final test was dropped from 40 feet with an impact velocity of over 50 ft/sec and all the eggs emerged unscathed. At this point the team decided to

maximize the amount of eggs in the foam pucks by using a layout design that allowed for 4 eggs to be nested inside of two pucks.

Mass (Slug)	0.0615		Mass (Slug)	0.0615		Mass (Slug)	0.0615		Mass (Slug)	0.0615	
Impact Velocity Vs Height with Tube											
h (ft)	9.704968944		h (ft)	16		h (ft)	28		h (ft)	40	
Vimpact (ft/s)	25		Vimpact (ft/s)	32.09984424		Vimpact (ft/s)	42.46410249		Vimpact (ft/s)	50.75431016	
Fimpact (lb)	19.21875		Fimpact (lb)	31.6848		Fimpact (lb)	55.4484		Fimpact (lb)	79.212	
	Time (s)	Survive? (Y/N)		Time (s)	Survive? (Y/N)		Time (s)	Survive? (Y/N)		Time (s)	Survive? (Y/N)
V-Test 1	0.82	6Y 0N	V-Test 1	0.9	6Y 0N	V-Test 1	0.9	6Y 0N	V-Test 1	1.2	6Y 0N
V-Test 2	0.9	6Y 0N	V-Test 2			V-Test 2			V-Test 2		
V-Test 3	0.73	6Y 0N	V-Test 3			V-Test 3			V-Test 3		
H-Test 4	0.7	6Y 0N	H-Test 4			H-Test 4			H-Test 4	1.3	6Y 0N
H-Test 5	0.65	6Y 0N	H-Test 5			H-Test 5			H-Test 5		

Table 7.4.1 Drop Test Results

**The V and H before each test stands for Vertical or Horizontal drop respectively*

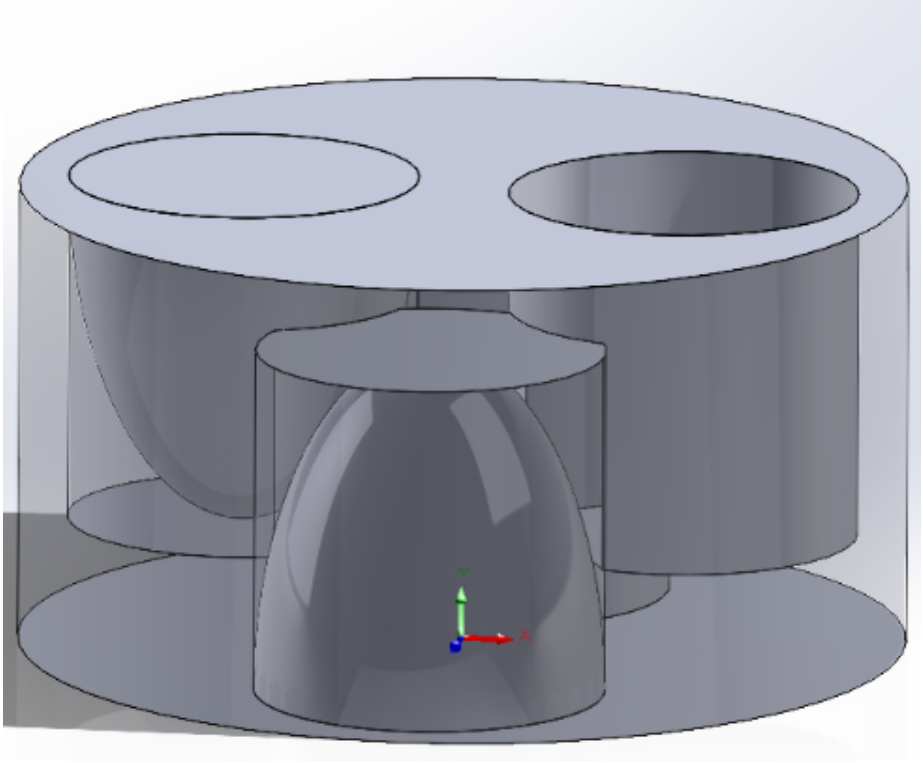

Figure 6.4.3 - Final egg layout

This design became the final iteration for how the eggs would sit within the rocket's payload bay. It was decided that the pucks would be stacked in series, for a total payload length of 24”. The wrapped pucks would be loaded from the top down, and sit underneath the avionics bay. The stack would sit on top of a centerplate that was installed during the manufacturing of the rocket. The centerplate acts as a fire wall between the motor and the payload bay. The pucks would be wrapped in cellophane with a handle taped to the top for easier extraction post launch. The cellophane provides a connective film that holds all of the pucks together, so when the user pulls on the handle, all of the pucks and eggs are extracted at once.

Figure 6.4.4 Pucks containing eggs stacked in series, wrapped in cellophane.

7 Design Analysis

7.1 Rocket Performance and Computational Fluid Dynamics Introduction

Computational Fluid Dynamics (CFD) is a method for solving fluid dynamic problems through use of a discretized mesh around an object that solves for the exact fluid properties at each cell. The conventional method for solving a fluid dynamics problem is through wind tunnel testing of either a scaled model or full scale prototype. The benefits of using CFD over a wind tunnel experiment are: ability to change model geometry and external conditions rapidly, quick compilation of data, low manual labor to complete a test, less equipment necessary - even when equipment is available, and no need for a physical model. The major downside of using CFD is the validity of those results. In this project - no experiments were conducted to solve for aerodynamic properties. In order to increase confidence in results, values from CFD were compared to approximated values generated by OpenRocket [31].

OpenRocket is a model rocket flight performance software that provides information about how a rocket will behave during its flight. OpenRocket is a powerful tool that was used for the baseline performance of the rocket in this project. However, OpenRocket estimates aerodynamic properties using Barrowman's equations [36] and other methods; according to OpenRocket technical documentation [31] "*One possible future enhancement that has also specifically been considered throughout the*

development is calculating the aerodynamic properties using computational fluid dynamics." These aerodynamic properties include the lift, drag, and normal forces; as well as pitching, rolling and damping moments. Here, these enhancements will be explored.

In Section 7.2 an overview of CFD setup will be shown. Then in Section 7.3 the methods for obtaining aerodynamic parameters will be presented. In Section 7.4, the procedures of rocket simulation are detailed. Section 7.5 compares CFD flight simulations to those obtained in OpenRocket. Finally, Section 7.6 attempts to validate Data by comparing different models.

7.2 CFD Setup

For this project 6 different flight configurations were analyzed. The first two cases analyzed were for the maximum loading conditions of the rocket fins. These conditions occurred at a maximum velocity (freestream velocity) of 450 ft/s, with wind sideslip angles (or angle of attack of the fins) of 5 degrees and 10 degrees. These simulations were conducted before the max velocity and sideslip angles were known with a high level of confidence. Therefore these values were assumed to be greater than anticipated to ensure that when pressure data of the fins was imported for Finite Element Analysis (FEA) the structural rigidity of the fins would be sufficient. The results from the FEA analysis of the fins are shown in Section 7.7.

The first step in CFD analysis is understanding the material and fluid properties at that condition and adapting the mesh and solvers to reach the most accurate

solution. For all cases, a Spalart Allmaras turbulence model was selected with coupled flow and ideal gas to reduce computation times. Because the vehicle is subsonic (Ma < 1) for the entire duration of the flight, and Reynolds numbers are relatively low for turbulent regimes, these assumptions were made. Below are the tabulated inputs along with corresponding meshing parameters for the max loading cases.

Inputs		*US Customary Units*
Vinf	450	ft/s
Density	0.07647426781	lb/ft^3
Dynamic viscosity	1.77E-10	atm-s
Atmospheric Pressure	1	atm
Standard Temp	537	°R
Meshing Parameters		
Characteristic Length	4	in
desired y+	1	
Prism layer Stretching	1.2	
Number of Prism layers	30	
Reynolds Number	954216.5232	
Cell Height Near Wall	0.00001625651703	ft
Total Cell Thickness	0.01921327786	ft
Boundary Layer Thickness	0.00785508852	ft
Final Number of Cells	1702605	
a (speed of sound)	1135.651917	ft/s
Mach	0.3962481755	

Table 7.1 StarCCM inputs for rocket under max loading conditions

In order to get pressure data on the fin: plane sections were created across the span of the fin at y/b = 0.2, 0.4, 0.6, 0.8, 0.95, 0.99 (see Figure.7.1). Pressure was plotted, normalized to the chord of the fin at these sections and tabulated to import into Ansys for FEA analysis. The study was conducted at sideslip angles of 5° and 10° using a coordinate transfer. Because all data is normalized to the geometry of the fin, in the event that the fin needs to be scaled - the same data can be used on the updated model. An example of a pressure plot can be seen below (Figure 7.2). These plots will be useful when finding the lift coefficient and validating data later in this report.

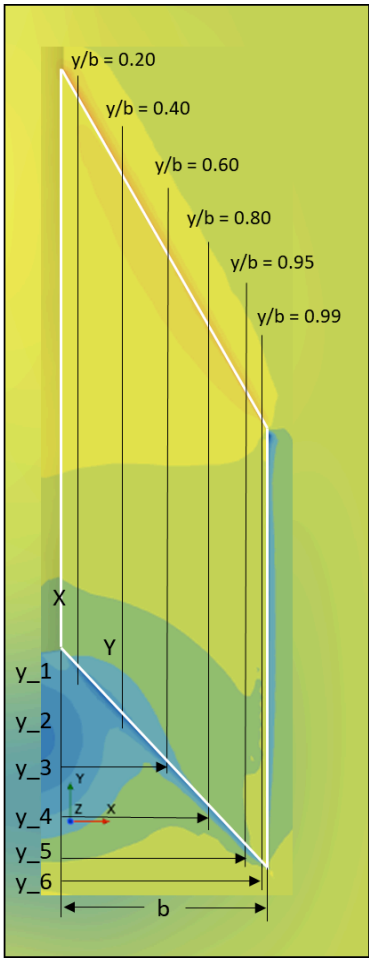

Figure 7.1 Sections of Fin used for Pressure Data

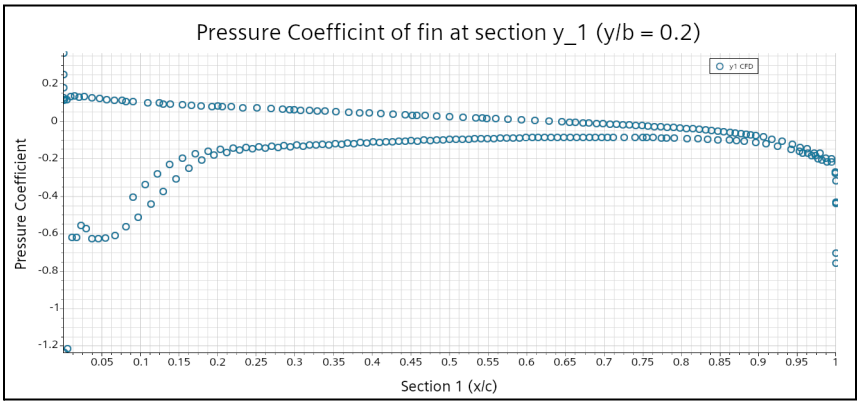

Figure 7.2 Pressure Data at Velocity of 450ft/s with 5° Sideslip

One of the most critical points in the rocket's flight is stabilization off the rail. As the rocket needs to incur a positive moment to adjust into the flow direction, the stability criteria that needs to be met is ($C_{m\alpha} > 0$). The next 4 cases analyzed were conducted for the rocket at low freestream velocity (V = 38ft/s) under sideslip angles of 1, 5,10 and 15 degrees. The results from these studies were used for flight simulation purposes. Similarly to the max loading conditions, a Spalart Allmaras turbulence model was selected with coupled flow and ideal gas. Inputs are listed below.

Inputs		*US Customary Units*
Vinf	38	ft/s
Density	0.07647426781	lb/ft^3
Dynamic viscosity	1.77E-10	atm-s
Atmospheric Pressure	1	atm
Standard Temp	537	°R
Meshing Parameters		
Characteristic Length	8	in
desired y+	1	
Prism layer Stretching	1.2	
Number of Prism layers	30	
Reynolds Number	161066.5365	
First Cell Height	0.0001612259522	ft
Total Cell Thickness	0.1905499813	ft
Boundary Layer Thickness	0.02242380983	ft
Number of Cells	1702605	
a (speed of sound)	1135.651917	ft/s
Mach	0.03346095704	

Table 7.2 StarCCM inputs for rocket under rail conditions

For all 6 cases a mesh of ~2 million cells was used. For the first several hundred iterations a coarse mesh of ~500 thousand cells was used, before the finer mesh was applied in order to reduce computation times by starting with a better initial guess. Higher cell counts were used at the nose and fins of the rocket where geometry was more complex. This was done to better encapsulate the fluid effects in these regions and reach a more robust solution. Prism Layer meshing was used to account for boundary layer effects, and those mesh settings are tabulated in Table 7.1 and 7.2.

Figure 7.3 Rocket Mesh Scene

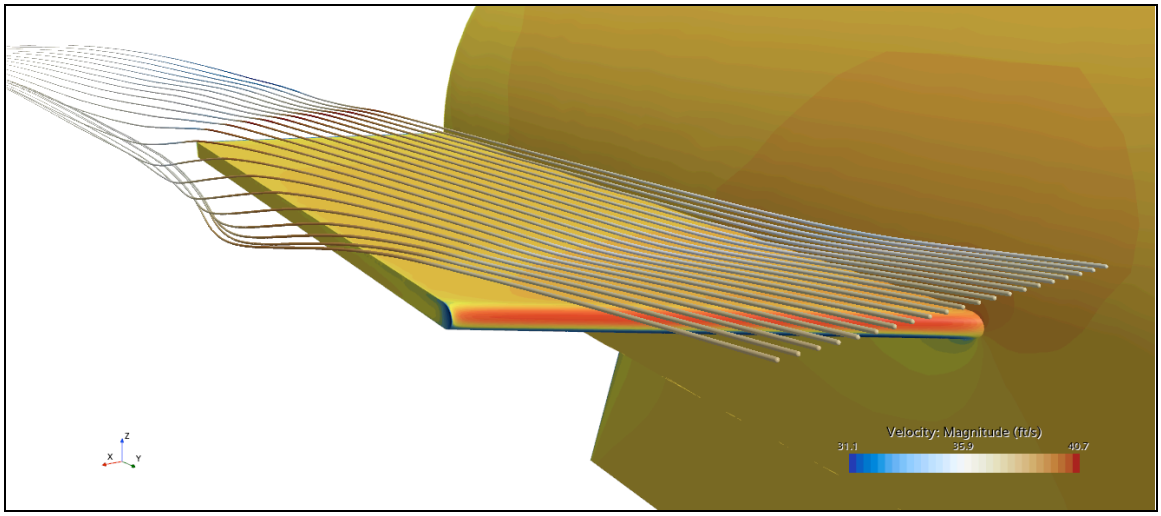

Figure 7.4 Fin Velocity Streamline View at 5° Angle of Attack

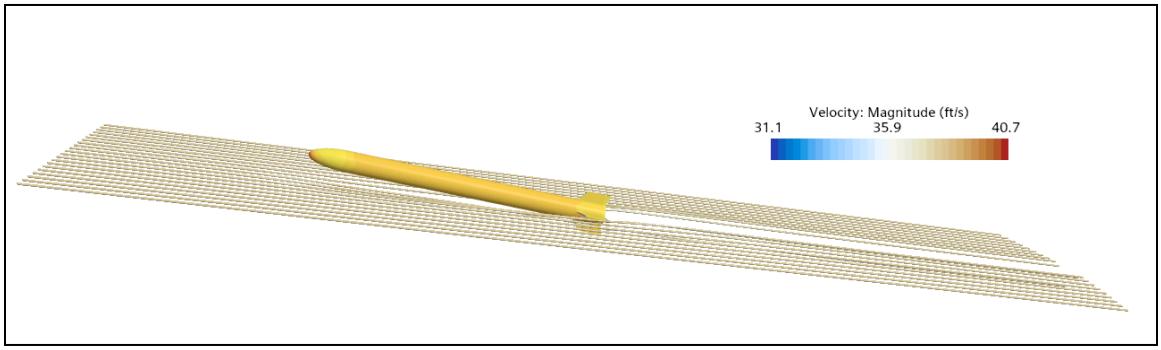

Figure 7.5 Rocket Velocity Streamline View at 5° Angle of Attack

7.3 Aerodynamic Parameters

V_R — *Relative Wind Velocity*

S_{ref} — *Reference Area*

d_{ref} — *Reference Distance*

ρ_∞	*Freestream Density*
q_∞	*Freestream Dynamic Pressure*
AR	*Aspect Ratio*
C_L	*Lift Coefficient*
C_D	*Drag Coefficient*
$C_{D,i}$	*Induced Drag Coefficient*
C_N	*Normal Force Coefficient*
CoM	*Center of Mass*
CoP	*Center of Pressure*
I_Y	*Longitudinal Moment of Inertia*
ω	*Angular Rotation*
$\dot{\omega}$	*Angular Acceleration*
q_m	*Pitch Angular Rotation*
M_0	*Base Pitch Moment*
C_{mm}	*Pitch Moment Coefficient*
C_{mqm}	*Pitch Damping Derivative*
C_{mmd}	*Pitch Damping Coefficient*
M_Y	*Total Pitch Moment*

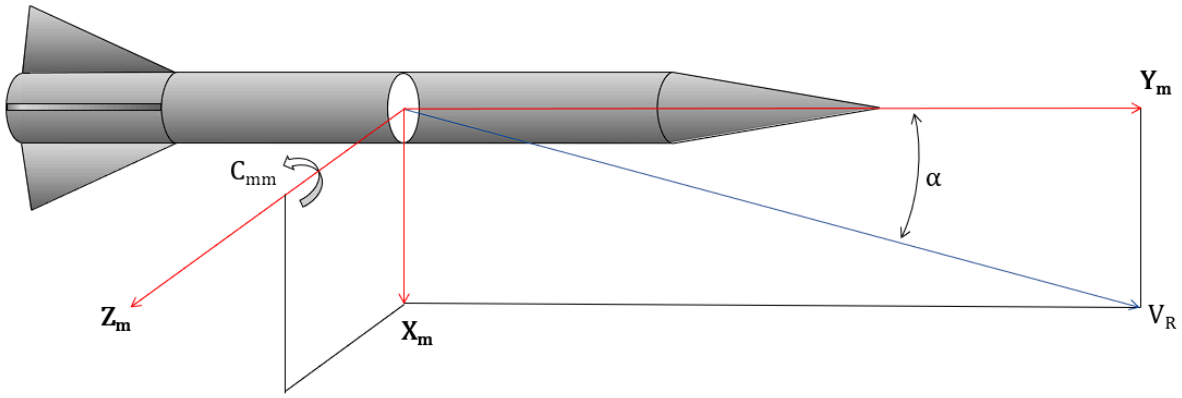

Figure 7.6 Rocket Body Reference Frame Coordinate System

Using CFD: values for the Lift force coefficient of the fins, Normal force coefficient of the nose cone, Drag coefficient of the system, and Moment coefficient of the body tube were found at sideslip angles from 0 to 15 degrees. In order to obtain the lift coefficient, section cuts were made along the fin and normalized to the chord. This data was integrated from the lower to upper surface of the fin (see Appdx. I. Pressure Integration Code) and averaged across the sections. All other coefficients were found using force reports in StarCCM+. The Mathematical representation of these coefficients can be found in Appdx. H. Keep in mind S_{ref} is the frontal area of the rocket and d_{ref} is the diameter of the body tube. As long as these reference values are constant, then they cancel out when solving for forces and moments. In order to apply these values to analyze the stability of the rocket, a curve fitting function was used to approximate the values between data points (Appdx. J. CurveFitting Code).

On the right, Error was analyzed for each of these coefficients. For a linear curve fit, the R^2 values for each of these coefficients was close to 1 - which implies a good approximation. However, looking at the graphs (Fig.10) shows that there is a negative moment generated by the body at 0 deg angle of attack.

```
######### Curve Fit Values (CL Fin) #########
Sum of Squares of Errors (SSE) =  8.82902e-03
Mean =  2.52142e-01
R squared = 0.940628
Standard error =  4.20215e-02

######### Curve Fit Values (CD Sys) #########
Sum of Squares of Errors (SSE) =  1.78771e-02
Mean =  6.92116e-01
R squared = 0.958180
Standard error =  5.97949e-02

######### Curve Fit Values (CN Nose) #########
Sum of Squares of Errors (SSE) =  2.26032e-07
Mean = -1.80294e-02
R squared = 0.999829
Standard error =  2.12618e-04

######### Curve Fit Values (CM Body) #########
Sum of Squares of Errors (SSE) =  3.49804e+00
Mean = -4.93908e+00
R squared = 0.939248
```

This is not physically possible in this example, as when the rocket is in line with the relative wind speed there should be no moment generated by the wind. Despite this physical impossibility, a positive moment is also generated by the fins at this angle (Fig.9), the two moments relatively cancel each other and the better curve fit between data points is desired. In order to get a better approximation more CFD or Experimental data points could be found, or a different numerical method could be used.

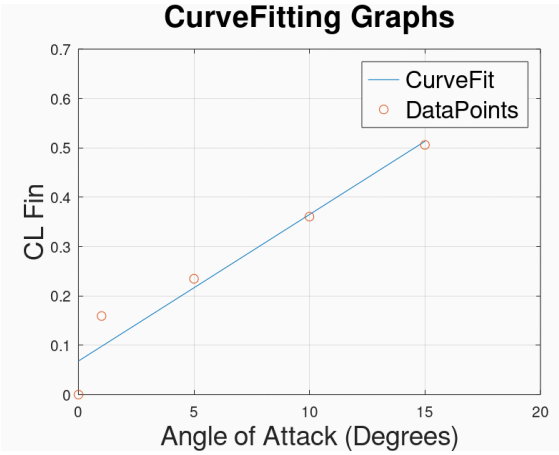

Figure 7.7 $C_{L,Fin}$ Graph

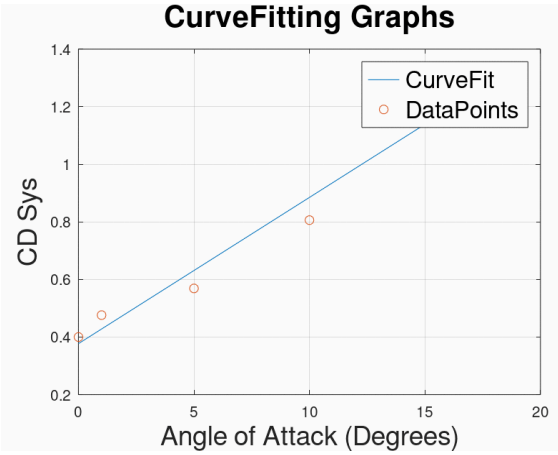

Figure 7.8 $C_{D,Sys}$ Graph

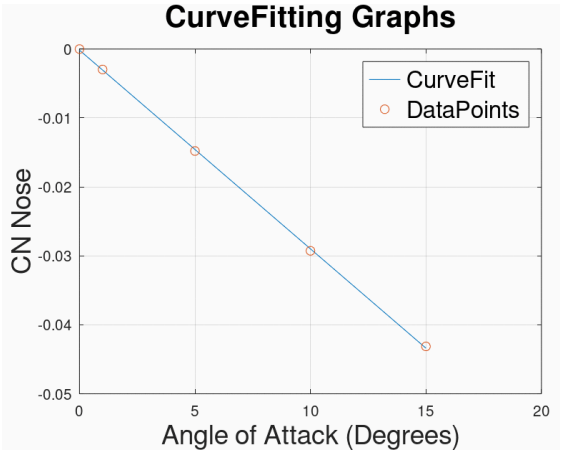

Figure 7.9 $C_{N,NoseCone}$ Graph

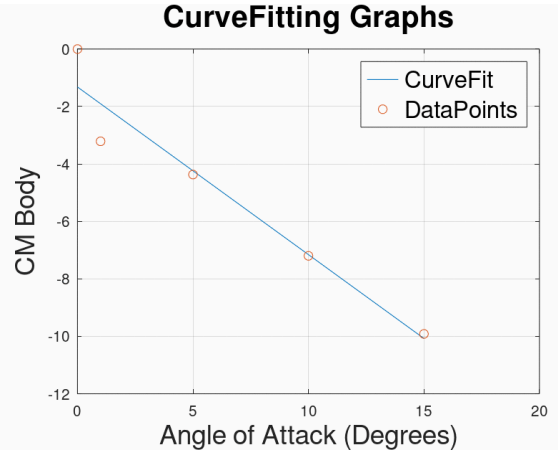

Figure 7.10 $C_{M,Body}$ Graph

Induced drag was also accounted for in drag coefficient derivation. The equation used was:

$$C_{D,i} = \frac{C_L^{\,2}}{\pi \cdot AR \cdot e} \qquad \textit{Equation (7.1)}$$

(Where e the efficiency factor is assumed at 0.7)

As all coefficients were found in the body frame, only the longitudinal location is needed to apply them for simulation. The moment coefficient of the body is easy, as it is applied at the center of mass of the rocket acting in a destabilizing motion. Drag coefficient acts parallel to the longitudinal frame and has no effect on stability. Both Lift coefficient and the Normal force coefficient of the nose act perpendicular but opposite to the longitudinal frame. Therefore, the center of pressure (COP) of these coefficients need to be addressed.

The Barrowman equations [33] give an approximation of where the center of pressure of a nose cone is. For an Ogive nose cone, the COP is approximately 46% the length of the nose cone measured from the tip of the nose. For all other nose cones, the

COP can be approximated at 66% the length of the nose cone measured from the tip of the nose. In this project, a parabolic nose cone was used, so the 66% length was approximated.

The COP of the fins was taken at the ¼ chord of the fin. This is a reasonable approximation to make for most wings. Looking at figure 7.2 shows the largest differential in pressure around that location, so this approximation was justified. To find the spanwise location of the center of pressure equation 7.2 was used, where the dimensions of the fin can be seen in figure 7.11.

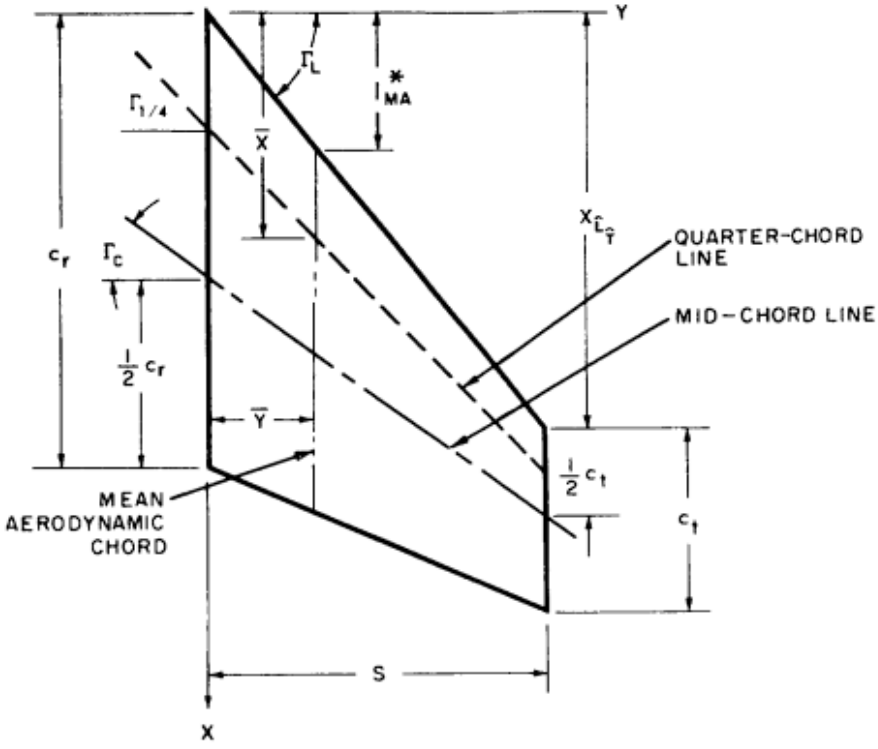

Figure 7.11 Fin Geometry and Aerodynamic Center [33]

$$Y_{AC,fin} = \left(\frac{S}{3}\right)\left(\frac{C_r + 2*C_t}{C_r + C_t}\right) \qquad \textit{Equation (7.2)}$$

The last aerodynamic coefficient that needs to be mentioned is the damping derivative in the longitudinal frame, as the rocket rotates about the longitudinal frame - air resists this motion which causes the rocket to stabilize. Without this derivative, the rocket would oscillate about the weathercocking angle (relative velocity vector) and be highly unstable. The traditional mathematical representation for this derivative C_{mqm} can be seen below in equation 7.3. In order to apply this derivative, it is transformed into the derivative C_{mmd} (equation 7.4) and acted against the pitching moment.

$$C_{mqm} = \frac{\partial C_{mm}}{\partial\left(\frac{q_m d_{ref}}{2V_R}\right)} \qquad \textit{Equation (7.3)}$$

$$C_{mmd} = \frac{q_m d_{ref}}{2V_R} \cdot C_{mqm} \qquad \textit{Equation (7.4)}$$

Because C_{mqm} is very hard to derive, it is often approximated using the lift coefficient. Here C_{mqm} is approximated as:

$$C_{mqm} = C_L\left(\frac{S_w}{S_{ref}}\right)\left(\frac{Y_{fin}}{C_{crit}}\right)^2\left(\frac{2.2}{V_R}\right) \qquad \textit{Equation (7.5)}$$

Where (S_w/S_{ref}) is an efficiency factor and $2.2\cdot(Y_{fin}/C_{crit})^2$ is used to approximate the damping derivative effect of the rest of the body

7.4 Rocket Simulation

In order to model the rocket's flight path, a first order ODE solver was programmed using MATLAB (see Appdx. K. Rocket Performance Program). The solver utilizes small time steps in order to calculate velocity, acceleration, altitude and drift at each time step until the entire trajectory of the rocket is compiled.

The stages of flight can be shown as:

1. Guided Flight: Rocket is on the pad, and flight path set to the orientation of the rail system
2. Powered Flight: Rocket is undergoing acceleration as propellant is being burned
3. Coasting Flight: Rocket is decelerating as motor provides no more thrust
4. Recovery: Rocket recovery system is deployed at or near apogee and rocket is in process of returning to earth
5. Touchdown: Rocket has returned to earth at a certain distance away from launch pad

To begin, initial conditions need to be declared. Air properties and gravity are assumed constant at STP as the rocket does not reach altitudes where these values significantly change. General dimensions of the rocket are needed, along with the initial center of mass and initial longitudinal moment of inertia. These can be easily found using equations 7.6 and 7.7. Where m_i is the mass of each component and y_i is the distance from the bottom of the rocket to the center of mass of the component.

$$I_Y = \sum_i m_i \cdot y_i^2 \quad \textit{Equation (7.6)}$$

$$CoM = \sum_i y_i \cdot \left(\frac{m_i}{m_{total}}\right) \quad \textit{Equation (7.7)}$$

These parameters are updated while the motor is burning, because as propellant is ejected from the rocket, the COM shifts forward to the nose of the rocket and the longitudinal moment of inertia decreases. To update these at each time step, a simple integration can be done assuming a constant mass flow rate of propellant $\dot{m}_p$

$$\dot{m}_p = \frac{m_p}{t_b} \quad \textit{Equation (7.8)}$$

$$I_Y \mathrel{-}= \int \dot{m}_p \cdot y_i^2 dt \quad \textit{Equation (7.9)}$$

$$CoM \mathrel{+}= \int y_{motor} \cdot \left(\frac{\dot{m}_p}{m_{total}}\right) dt \quad \textit{Equation (7.10)}$$

Here t_b is the burn time time of the propellant and m_p is the mass of the propellant obtained from specifications by the manufacturer [35].

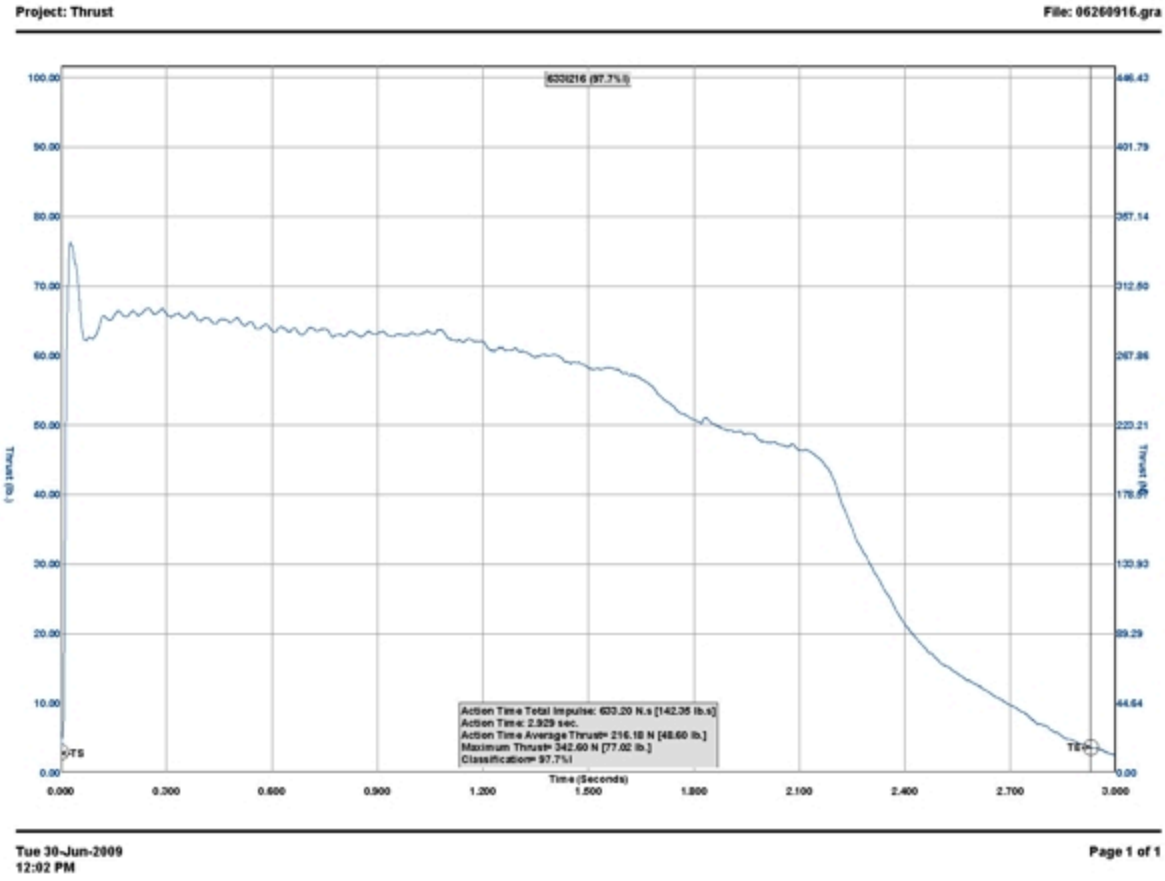

Figure 7.12 Cesaroni 636I216 Thrust Curve [34]

Thrust can be integrated across the flight by interpolating between known thrust data points during the burn time of the rocket. The result is a thrust curve (Figure 7.11). These data points were obtained from *Thrustcurve.org* [34] and incorporated into the code using a linear interpolation method.

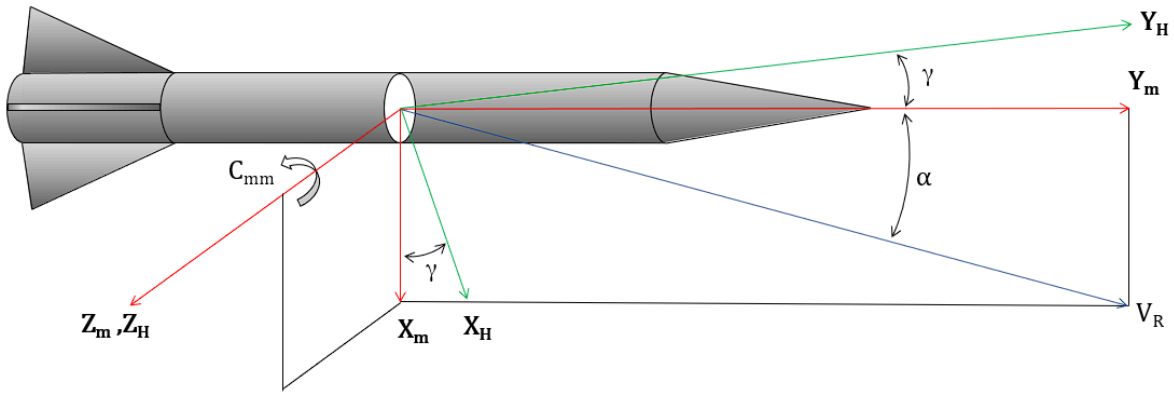

Figure 7.13 Body Frame And LVLH Frame

Next, a new coordinate system is defined as the Local Vertical, Local Horizontal (LVLH) coordinate system. Here, Y_H is defined as pointing radially out from the tangent plane of the earth's surface, and X_H points in the direction of the local horizon. To convert between the Body Frame to LVLH Frame the angle γ (Flight Path Angle) is used. The flight path angle will define the position of the rocket relative to the earth.

Rocket velocity and acceleration is defined in the body frame pointing in the Y_m direction. These parameters are defined by the thrust, drag and gravitational deceleration of the rocket. Both thrust and drag are defined in the body frame in the Y_m direction, but gravity is applied in the Y_H direction. Because γ is small for most of the flight, this discrepancy is ignored.

$$a = (T - D - g/m) * m \quad \textit{Equation (7.11)}$$

$$v = \int a \cdot dt \quad \textit{Equation (7.12)}$$

In this program, a wind velocity vector is specified in the X_H direction. As rolling moments are ignored for this code, velocity can only be specified in the X_H , Y_H plane. This velocity can be made unsteady by applying a random standard deviation to the speed. A new angle can then by defined as the tan of the rocket velocity which points in the Y_m direction and the wind velocity that points in the X_H direction. This angle is the sideslip angle or weathercocking angle, and is the angle which the rocket tends toward. Now define α:

$$\alpha = tan^{-1}\left(\frac{V_{wind}}{V_{Rocket}}\right) - \gamma \qquad \textit{Equation (7.13)}$$

From here, all aerodynamic coefficients can be calculated at each time step using the curve fitting function mentioned in section 7.3. However, The flight path angle is still unknown. This is solved from the angular impulse and momentum equation.

$$I_Y \omega_1 + \sum \int_{t1}^{t2} M dt = I_y \omega_2 \qquad \textit{Equation (7.14)}$$

$$\omega_2 - \omega_1 = \frac{M_Y}{I_y} dt \qquad \textit{Equation (7.15)}$$

$$\dot{\Delta\omega} = \frac{M_Y}{I_y} \qquad \textit{Equation (7.16)}$$

Where,

$$M_Y = M_0 + M_d = q_\infty S_{ref} d_{ref} (C_{mm} + C_{mmd}) \qquad \textit{Equation (7.17)}$$

Now, set q_m equal to angular rate

$$q_m = \int \dot{\omega} \cdot dt \quad \textit{Equation (7.18)}$$

$$\gamma = \int q_m \cdot dt \quad \textit{Equation (7.19)}$$

The last parameters that need to be solved for are the altitude achieved by the rocket, and the drift of the rocket.

$$h = \int v \cdot cos(\gamma) \cdot dt \quad \textit{Equation (7.20)}$$

$$x = \int v \cdot sin(\gamma) \cdot dt \quad \textit{Equation (7.21)}$$

Once Apogee is achieved, drag coefficient is set to that of the parachute, and Gamma is set equal to the weathercocking angle.

The procedure of the code is as follows:

1. Initialization of the rocket on the pad (t=0)
2. Evaluate point at which rocket is in flight
3. Compute Thrust, CoM and Moment of Inertia
4. Solve for Angle of Attack
5. Compute Aerodynamic Coefficients
6. Solve for Flight Path Angle
7. Compute Wind variation, Acceleration, Velocity, Altitude and Drift
8. Advance Time Step

7.5 Flight Performance Analysis

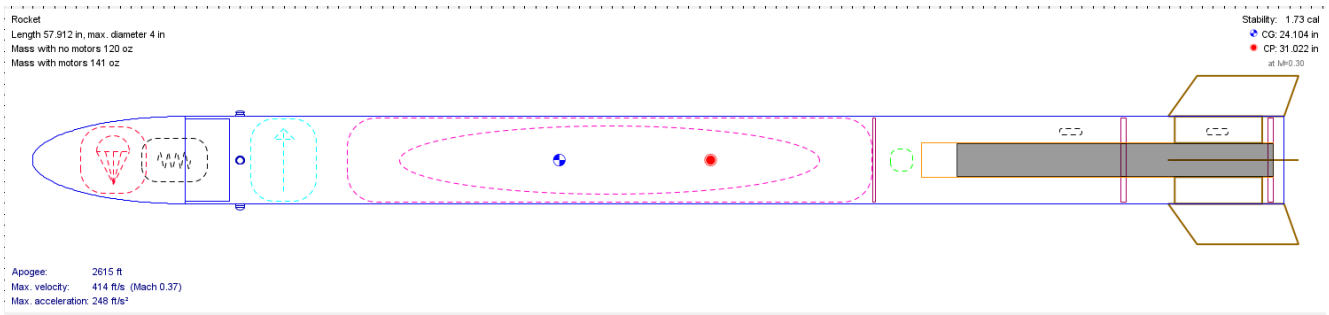

Figure 7.14 Rocket Design Geometry in OpenRocket

In order to get the best comparison between OpenRocket and MATLAB flight simulations, the same initial conditions need to be applied. Mass was measured on launch day and was identical in both simulations at 140oz. In addition, COM and Moment of Inertia were set equal in both simulations. Finally a constant wind velocity was set at 10 ft/s in the X_H direction. The general rocket design overview that was input into OpenRocket can be seen above in Figure 7.14. From the figure, several key parameters such as the Max Velocity, Apogee and Max acceleration are readily available.

```
######### Rocket Data #########
Rocket Max Altitude = 2372.76 ft
Rocket Max Velocity = 390.986 ft/s
Rocket Max Acceleration = 240.606 ft/s^2
Rocket Empty Mass = 8.46709 lbs
Rocket Time to Apogee = 12.608 s
Rocket Average Drag Coefficient = 0.5304

######### Rocket Recovery Data #########
Rocket Descent Rate = -18.1719 ft/s
Rocket Drift = 1198.82 ft
Wind Speed = 10 ft/s = 6.81818 mph

######### Rail Conditions #########
SideSlip Angle Off Rail = 9.09131 deg
>>
```

Figure 7.15 Rocket Performance Values Modeled using MATLAB

From Figure 7.14, it can be seen that MATLAB estimates are lower than OpenRocket. Max Altitude has dropped from 2616 ft to 2372 ft. Max Velocity has dropped from 414 ft/s to 390 ft/s. And Max Acceleration has dropped from 248 ft/s^2 to 240 ft/s^2. These drops in performance can be attributed to the difference in drag coefficient between models.

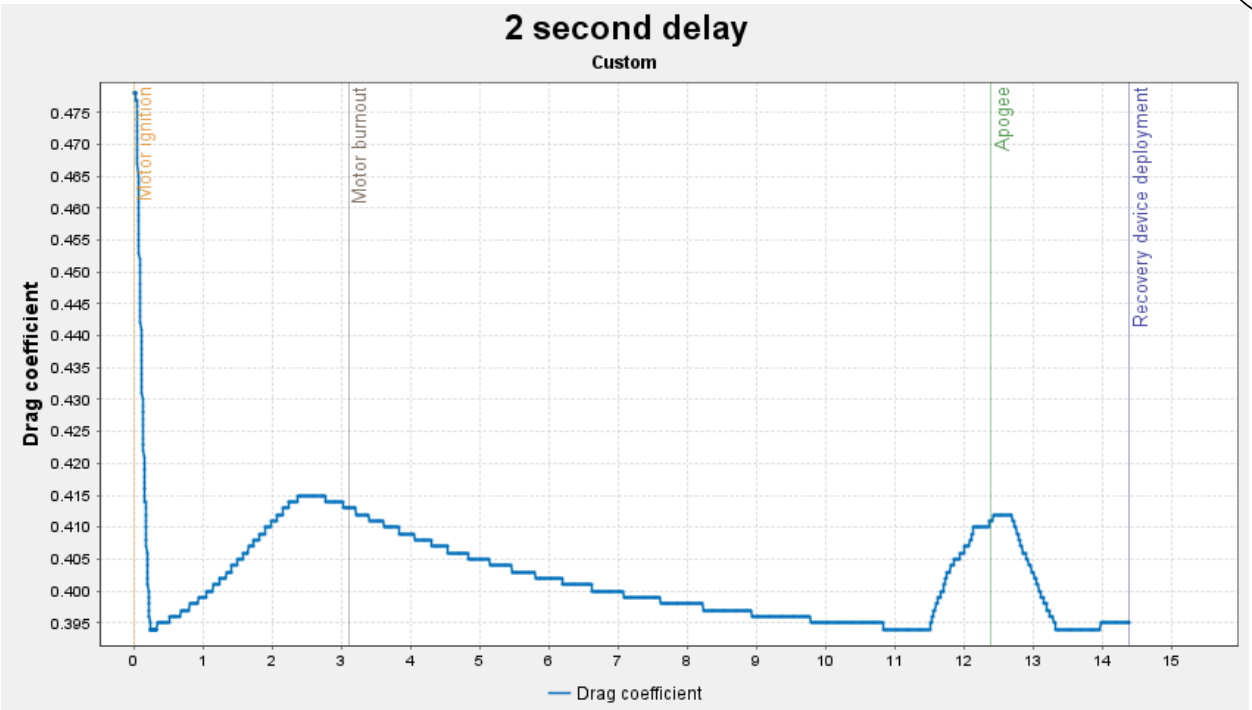

Figure 7.16 OpenRocket Drag Coefficient Plot

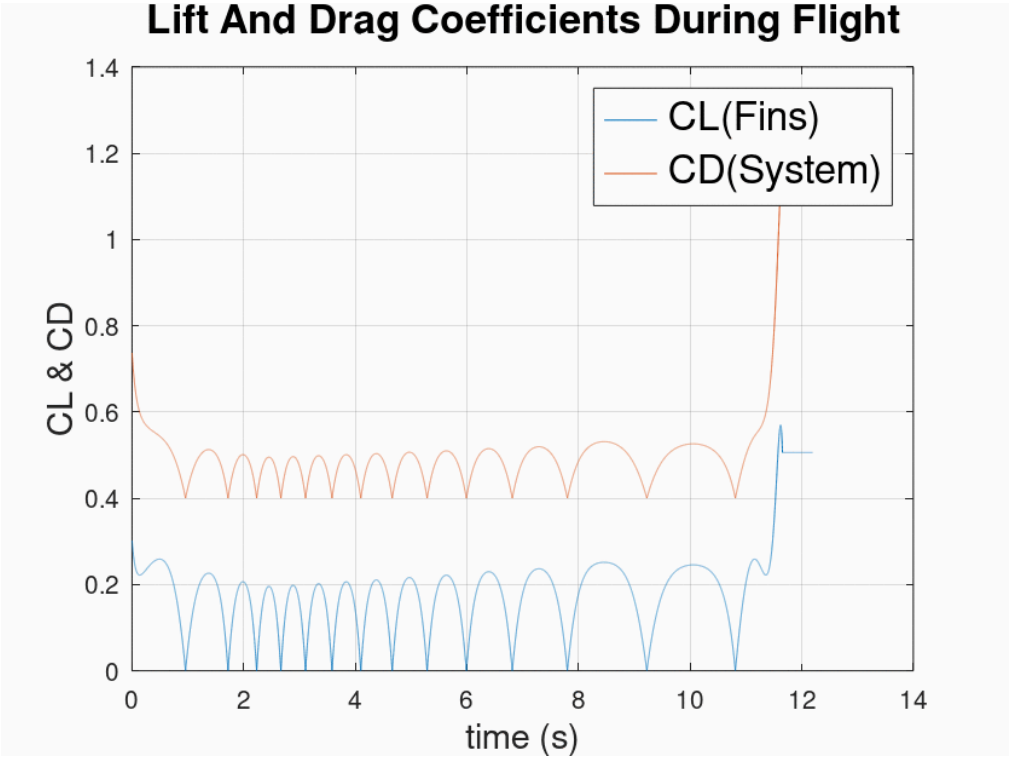

Figure 7.17 MATLAB Drag Coefficient Plot

By comparing Drag coefficient values between OpenRocket and MATLAB, (Figures 7.16 and 7.17) It can be seen that drag in OpenRocket does not oscillate compared to values from MATLAB. OpenRocket drag increases at higher velocities while MATLAB drag does not. According to OpenRocket technical documentation: “The drag coefficient scaling function is a two-part polynomial function that starts from 1 at α = 0◦ , increases to 1.3 at α = 17◦ and then decreases to zero at α = 90◦ [31]”. This scaling factor does not increase much while the rocket is at low sideslip angles, whereas drag found from CFD does.

OpenRocket also adjusts drag coefficient for velocity increase - this is the curve seen while the rocket is in powered to coasting flight. Because the rocket in this simulation is subsonic this effect was not accounted for in CFD. Averaged drag coefficient for MATLAB simulations can be seen in 7.15 at 0.53 whereas OpenRocket is around 0.412. This difference in drag coefficient is enough to drop the simulated altitude from OpenRocket to MATLAB by 250ft. However, as both simulations result in a targeted apogee larger than the requirement of 2000 ft AGL this brought confidence that requirement would be satisfied.

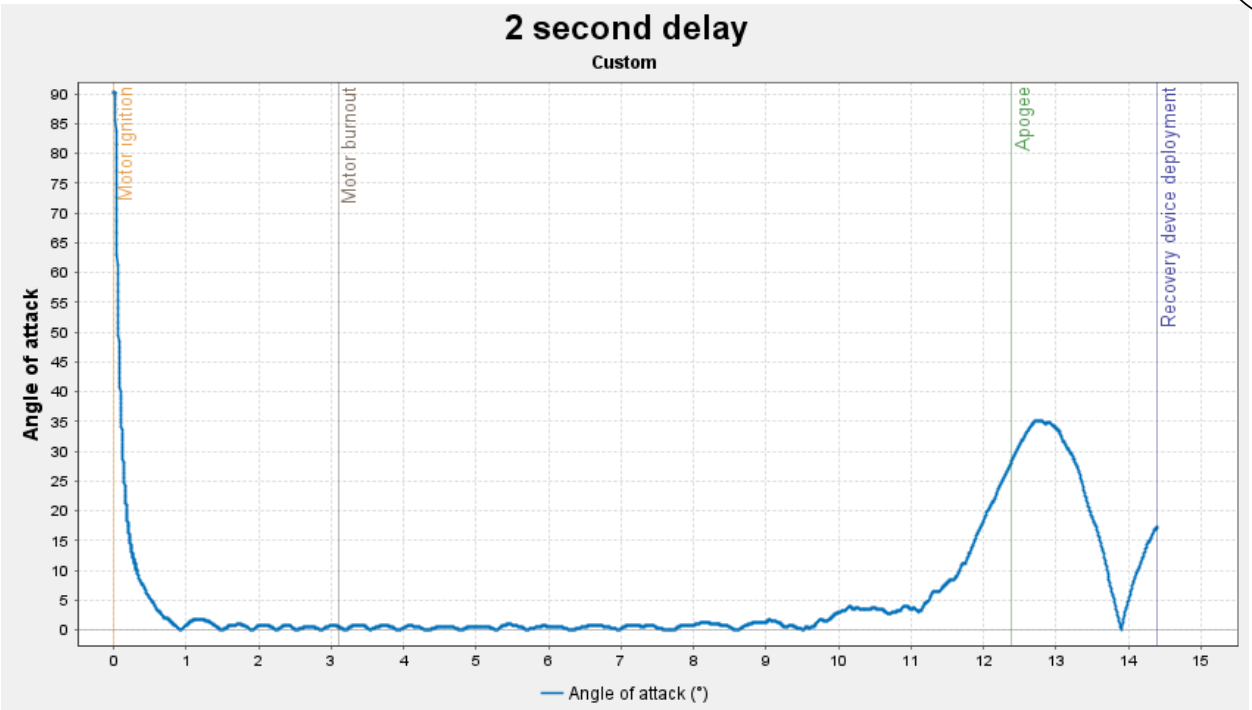

Figure 7.18 OpenRocket Angle of Attack Plot

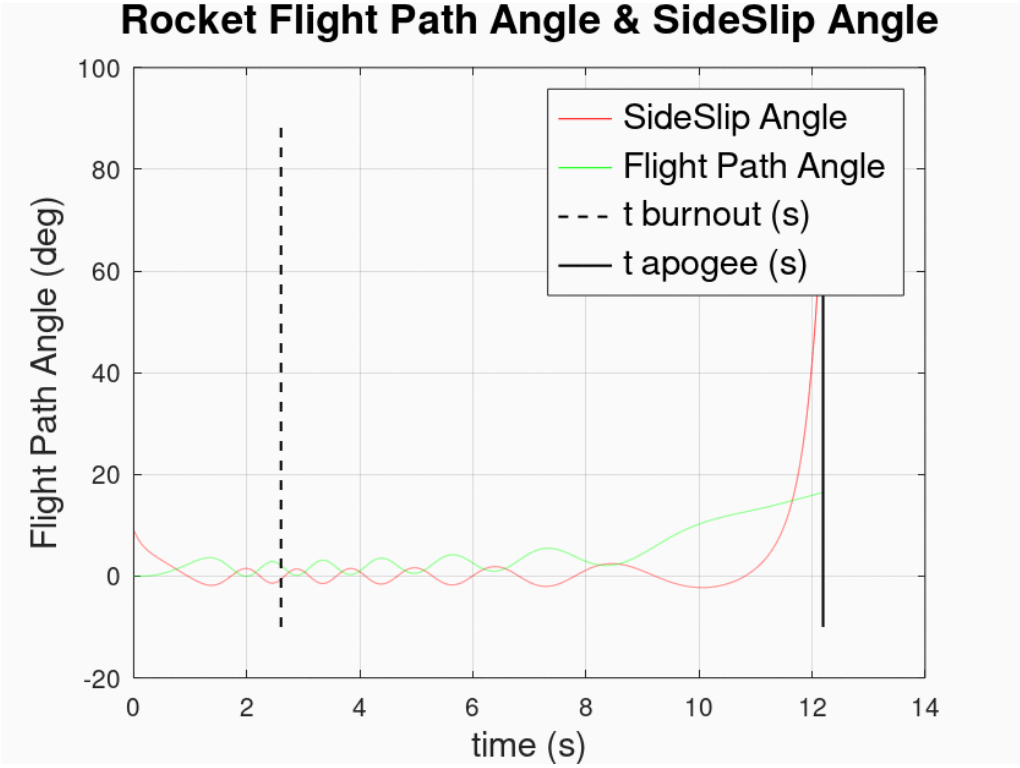

Figure 7.19 MATLAB Stability Angles Plot

The stability requirement of ($C_{m\alpha} > 0$) can be visually represented by the Angle of Attack plots in Figures 7.18 and 7.19. If ($C_{m\alpha} > 0$) stability requirement is not met, the angle of attack oscillations will increase across time steps. One key difference between OpenRocket and MATLAB angle of attack plots is that the angle of attack in OpenRocket never goes below 0°. This is because this plot is the absolute value of α, therefor the change in α can be assumed to be two times the amplitude of each oscillation here. OpenRocket α varies approximately $\pm$ 0.5°, while MATLAB α varies approximately $\pm$ 1.5°. This larger simulated α variation in MATLAB helps to explain the increase in drag coefficient. Low reduction in the amplitude of the Angle of Attack over time in MATLAB shows that the damping ratio ζ is close but below 1.0, whereas a higher reduction of Angle of Attack amplitude in OpenRocket shows that ζ is closer to 0.

In conclusion, OpenRocket simulations suggest that the rocket will weathercock significantly, whereas MATLAB simulations suggest that the rocket will not weathercock as much but not be as stable compared to OpenRocket simulations. Both simulations suggest that the rocket will achieve the target altitude so a test launch is a go.

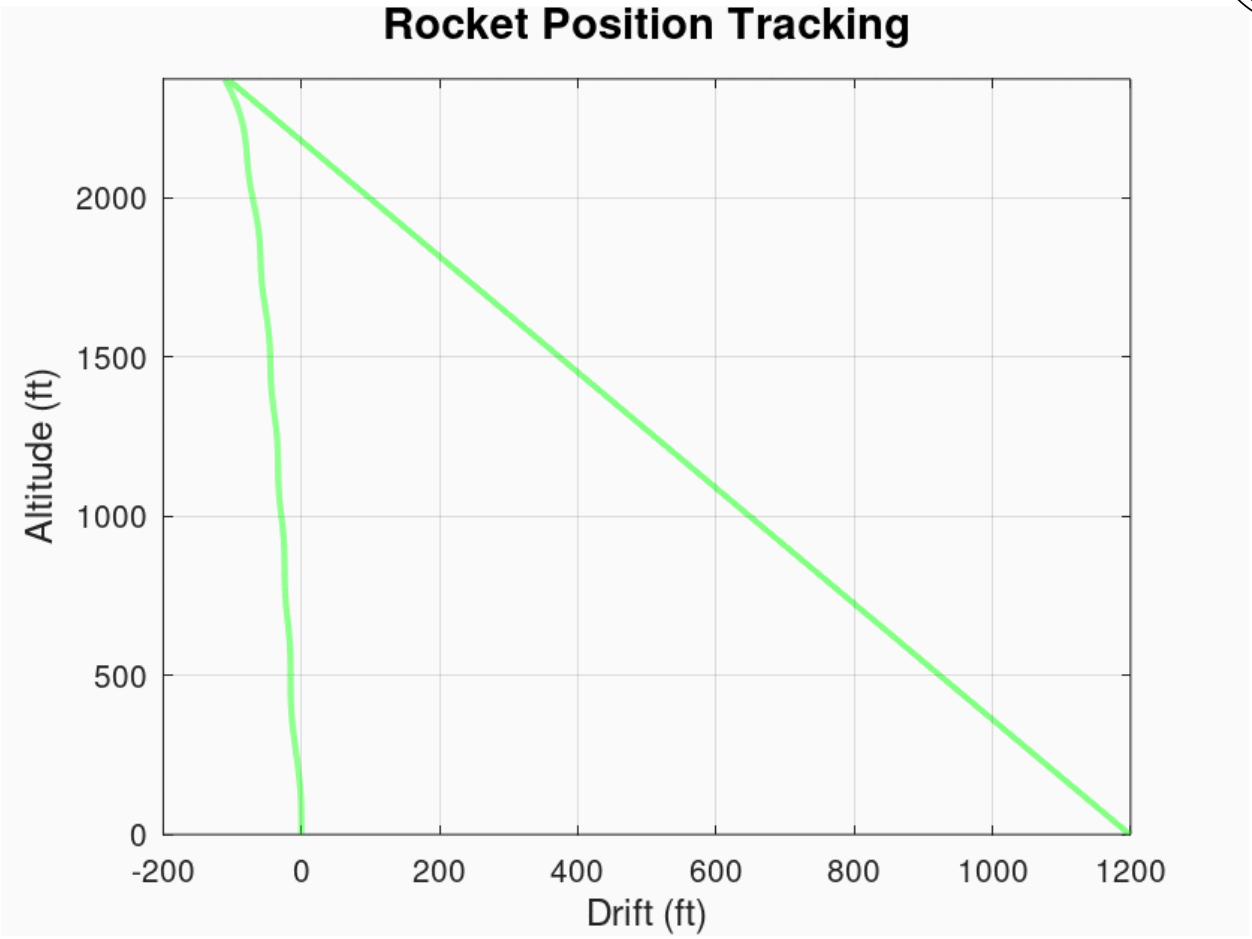

Figure 7.20 MATLAB Simulated Flight Path

7.6 Comparison with Data

One estimation that can be done to compare CFD results is Thin Airfoil Theory. Because the rocket fin is a thin flat plate with no camber, a simple estimation can be done for the delta Cp of the rocket. Here the vortex strength is plotted along the chord of the rocket defined by γ(θ). θ corresponds to a location on that line ranging from 0 at the leading edge of the fin to π at the trailing edge of the fin. α is the angle of attack of the fin (5° in this example) with a freestream velocity of 450ft/s. Using equations 7 and 8,

ΔC_p can be plotted normalized to the chord of the fin. The Results are compared and can be seen in Figure 7.21.

$$\gamma(\theta) = 2\alpha V_\infty \frac{(1+cos(\theta))}{sin(\theta)} \qquad \textit{Equation (7.22)}$$

$$\Delta C_p = 2\frac{\gamma(\theta)}{V\infty} \qquad \textit{Equation (7.23)}$$

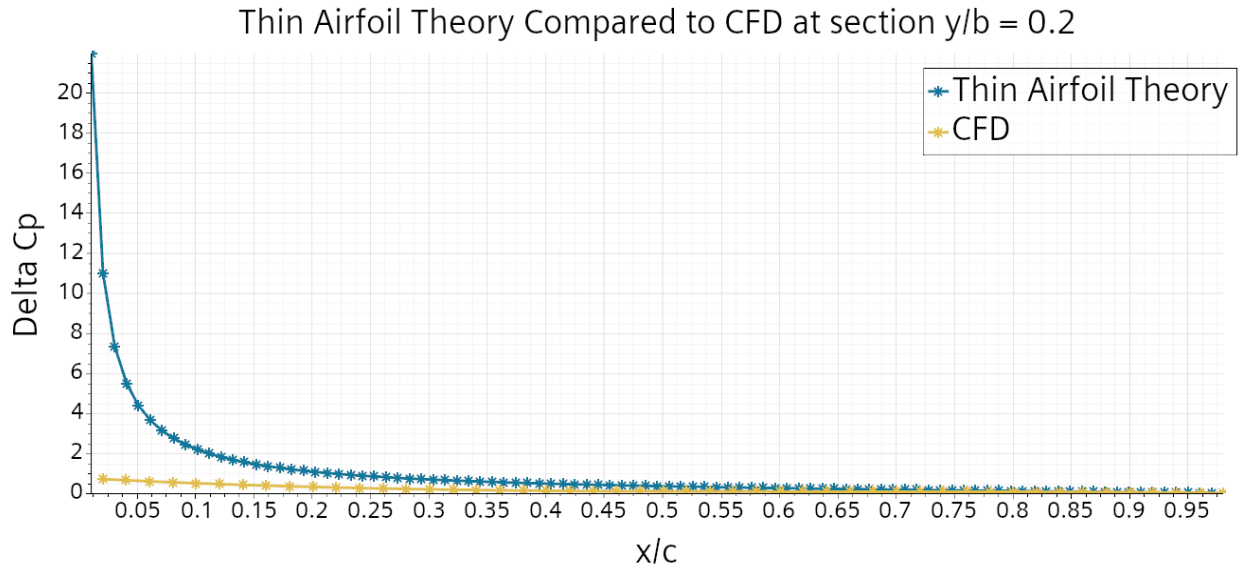

Figure 7.21 CFD results compared to Thin Airfoil Theory at Velocity of 450 ft/s with 5° Sideslip

At x/c < 0.2 thin airfoil theory does not provide a valid approximation as Cp tends to infinity, however values past this point are a better comparison. Still, thin airfoil theory provides much better results than found using CFD. At y/b = 0.2 the boundary layer created by the rocket body can create turbulence on the fin, which is not modeled in

Thin airfoil theory. Even though there is a large discrepancy between results, CFD results should be lower - this experiment increases confidence in CFD results.

Xfoil was also used to compare data to CFD, a inviscid model was used at low mach numbers and angle of attacks of 5, 10, and 15 degrees:

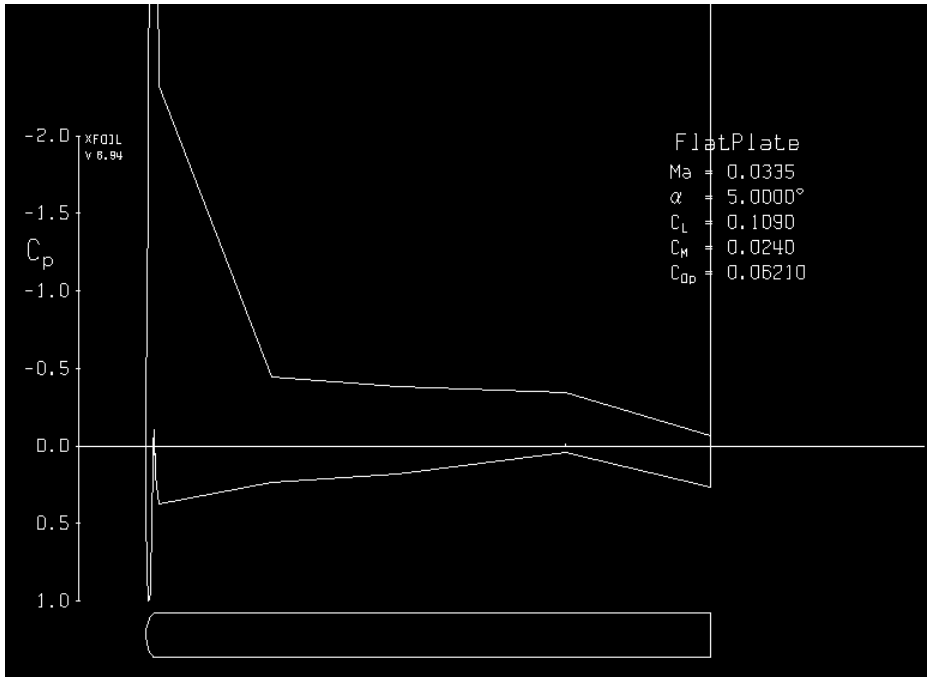

Figure 7.22 Xfoil Cp Plot and Angle of Attack 5°

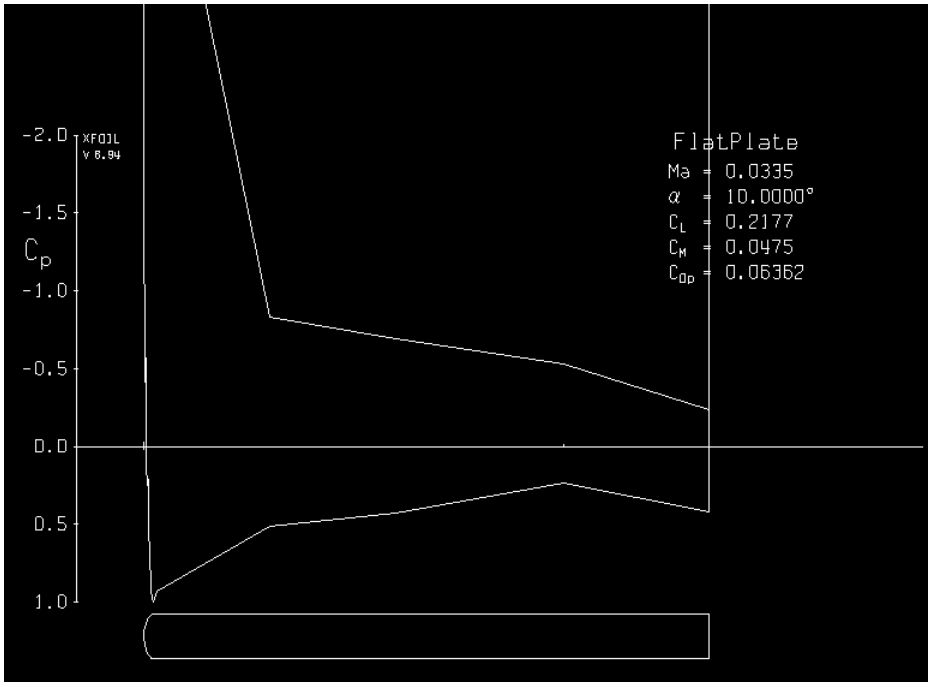

Figure 7.23 Xfoil Cp Plot and Angle of Attack 10°

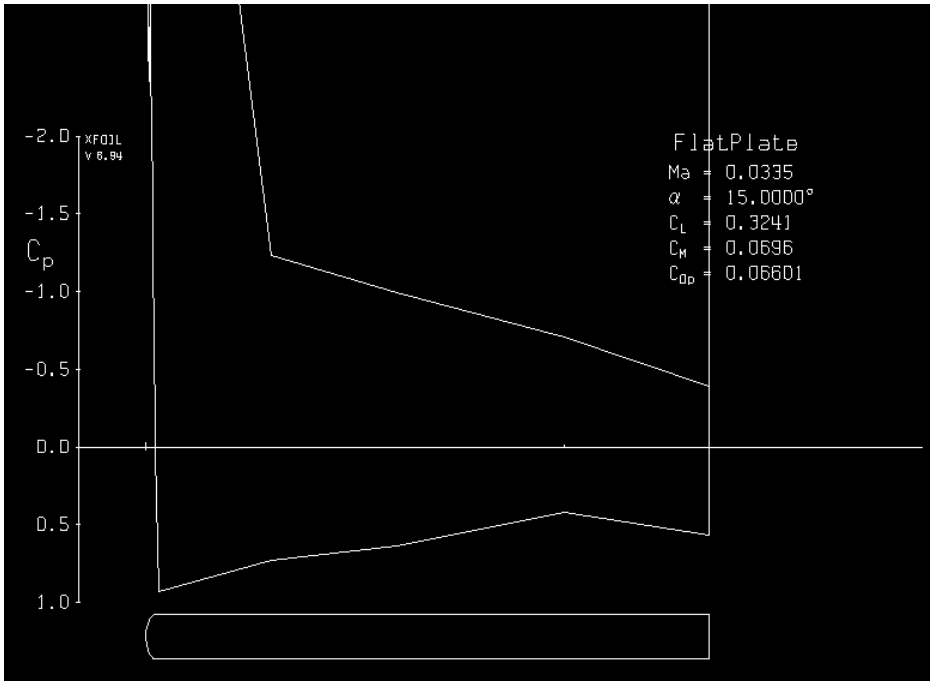

Figure 7.24 Xfoil Cp Plot and Angle of Attack 15°

At 5 degrees angle of attack, Lift coefficient percentage difference between CFD and Xfoil is 73%. At 10 degrees angle of attack, percentage difference is 49% and at 15 degrees angle of attack, percentage difference is 44%. Clearly, there is a wide margin of difference between both models. This difference has not been explored, but is a cause for uncertainty in modeling.

7.7 Finite Element Analysis

Each subcomponent of the rocket will experience unique loading conditions throughout the course of flight and recovery. The team performed FEA simulations on all the critical components of the rocket to generate numerical values for stress and deformation. These values allow us to effectively mitigate and potentially remove some of the risks aforementioned.

To get a better understanding of how dynamic pressure would affect the nose cone, an FEA analysis was performed using Ansys software. Using OpenRocket software to simulate a launch, our current model shows a maximum velocity of 354.33 ft/s. At sea level, this gives a dynamic pressure of 1.036 psi.

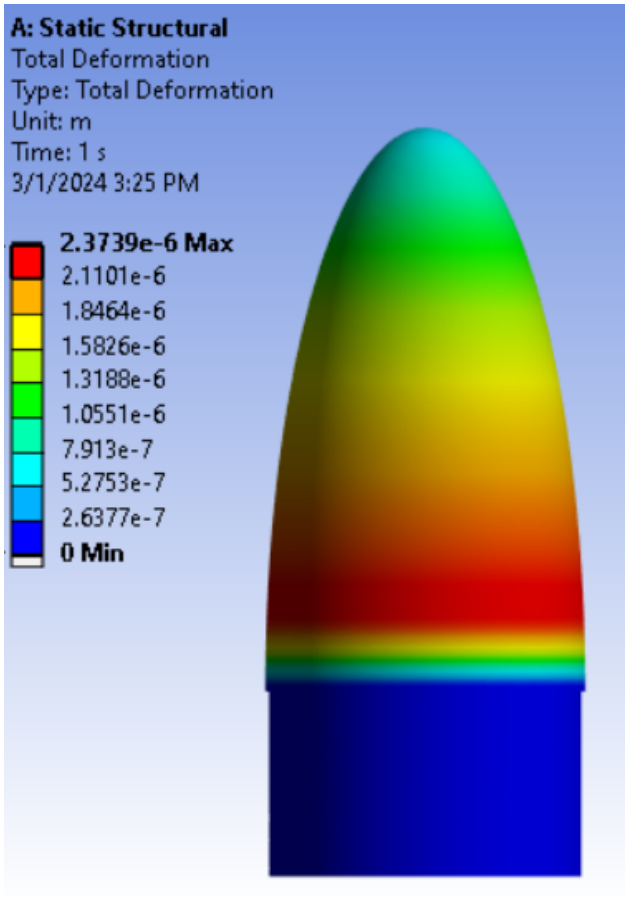

Figure xx. Dynamic Pressure analysis

The analysis shows that the maximum deformation would be 2.3739 x 10^-6 meters, or 6.49 x 10^-7 inches. The maximum equivalent stress acting on the nose cone will be 17.7 psi, while the elastic strain will be 5.3505 x 10^-5. The probability of fracture occurring during flight is minimal. The nose cone was 3-D printed and a thorough inspection was performed after printing was completed. We ensured there was consistent thickness and uniformity over the entire nose cone.

A Cessaroni I-216 rocket motor produces 85.4 lbs of thrust. The dynamic pressure acting on the fins, during flight, will be 1.036 psi. The analysis shows the total deflection of the fins, during flight, will only be 7.8187 x 10^-6 meters or 2.14 x

10^-6 inches. The maximum equivalent stress was calculated to be 1324.35 psi, while the maximum elastic strain is 0.0013044. The probability of structural damage to the fins, occurring during flight, is low.

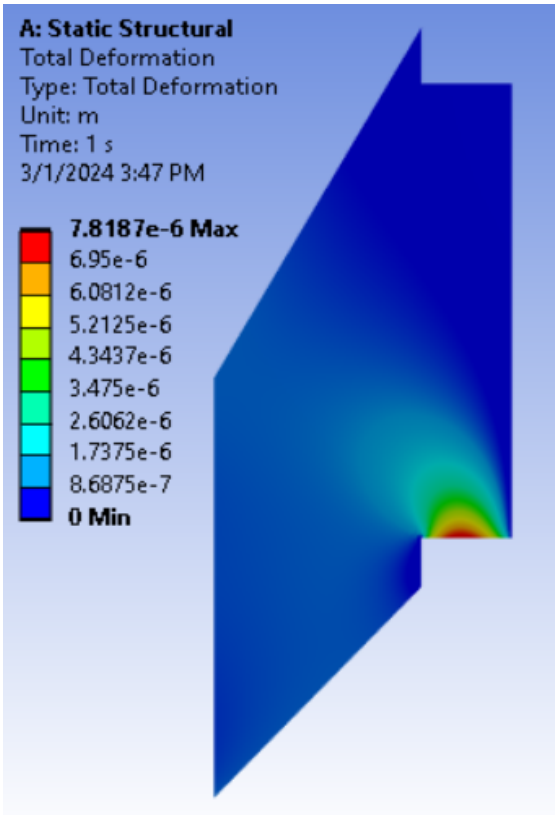

Figure xx. Maximum deflection from thrust and Dynamic Pressure

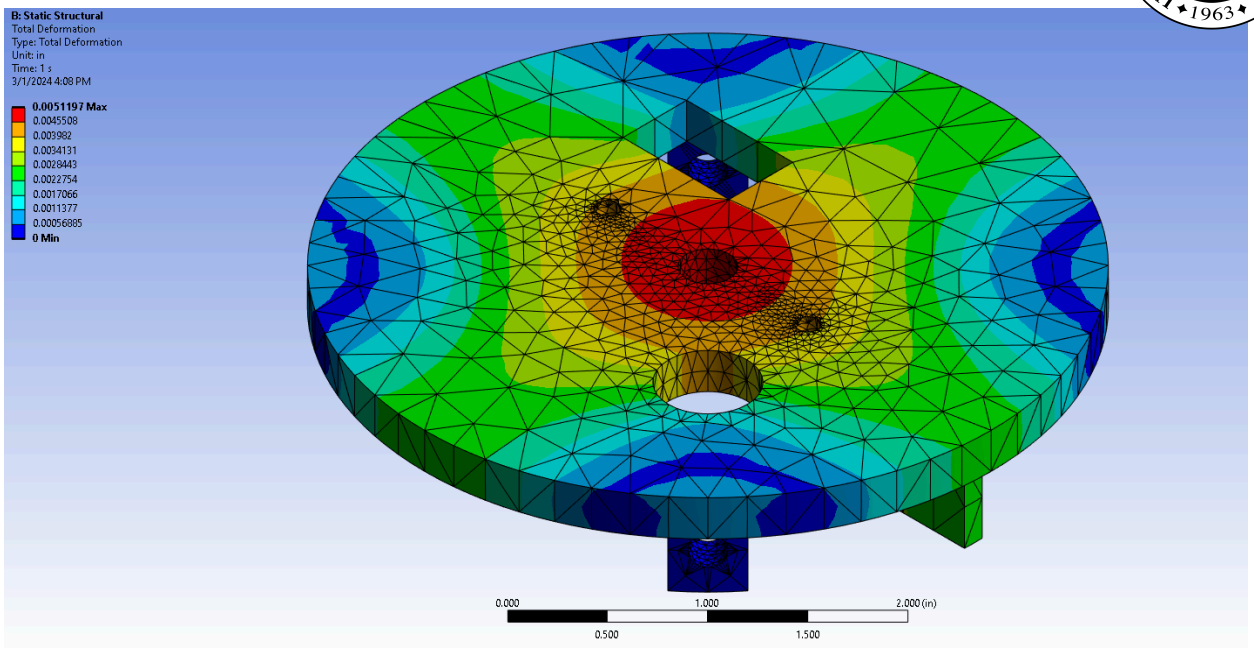

Figure xx. Total deformation of locking top from thrust

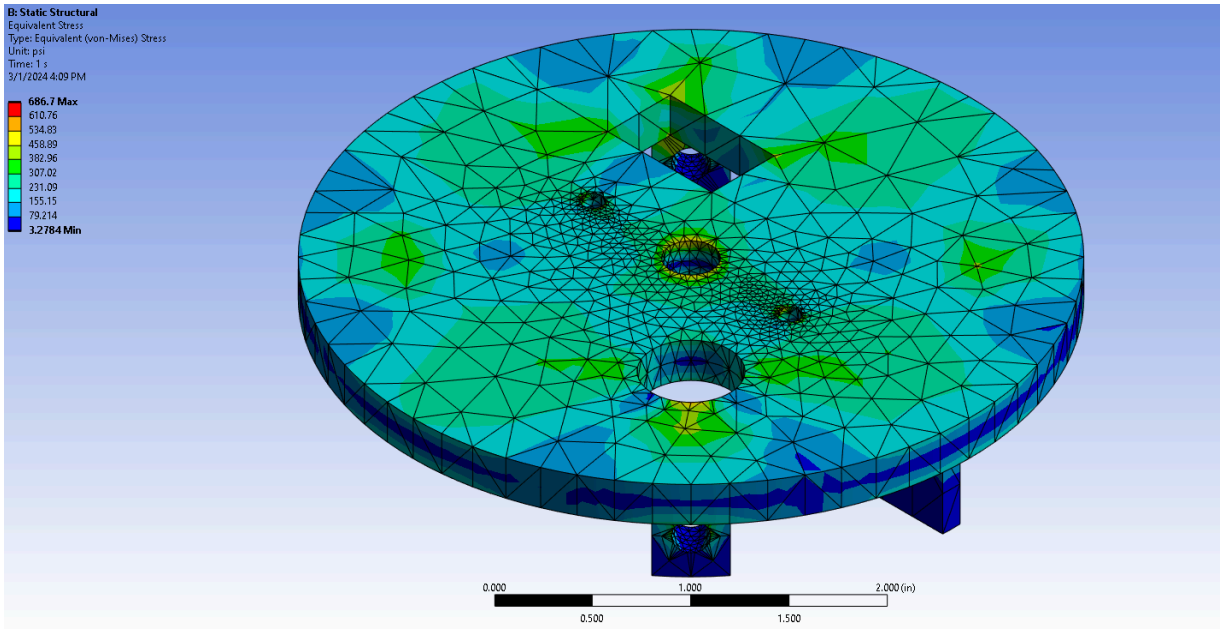

Figure xx. Total stress of locking top from thrust

The above images show that the forces acting on the top are of no concern for failure during launch and the locking top mechanism is able to withstand these

forces. With the max thrust of 85.315 lbf coming from the Cesaroni I216 motor, there will be an estimated pressure of 9.427 psi acting on the bottom of the plate. This will cause a deformation of 0.005 in. at the middle of the plate.

Another failure point for the locking top is the force upward when the parachute is deployed that will pull the locking top up. The FEA that was done on the locking top given these circumstances was also conducted and the results in the images below show that the locking top is still able to withstand the force generated by the parachute pulling up.

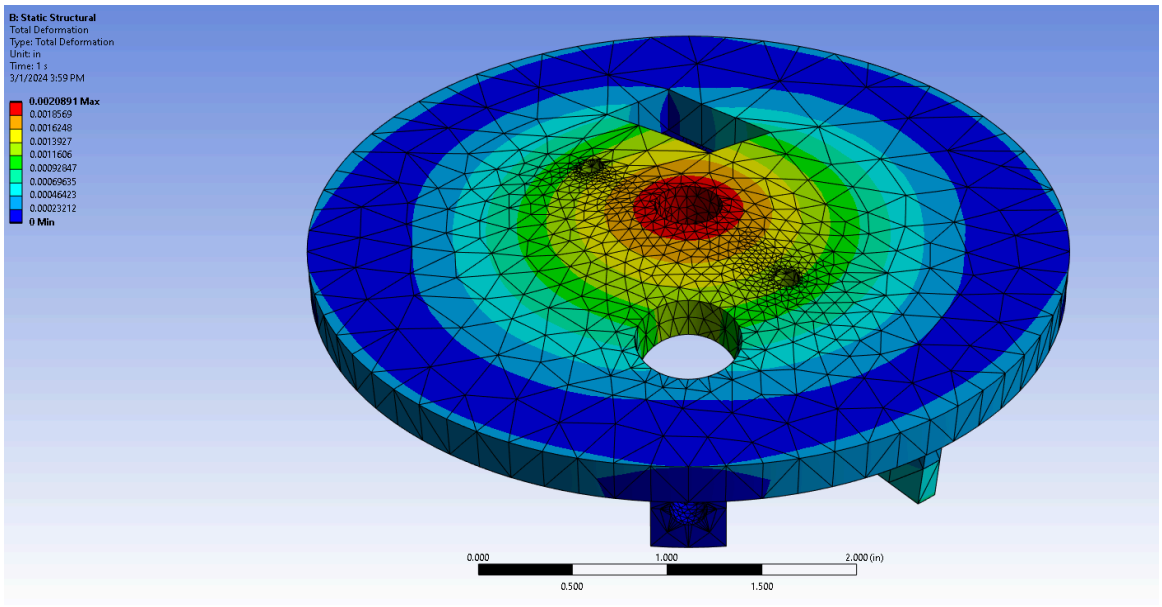

Figure xx. Total deformation of locking top from parachute

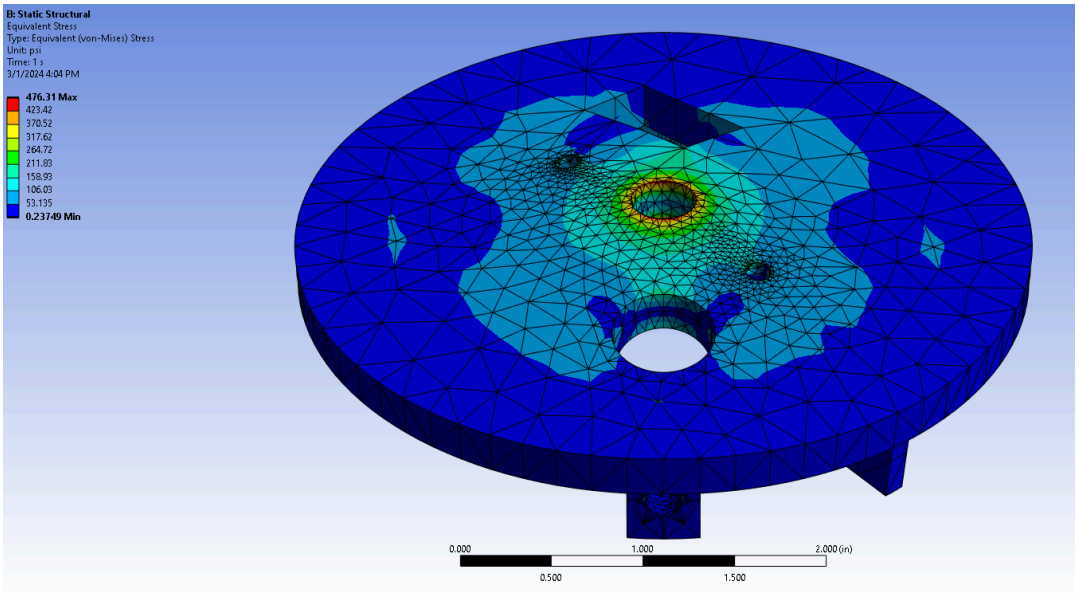

Figure xx. Total stress of locking top from parachute

The parachute pulling up on the hole at the center of the plate, which is where the I-bolt will be screwed into, causes a pressure on that hole of 37.7 psi. The analysis from Ansys is that there will be a total deformation of 0.002 in. at the center of the plate around where the bolt is pulled up at. Once again, the forces that will be acting on the plate are of no concern for failure during the flight.

The image below shows an FEA on the plate with a pressure of 185 psi, which is just under 20 times as much as is expected to be acting on the plate. This pressure results in a deformation of 0.1 in. at the center of the plate. This deformation is the maximum deformation that is acceptable in this project, but a pressure that high is extremely unexpected and thus there is high confidence in the design of the plate.

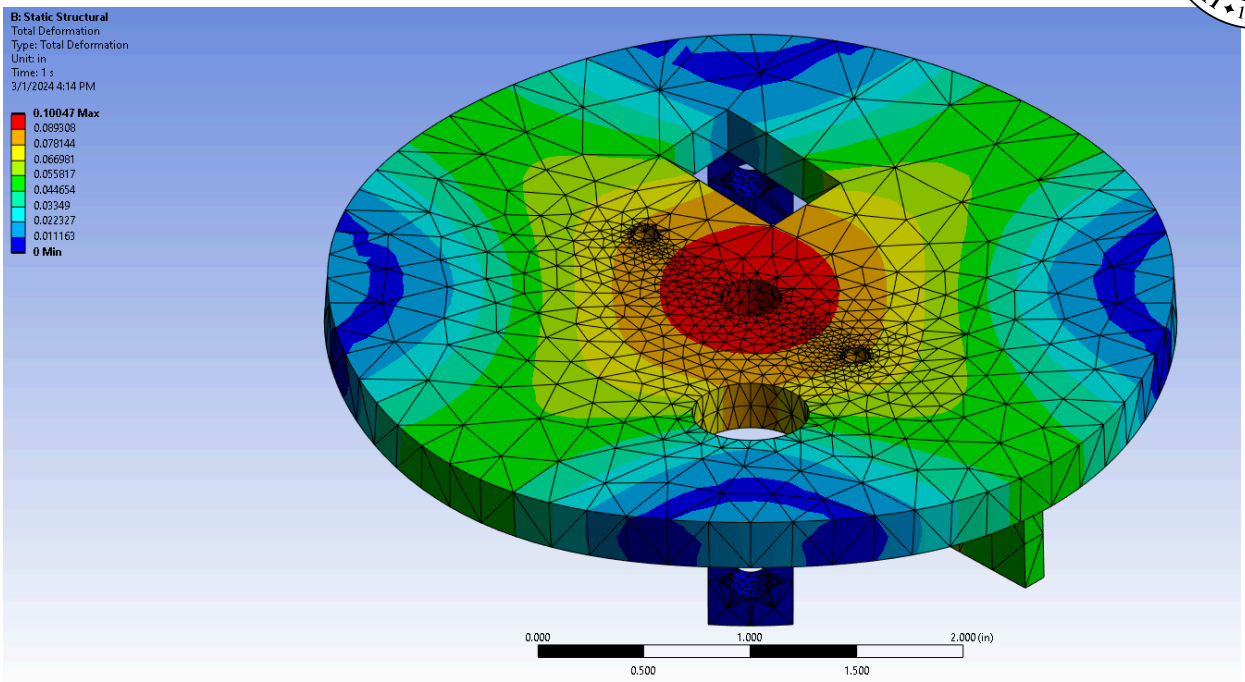

Figure xx. Max allowable deformation of 0.1 inches

The initial launch of the rocket on March 16 helped validate our analysis of the above pieces and showed that they could withstand the forces experienced by the rocket during flight, even when the flight did not go as intended. The polycarbonate material utilized to manufacture these parts proved to be strong enough and is the material that will be utilized moving forward to the final launch of the rocket.

8 Final Design and Engineering Specifications

Overall Rocket:

The final rocket assembly is shown below assembled in Solidworks and details all of the major components of our rocket.

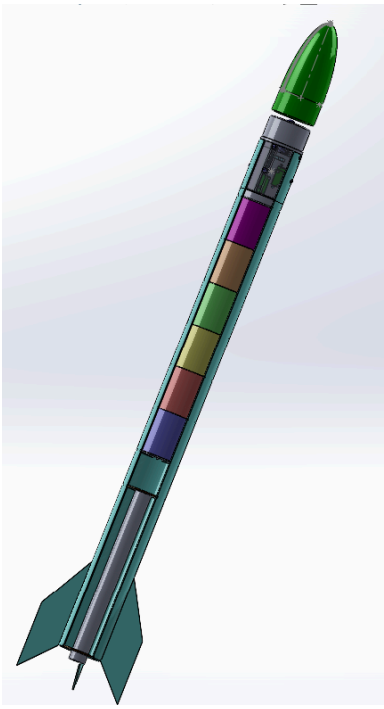

Figure 8.1 Rocket Assembly

Nose Cone:

The nose cone was 3-D printed in a polycarbonate material. As can be seen in figure 8.3 we had some design restrictions due to our manufacturing choice. The max height that the 3-D printer could print was 9.2”. So we had to balance the shoulder height selection with nose cone height which can affect the overall stability of the rocket. Ultimately we chose to make the shoulder of the nose cone 2” and the nose cone length 7”.

Figure 8.2 Nose Cone

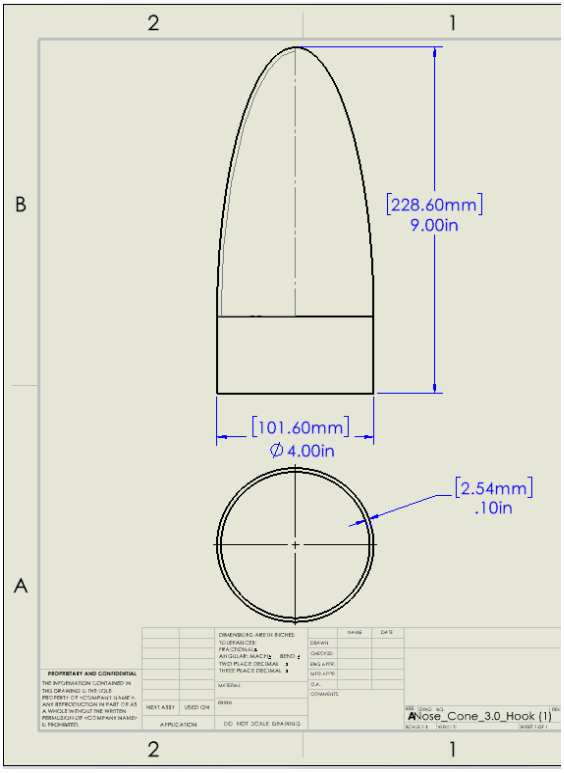

Figure 8.3 Nose Cone Drawing

Avionics Bay:

The entire avionics bay was 3-D printed in a polycarbonate material. Some key design parameters to consider were the restriction of the diameter or width to 3.9” to accommodate the inside diameter of the body tube. We also designed the avionics bay to not impede on the inside volume of the nose cone and the body tube so there was enough space to store the parachute and payload. This was achieved by designing and manufacturing a coupler product that could give the nose cone the space it needed for parachute storage and still store the avionics bay in the body tube. Using an additive manufacturing resource allowed us to complete the production of these products within 1 day while keeping the cost very low. The average cost per print was in the range of $3 - $4 depending on the infill percentages of the design.

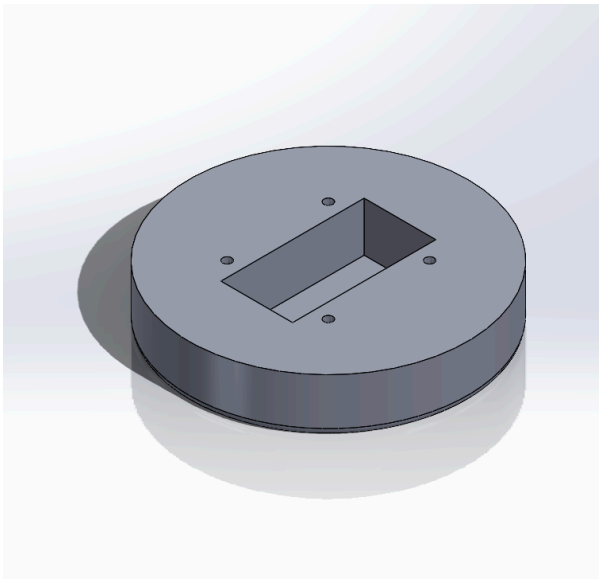

Figure 8.4 Battery Pack

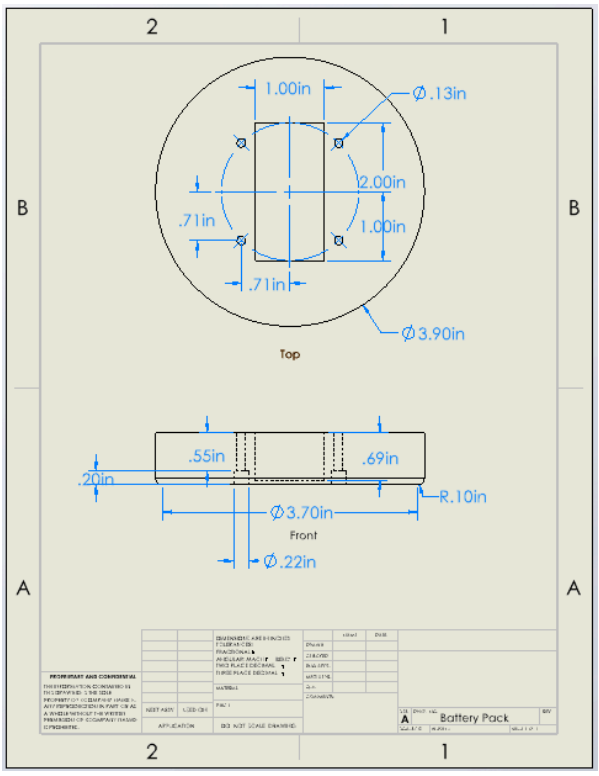

Figure 8.5 Battery Pack Drawing

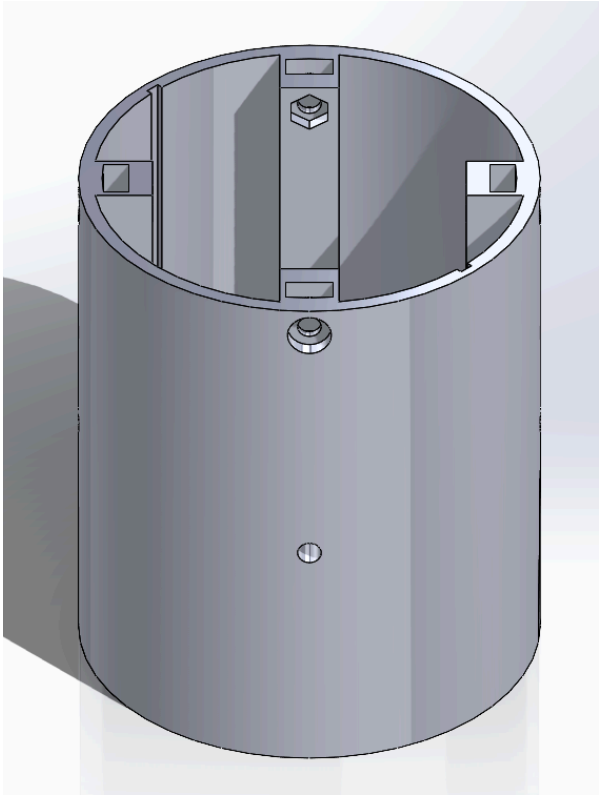

Figure 8.6 Avionics Cylinder

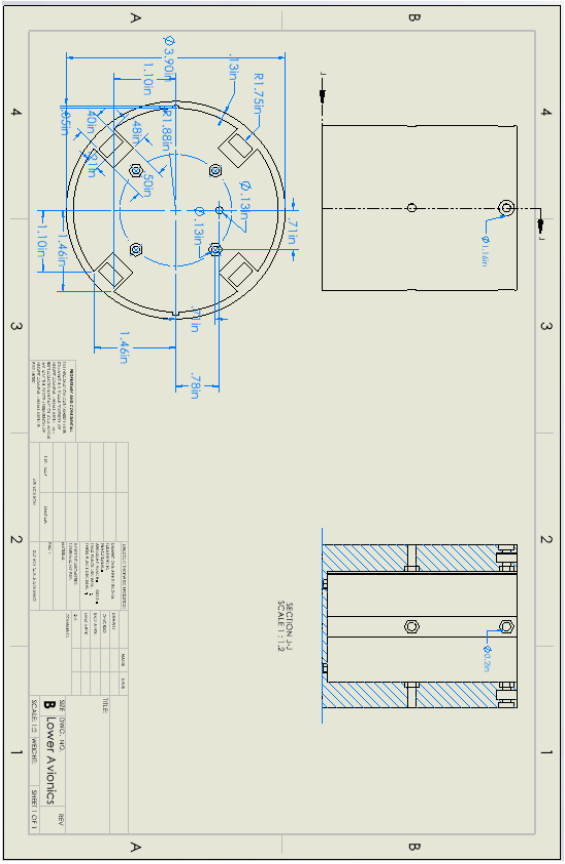

Figure 8.7 Avionics Cylinder Drawing

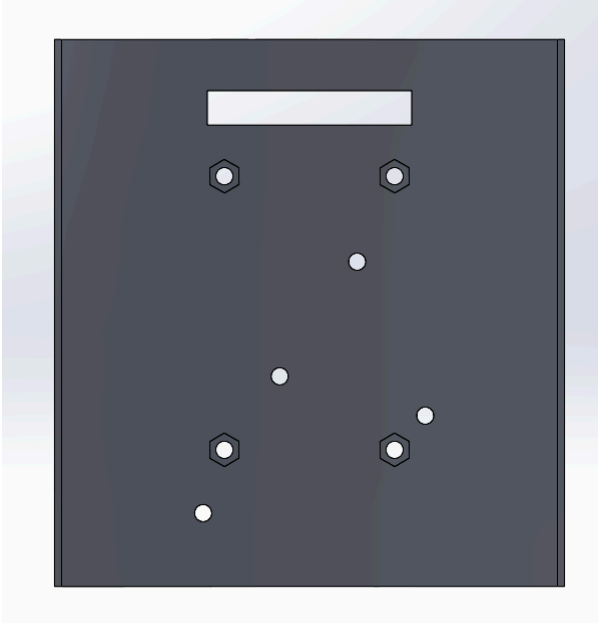

Figure 8.8 Avionics Board

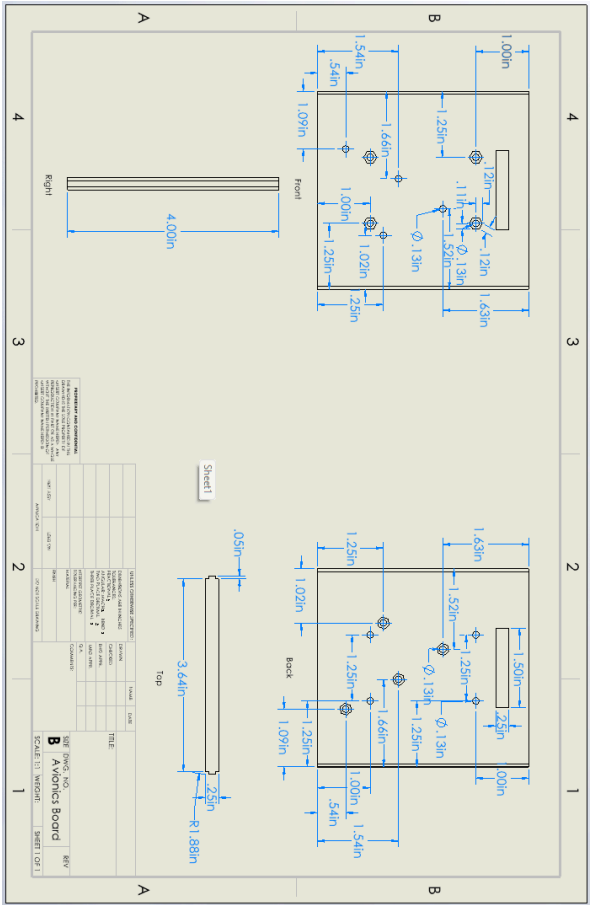

Figure 8.9 Avionics Board Drawing

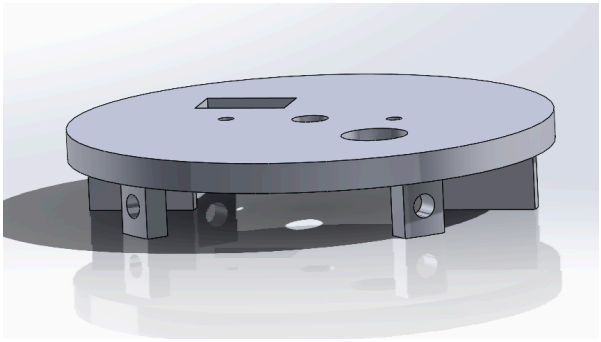

Figure 8.10 Coupler

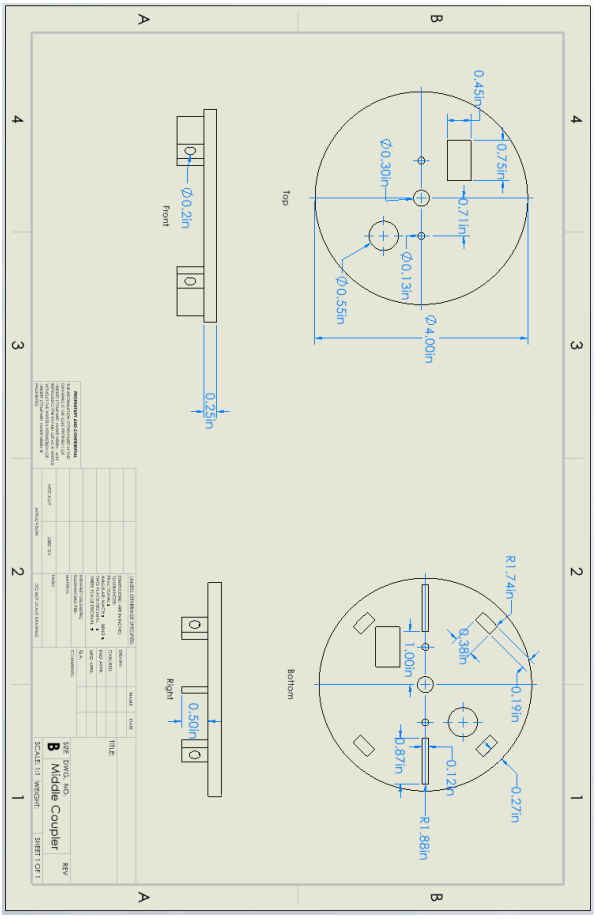

Figure 8.11 Coupler Drawing

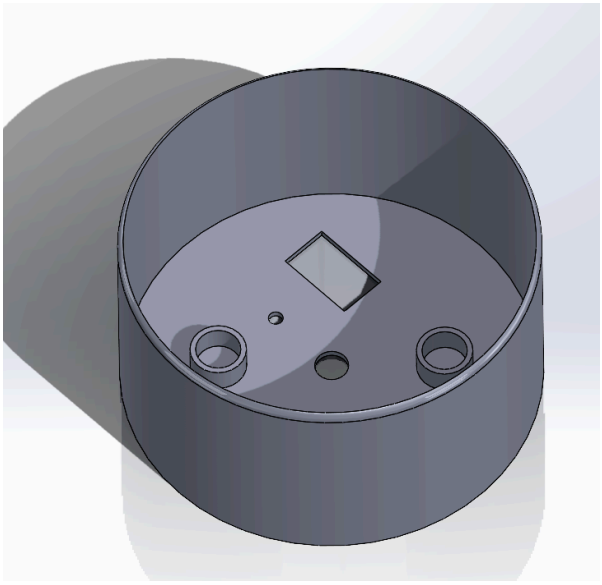

Figure 8.12 Avionics Upper

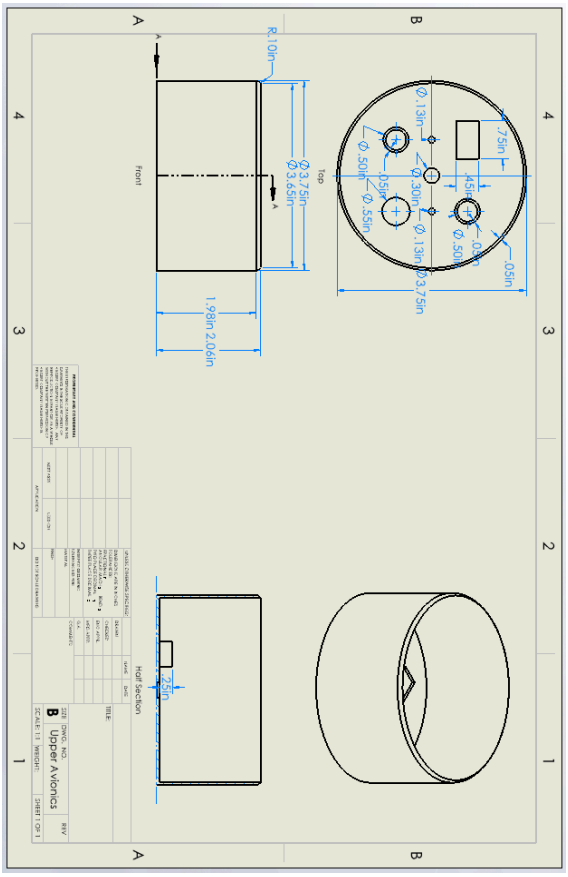

Figure 8.13 Avionics Upper Drawing

Centering Rings:

The centering rings we originally used were ⅛” thick made from balsa wood. After experiencing centering failure during our first launch we realized the balsa wood did not have the structural integrity we needed to hold the motor in place. After realizing this we switched over to quart inch thick pine centering rings that had a much higher strength.

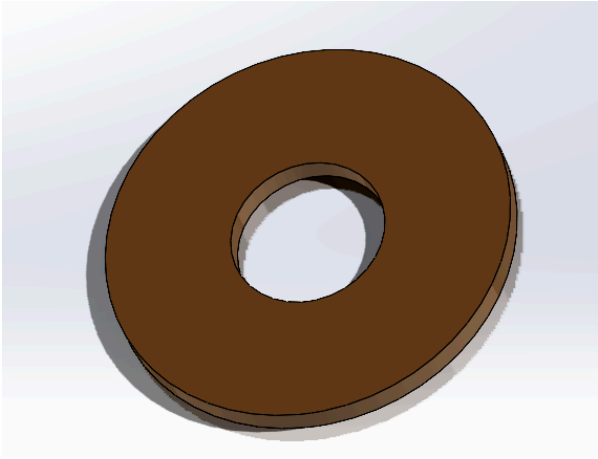

Figure 8.14 Centering Rings

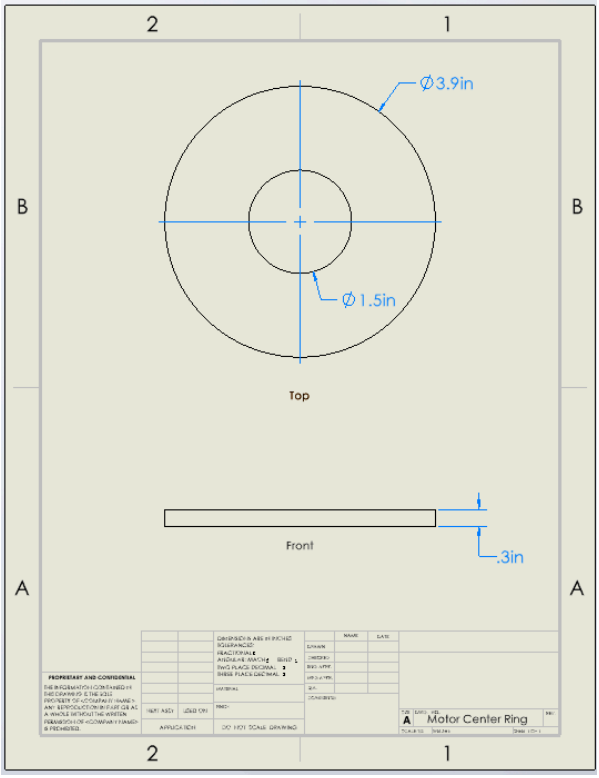

Figure 8.15 Centering Rings Drawing

Fins:

The fins of the rocket were made from ⅛” thick made from balsa wood. The balsa wood was used for the test launch and the final launch. The fin geometry was a mixture of trapezoidal and free form to try to get the max stability for the rocket.

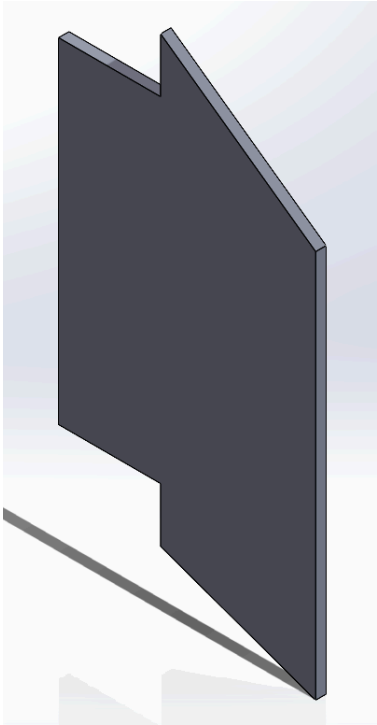

Figure 8.16 Fins

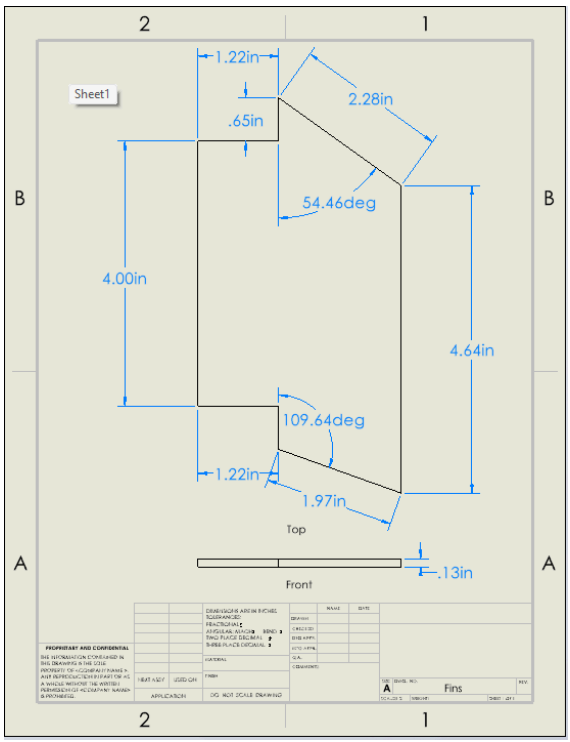

Figure 8.17 Fins Drawing

Parachute:

Initially we started with a 58” parachute to lower the descent rate of the rocket for max protection of the eggs. Due to the parachute taking up too much room and the shroud lines sticking together we decided to go with a 36” parachute once we realized the eggs could survive a much higher descent rate than initially anticipated. The 36” parachute has 8 Mil-C5040 type IA shroud lines, a 3” apex vent, a 1.9-oz rip stop nylon, and a drag coefficient of 1.3.

The final payload design was simplified to consist of EVA form, plastic wrap, and a bottom set plate. Initially the design was to use a rail system to securely fasten

the payload into the rocket. This design only allowed for 2 eggs to be placed within every 4 in of form resulting in a total of 12 eggs. However, after further discussion on the practical usage of the rail system it was decided to scrap the rails and instead use 3.8 in diameter foam pucks that encased 2 eggs every 2 in. As seen in *Table 10.1 in version 3*, this allowed us to effectively double the payload carrying size compared to version 1 and more efficiently use the space dedicated to the payload. Removing the rail system also decreased weight while increasing protective ability. From initial payload testing the EVA pucks were about to successfully protect eggs in free fall from a height of 48 ft. Giving us confidence in removing the rail system and adding more foam for simplicity and protection. The plastic wrap was added as a way to firmly package each individual puck as one payload system. Adding a makeshift handle made of duct tape at the top made removal of the pucks extremely easy and most importantly safely without damage.

Figure 8.18 Prototype Payload Bay

Rocket Payload Configuration and Sizing				
Total Height (in)	24			
Rocket Radius (in)	1.85			
Total Payload Volume (in^3)	516.1008411			
Egg Max Radius (in)	0.78			
Egg Length (in)	2.25			
Egg Volume (in^3)	5.734034911			
Version 1				
Stack Height (in)	4		*Version 3*	
# of Eggs Per Stack	2		Stack Height _1 (in)	1.5
# of Stacks	6		Stack Height _2 (in)	2
Total # of Eggs	12		End-Caps (in)	1.5
Volumetric Efficiency	0.1333235939		# of Eggs Per Stack	2
			# of Stacks (_1 + _2)	6
Version 2			Total # of Eggs	24
Stack Height (in)	2		Volumetric Efficiency	0.2666471877
End-Caps (in)	2		Percentage Increase (%)	**20**
# of Eggs Per Stack	2			
# of Stacks	10			
Total # of Eggs	20			
Volumetric Efficiency	0.2222059898			
Percentage Increase (%)	**66.66666667**			

Table 10.1 Payload Efficiency

Each Puck had two semi spherical sections carved out on the top and bottom using a make-shift drill that consisted of a golf ball attached to a drill bit see in *figure 8.2*.

Figure 8.19 Egg Drill Bit

9 System Evaluation

9.1 Test Flight and Post Flight Evaluation

A test flight was performed after all of the above analysis was completed and a version 1 of the rocket was manufactured. The test flight was semi successful as the avionics did not record the apogee height, the GPS tracker switched off during flight, the parachute did not inflate properly and the motor mount failed. With all these points of failure 1 out of 24 eggs flown survived, which stands as a testament to the payload bay design. Figure 9.1.1 below shows the damage done to the rocket and payload after recovery.

Figure 9.1.1 - Damage done

The image on the left shows the underside of the rocket where the nozzle should be extruding from the bottom. As shown the nozzle and motor have been pushed into

the rocket causing the upper two sets of centering rings, and the lower set plate to be destroyed. Luckily the strength of our payload locking mechanism held the motor inside the rocket, however the lower section of the payload was destroyed due to the thrust of the motor and the instability occurring during flight, this damage is shown in the left image of figure 9.1.1. This failure was caused from poor adhesion in the motor mount. The original design of the motor mount had the aluminum motor casing directly adhered to the centering rings with high strength epoxy. Although the results of motor mount FEA simulations showed that the load on the rings was less than the adhesion strength of the epoxy, that data was assuming perfect adhesion between the components. As the team has learned that was not the case with the material selections. The motor mount will need to undergo a redesign before the next launch.

Another failure point during the test launch was the recovery system. After apogee the parachute failed to inflate. This failure is primarily due to the parachute being too large and packed too tightly into the given area. Another cause of the failure was the parachute material. The shroud lines of the parachute stuck together like velcro and did not allow the parachute to properly inflate. These failures caused the rocket to fall nose first from approximately 1800 feet (although not verified on this flight) leading to the upper portion of the payload to be destroyed as shown in the right image of figure 9.1.1. The fix to correct this failure point is to switch to a smaller parachute with thicker shroud lines. Although this will increase the velocity at which the rocket lands, we know from payload testing the payload will survive the higher velocity at impact.

The final failure point came from the avionics system. The altimeter failed to store any useful flight data and the GPS tracking unit switched off after the rocket left the pad.

The failed data storage was caused by user error. Upon recovery the avionics system was powered off before the data could be transmitted through the Featherweight UI app. This was unfortunate but it is a simple fix to correct the failure point. The vibrations that occur during takeoff slide the on/off switch on the tracking unit powering of the tracking capabilities. This can be reminded by simply tapping the power switch in the “on” position.

Altogether, the team was impressed that one of the 24 eggs were able to survive this initial launch. With the rocket striking the ground nose first at a high velocity and the motor smashing into the pucks in the back, the payload bay design was still able to provide enough protection for one egg in the middle of the stack. If the previous failure points mentioned above are able to be fixed - There is a high likelihood of returning most if not all 24 eggs intact.

9.2 Further Evaluation

After the initial test flight the lower end of the rocket needed to be cleaned, evaluated, and prepared before the final flight. Figure 9.2.1 below shows the internal damage after the lower most centering ring was removed.

Figure 9.2.1 - Disassembled rocket lower

Focusing on the left image in the figure above the remnants of the middle centering ring can still be seen. This damage profile leads us to believe that the motor casing slid through the centering rings and as the motor accelerated it bounced around inside the body tube, destroying the middle and upper centering rings, and the lower set plate. The image on the right of figure 9.2.1 shows the only external damage on the body and this is easily repaired with epoxy and sanding.

Figure 9.2.2 - Cleaned rocket lower

Figure 9.2.2 shows the body tube after the remnants of the centering rings and fins have been removed. This cleaning process was done utilizing a dremel and a drill with a wheel sander attachment. These tools allowed for the complete removal of the balsa wood remnants and any scrambled eggs left over from the test flight. This is the starting point for the lower end of the rocket to be rebuilt.

9.3 Final Flight

The final launch of this rocket was April 20th, 2024 marking approximately 7 months since the start of the project. Before final flight the motor mount was redesigned, the parachute was changed, and more hands-on experience with the avionics was obtained. The changes we made for the new motor mount and the size reduction of the parachute offset each other and the overall mass of our rocket was approximately the same as the initial test flight, meaning the target apogee and the avionics settings remained unchanged.

The figures below show the first 3 stages of the flight captured on video.

Figure 9.3.1 - Leaving pad

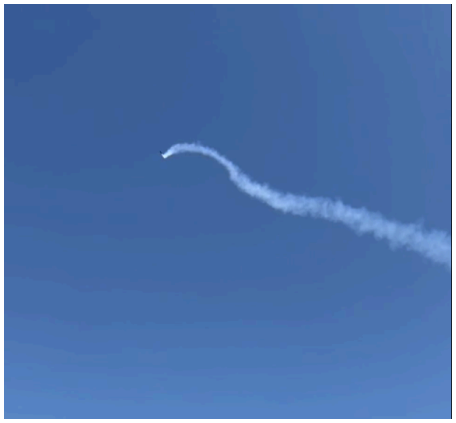

Figure 9.3.2 - Begins to corkscrew

Figure 9.3.3 - Flattens out

As Shown in figure 9.3.1 the rocket leaves the pad unstable and begins to head northwest with an approximate 45° angle of attack. Figure 9.3.2 shows the rocket beginning to corkscrew, similar to the test flight. Unlike the test flight however, this corkscrew begins much later in the flight. Figure 9.3.3 shows the rocket's path does flatten out after three corkscrews. The path flattens out after the burn time of the motor is complete suggesting that another motor mount issue occurred on this flight attempt. Not shown in the videos taken is the avionics activating. The avionics gave a live flight altitude reading of approximately 1200 feet and separated the rocket shortly after. The parachute successfully deployed and inflated, however, due to the trajectory of the rocket when the parachute inflated the connection point to the shock cord failed and the parachute separated from the rest of the rocket causing the rocket to continue on its flight path while the parachute drifted on its own. The GPS tracker installed in the avionics displayed the location of the rocket in the app; however, the area was dense with trees, tall grass, and various other brush. A redundant "screamer" was installed

before flight but it separated from the rocket sometime during the back half of the flight, likely on impact.

Figure 9.3.4 - Debris map

Figure 9.3.4 shows the locations of a few important points. The red circle in the bottom right is the approximate launch site. The blue circle on the left is the approximate location of the rocket shown by the GPS tracker. The orange and green circles are the locations of the debris found from our rocket. The orange circle is the approximate location of where the “screamer” was found and the green circle is the approximate location of where a burnt up black powder charge was found with our signature blue latex glove packing.

Unfortunately after many hours of searching, the rocket was unable to be recovered so it is unknown if any eggs survived this flight. With that said the how and why the flight failed is all speculation and estimated based on the footage taken. The

most likely causes for the failed flight are low velocity off the rail, motor mount failure, and a parachute connection point not designed for sideways deployment.

10 Significant Accomplishments and Open Issues

As of March 18th, the first fully functional build of our product was successfully manufactured and assembled. To get to this point, multiple manufacturing processes had to be refined and prototyped in order to ensure the final build would fit together as designed. As well as tests of proper folding techniques for parachutes and black powder charges. Some of the bigger manufacturing issues was the creation of the fin slits on the body, assembly of the avionics bay and nose cone, as well as placement of centering rings within the tube.

Accomplishments

One of the first major accomplishments was the assembly and functions check of the avionics bay and nose cone. The avionics bay acts as the brain of the rocket and therefore carries high importance and with that importance came weight. Besides the payload and motor the avionics bay was the heaviest component. The avionics bay came in 3 separate parts. From top to body we have the coupler, then the housing group for the Blue Raven, and finally the battery storage. These 3 parts were 3D printed then assembled via glue and screws. With the assembly of these 3 parts complete it was then time to smooth out any contact surfaces that prevented a smooth fit. This took the team approximately a total of 3 hours to complete and securely fit within the body tube and nose cone.

Figure 10.1 Avionics Bay Assembly

Figure 10.2 Avionics Bay Assembly

The next major accomplishment for the build was the alignment of the fin slits on the tube. The fin slits are where the shoulder of the fin will be placed and glued to in order to stabilize the rocket. Due to the importance of a stable flight the multiple methods of cutting the slits out were discussed and compared to determine the most accurate method of manufacturing. In the end we decided to use our fin jig, a device used to help hold the fins in place while the epoxy dries, was used to mark the specific location and width of each fin slit. As a result of careful analysis and comparison of

alignment methods the fin slits were spaced evenly and fit firmly against the body. To avoid this delay again for future builds a secondary fin jig will be printed that will help align the fin slit placement.

Figure 10.3 Fin slits

Another major assembly milestone was the placement and design of the centering rings. Upon the cutting of the balsa wood centering rings the team felt uneasy about how easy it was to bend the rings. To strengthen the rings without increasing the weight, it was decided to double the thickness of each ring by stacking another ¼” ring on top. Making sure to offset the placement by 90 degrees in order to have the wood fibers alignment be perpendicular to one another. This greatly increased the strength while still remaining extremely light in weight. Once the rings were improved the placement within the rocket was at first challenging due to limited space and visibility to properly apply any adhesive. This was overcome by using a custom made rocket pole. This rocket pole consisted of a rounded flat top that ensured the placement of any ring would be even and flush. While one end of the ring was set with the rocket pole the

other end was being pushed in by the motor casing that created a sandwich with the rings being held in place as the epoxy set.

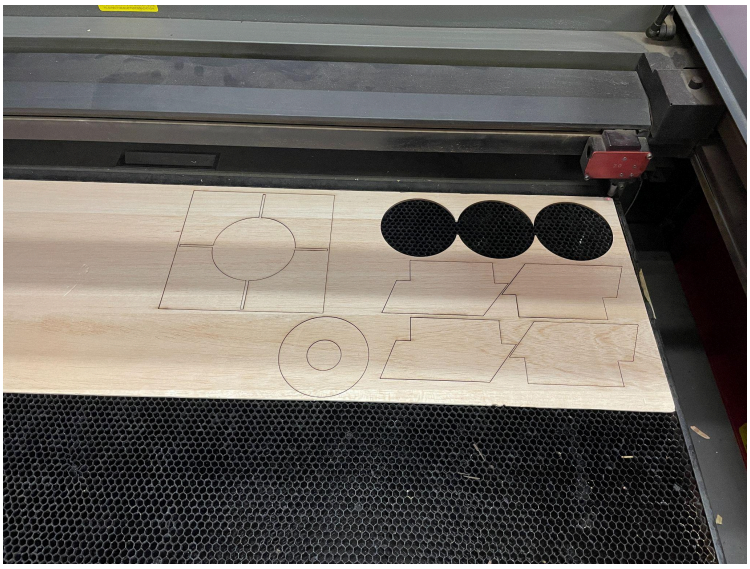

Figure 10.4 Centering Rings, Fins and Fin Jig Cut Out

Lastly, the most technical accomplishment we faced was the research and understanding of our e-matches. The Ematches were first thought to be ignited by a simple electrical charge supplied by the Blue Raven. After initial testing it was discovered this was not the case. Further research showed the Ematches used in testing needed a coat of fuel on the tip in order to ignite the black powder. This issue allowed us to gain more knowledge on black powder ignition devices as well as how to create our own ignition fuel. Upon initial testing of the e-matches with black powder, there was no pop of the nose cone due to the lack of fuel on the e-matches. After the research was conducted, the team was able to create the fuel and apply it to the e-matches and successfully utilize them to light the black powder and pop the

nose cone off in testing. These tests helped validate that during the launch, the nose cone will successfully pop off of the rocket at the intended time, allowing the parachute to fall out and deploy.

Open Issues

After the test launch multiple issues were discovered during the rocket's flight. First was the failure of the centering rings to keep the motor in place and properly transfer the thrust produced by the motor to the rest of the body. This was a result of not having a proper motor mount and adhering the centering rings directly to the motor casing. To avoid this failure in the next launch a sufficient motor casing must be inserted to more securely fasten the motor and properly distribute the forces produced within the body of the rocket.

Figure 10.5 Centering Ring Failure

The next failure was the parachute not fully deploying after the black powder charge. Upon detonation of the black powder the nose cone was successfully blown off, however the parachute was unable to open and therefore caused the rocket to

impact the ground at terminal velocity. This may have been caused by two separate faults. First was the parachute being too large for the given space within the nose cone requiring too many folds. The other is the residue the black powder leaves after ignition causes the shroud lines to stick together. Many tests of black powder were done prior to the launch and each test was conducted with the parachute inside the nose cone. After the black powder had been fired numerous times, the residue caused the shroud lines of the parachute to stick together making it difficult for them to untangle. The combination of these two negative effects cause a critical failure in the design. To avoid this in the final launch a small parachute will be used and with different shroud line material to be less affected by any residue that the black powder may release.

The last issue uncovered was upon launch the internal tracking unit was switched off. This caused locating the device to be much more difficult than it should have been. The corrective action will be to tape down any switches in the “On” position to avoid any vibration switching them back off.

11 Conclusions and Recommendations

On April 20, 2024, the final iteration of the rocket “Tycho” was launched with a payload of 24 eggs and an intended apogee of at least 2,000 feet. After the initial test launch in March and a thorough analysis of what went wrong, the following changes were made to the rocket. First, the centering rings that hold the rocket motor in place were redesigned using pine rather than balsa wood. This change added a bit more weight to the rocket but gave us confidence that the motor would be held in place for the final launch. Second, the parachute was changed from a 58” parachute to a 36” parachute, allowing for it to fit inside the nose cone more comfortably without worry of tangling as it did in the initial test launch. Finally, further testing was done on the avionics unit to ensure that all systems would be running smoothly during the final launch.

Ultimately, the final launch still had some minor issues that needed to be addressed. Once launched, the rocket immediately began to launch at an angle rather than straight up and eventually began to launch parallel to the ground causing it to fly very far away from the launch pad. Once again, the rocket went up in a corkscrew motion rather than a straight flight. Due to the similar nature of both the test flight and the final launch, a motor mount failure is believed to have occurred. The epoxy that was used for the final launch had a temperature rating of 250F, it is possible that some debonding could have occurred on the pad while the rocket internal temperatures were recorded at 100F. With the Motor itself heating the epoxy during launch, this is a possible explanation of the failure.

Epoxy application error could be another explanation for the failure. Improper mixing of the two compounds could result in less strength. Not applying enough epoxy could also mean that the overall strength was not enough to hold the motor in place.

Another possibility is that the rocket weathercocked into the wind too rapidly during the initial launch. A lower velocity than anticipated off the rail system, with a strong gust off the rail could have caused the initial weathercocking angle to be very high and caused the large initial destabilization of the rocket.

Another possibility is that the rocket may have had fins that were stable for a standard L1 rocket with an I-class motor, however our rocket was also carrying a payload of 24 eggs in it. This added mass that sat closer to the top of the rocket very well could have caused the center of gravity to move too far to the top of the rocket causing a stability error, regardless of the fin design. Additionally, our rocket design included an avionics bay that was printed with a polycarbonate filament which once again adds mass higher up on the rocket.

All of these parameters could have caused a center of gravity shift that may not have been fully accounted for, causing an unstable flight for the rocket. One recommended solution to this issue would be to increase the size of the fins in an attempt to counteract the center of gravity shift and create a more stable flight for the rocket. Another possible solution would have been to try to shift the center of gravity down by either reducing the number of eggs or printing the avionics bay out of a lighter filament.

A solution which would have been researched since the final launch would be to add an additional set of fins closer to the top of the rocket. Similar to how military

missiles have multiple sets of fins to improve control, a small second set of fins added higher up on our rocket would have moved the center of pressure closer to the center of gravity. Ultimately, this solution could increase the stability of the rocket given how high the center of gravity is and could also reduce weathercocking. However, if the front fins are made too large then the center of pressure goes too far forward and the stability reduces drastically causing a very unstable flight for the rocket. A rocket with multiple fin sets could look similar to the one in the image below.

This design with multiple fin sets was seen at the launch on other rockets for similar reasons - a center of gravity that is too high up on the rocket. The additional fins are not meant to be larger than the fins at the bottom of the rocket, but are there to provide additional stability towards the top. Any of these recommended solutions could

have solved the issue that our rocket kept having with the “swirl” launch path on the way up.

Another point of failure occurred during parachute deployment. For the initial test launch, Tycho was using a 58” parachute that proved to be too big for the space where it was being housed during launch. In order for it to fit, the parachute had to be improperly folded and the shock cord had to be wrapped around multiple times more than recommended. This proved fatal when the rocket failed to achieve apogee and began its rapid descent back to Earth. The redundant recovery system engaged and deployed the chute when the rocket achieved a specific descent rate. Due to the added folding, and wrapping of the shock cord, the parachute did not have time to unwrap, unfold and inflate and Tycho impacted the ground at a high rate of speed. It is recommended to follow proper parachute packing techniques and use a parachute that can comfortably sit in the space allotted.

On April 20th, 2024, Tycho launched with a goal of achieving 2000 feet and safely returning to Earth with the payload fully intact. The changes made to the recovery system consisted of replacing the 58” parachute with a 36” chute. As it was stated before, the launch did not go as planned. Tycho was flying parallel to the Earth, in a parabolic arc, when the parachute was deployed. Because the rocket was not flying vertically, it was being accelerated by the force of gravity. The rocket was traveling so fast, that when the parachute deployed and inflated, it was completely separated from the rocket. Since the rocket was never recovered, the team is not sure if the force caused the eyebolt connecting the shock cord to the rocket to fail, or if the shroud lines connected to the shock cord failed. It is recommended that in the event of a high speed

deployment, longer shock cords should be used to allow for the parachute to induce some kind of drag for a period of time before parachute inflation.

References

[1] 6074, B. J. D. D. 2014 P., Squeaker 'BentRider Legacy Member
Join Date: Jul 2005 Posts: 2257, The Toecutter
Join Date: Aug 2017 Posts: 1778, 6155, purplepeopledesign J. D. J. 2008 P., & Carbon midracer
Join Date: Aug 2015 Posts: 1743. (n.d.). *Announcement*. BentRider Online Forums. https://www.bentrideronline.com/messageboard/forum/main-category/specialty-discussions/velomobiles/141867-nose-cone-advice-needed

[2] *Anycubic Kobra 2 max*. ANYCUBIC. (n.d.). https://www.anycubic.com/products/kobra-2-max?msclkid=c5302ac324d51a1c49184fc57d94463a&utm_source=bing&utm_medium=cpc&utm_campaign=Smart%2B-%2B%E7%BE%8E%E5%9B%BD%2B823%2F914&utm_term=4586887642454984&utm_content=%E4%BA%A7%E5%93%81%E8%B4%AD%E7%89%A9

[3] Apogee Components, I. (n.d.-a). *Apogee components - 2.56in Blue Tube*. Model Rockets & How-To Rocketry Information. https://www.apogeerockets.com/Building_Supplies/Body_Tubes/Blue_Tubes/2-56in_Blue_Tube

[4] Apogee Components, I. (n.d.-a). *Apogee components - adrel altimeter*. Model Rockets & How-To Rocketry Information. https://www.apogeerockets.com/Electronics-Payloads/Altimeters/Adrel-Altimeter

[5] Apogee Components, I. (n.d.-a). *Apogee components - chute release*. Model Rockets & How-To Rocketry Information. https://www.apogeerockets.com/Electronics-Payloads/Dual-Deployment/Chute-Release

[6] Apogee Components, I. (n.d.-c). *Apogee components - easymega flight computer*. Model Rockets & How-To Rocketry Information. https://www.apogeerockets.com/Electronics-Payloads/Dual-Deployment/EasyMega

[7] Apogee Components, I. (n.d.). *Model rockets & how-to rocketry information*. Model Rockets & How-To Rocketry Information. https://www.apogeerockets.com/

[8] Apogee Components, I. (n.d.-f). *Peak of flight newsletter : Apogee rockets, model rocketry excitement starts here*. Peak of Flight Newsletter : Apogee Rockets, Model Rocketry Excitement Starts Here. https://www.apogeerockets.com/Peak-of-Flight/Newsletter546

[9] *Ask US - rocket nose cones and altitude*. Aerospaceweb.org | Ask Us - Rocket Nose Cones and Altitude. (n.d.). https://aerospaceweb.org/question/aerodynamics/q0151.shtml

[10] *Blue Raven*. Featherweight Altimeters. (n.d.). https://www.featherweightaltimeters.com/store/p25/Blue_Raven_Permalink.html

[11] Dahlke, G. (n.d.). Technical Workforce Development Program Student Guide. https://drive.google.com/file/d/1u9kcBNpWpPmD8AWSRdFQl-sAGE6qauyl/view?usp=sharing

[12] Department of Physics and Astronomy at Douglas College, & OpenStax. (n.d.). *8.7 introduction to Rocket Propulsion*. xDouglas College Physics 1107 Fall 2019 Custom Textbook. https://pressbooks.bccampus.ca/introductorygeneralphysics1phys1107/chapter/8-7-introduction-to-rocket-propulsion/

[13] Gohd, C. (2022, January 27). *SpaceX snags $102 million contract to rocket military supplies and humanitarian aid around the world: Report*. Space.com. https://www.space.com/spacex-air-force-102-million-dollar-contract-rocket-transport

[14] *High Power Rocket Safety Code - National Association of Rocketry*. NAR. (2022, September 19). https://www.nar.org/safety-information/high-power-rocket-safety-code/

[15] Huckins, E. K., Center, L. R., & Hampton Va., L. S. (n.d.). NASA technical note - NASA. https://ntrs.nasa.gov/api/citations/19700005898/downloads/19700005898.pdf

[16] *Introduction to EX Rocket Design*. Richard Nakka's Experimental Rocketry Site. (n.d.). https://www.nakka-rocketry.net/RD_body.html

[17] James. (2021, June 4). *What are Model Rocket Recovery Methods?*. CoolRocketStuff. https://coolrocketstuff.com/model-rocket-faq/what-are-model-rocket-recovery-methods/

[18] Jan, D. L., Davidson, B. D., & Moore, N. R. (n.d.). N91-10309 - NASA Technical Reports Server (NTRS). https://ntrs.nasa.gov/api/citations/19910000996/downloads/19910000996.pdf

[19] Koroghlian, A. (2022, December 23). *The history of the logistics and Shipping Industry*. Diversified Transportation Services. https://www.dtsone.com/the-history-of-the-logistics-and-shipping-industry/

[20] Li, Y., Jiang, C., Mao, L., & Li, M. (2020, March 19). *Study on Transient Dynamics and Aerodynamic Characteristics of a New Type of High-Damping Four-Winged Rotating Parachute Inflation Process*. Mathematical Problems in Engineering. https://www.hindawi.com/journals/mpe/2020/2361534/

[21] The lunar handbook. (n.d.). http://www.lunar.org/docs/handbook/handbook.shtml

[22] Mecalux. (n.d.). *Logistics history: Origin and development*. Interlake Mecalux, Warehouse solutions. https://www.mecalux.com/blog/logistics-history-origin#:~:text=Antiquity%3A%20the%20origin%20of%20logistics,establishing%20strategic%20routes%20and%20warehouses

[23] Miniature Autonomous Rocket Recovery System - Naval Postgraduate School. (n.d.-b). https://nps.edu/documents/106608270/107784480/Snowflake+-+Yingling+-+Miniature+Autnomous+Rocket+Recovery+System+-MARRS.pdf/0a9d66f2-977b-4175-9116-5d5cedd3f96f?t=1456349023000

[24] NASA. (2022, August 31). *Go to NASA Glenn Home*. NASA. https://www.grc.nasa.gov/

[25] *Online materials information resource*. MatWeb. (n.d.). https://www.matweb.com/index.aspx

[26] *Original Prusa mini+ semi-assembled 3D printer: Original Prusa 3D printers directly from Josef Prusa*. Prusa3D by Josef Prusa. (n.d.). https://www.prusa3d.com/product/original-prusa-mini-semi-assembled-3d-printer-4/

[27] *Polylactic acid (PLA) Filament Review*. JuggerBot 3D. (2023, August 10). https://juggerbot3d.com/pla-filament-review/

[28] *Rocket basics*. Eclipse Rocketry Ltd. (n.d.). http://eclipserocketry.com/basics.html

[29] *Unit D : Aerodynamics & flight 2*. Kurpinski's Class. (n.d.). https://www.kurpinskisclass.com/new-page-5

[30] Watts, G., & Mccarter, J. (2012). *Missile Aerodynamics for Ascent and Re-entry*. 20130003336.pdf (nasa.gov)

[31] Niskanen, S., Development of an Open Source model rocket simulation software, M.Sc. thesis, Helsinki University of Technology, 2009. OpenRocket — Documentation

[32] *ISSUE 197 - November 20 , 2007 Basics of Dynamic Flight Analysis The Damping Ratio INSIDE: • Basics of Dynamic Flight Analysis Damping Ratio • Defining Moment Canard • Question & Answer Corner*. (n.d.). Newsletter197.pdf (apogeerockets.com)

[33] *Barrowman Equations*. (n.d.). Mae-Nas.eng.usu.edu. Barrowman Equations (usu.edu)

[34] *Cesaroni 636I216-14A • ThrustCurve.* (n.d.). Www.thrust curve.org. Retrieved April 24, 2024, from Cesaroni 636I216-14A • ThrustCurve

[35] - || *Pro-X* || - *A better way to fly - - Cesaroni Technology Incorporated*. (n.d.). Pro38.com. Retrieved April 24, 2024, from - || Pro-X || - A better way to fly - - Cesaroni Technology Incorporated (pro38.com)

[36] Barrowman, J., & Washington, D. (n.d.). *THE PRACTICAL CALCULATION OF THE AERODYNAMIC CHARACTERISTICS OF SLENDER FINNED VEHICLES*. 20010047838.pdf (nasa.gov)

Appendices

A. Customer Requirements

Customer Requirements	
Requirement (RIN)	**Target Values/ Range**
[LRS - 01] Geometry	N/A
[LRS - 02] Materials	NAR L1 Compliant
[LRS - 03] Flight	Greater than or equal to 2000 ft AGL
[LRS - 04] Stability Controls	$1.2 \leq Stability\ (cal) \leq 1.8$
[LRS - 05] Sensory Systems	Ensure precision of the system has a standard deviation less than 100ft
[LRS - 06] Internal Measurement Unit	N/A
[LRS - 07] Recovery	Cargo remains unchanged from initial packaging
[LRS - 08] Parachute	Reduces velocity to less than 25 ft/s
[LRS - 9] Payload	Greater than or equal to 1 chicken Egg
[LRS - 10] Protection	Keeps payload intact at an impact at 25 ft/s
[LRS - 11] Propulsion	N/A
[LRS - 12] Motor Type	NAR designated H or I motor
[LRS - 13] Logistics	LRS remains functional after configuration changes and usage
[LRS - 14] Transportation	No single part shall be longer than 5ft 6in

Customer Requirements	
[LRS - 15] Safety	Guideline review
[LRS - 16] Arming system	Successful test launch
[LRS - 17] Environmental Conditions	Avg Winds: 9.1 knots Avg high/low Temp: 80/65℉ Humidity: 36%
[LRS - 18] Launch Interface	Successful test launch
[LRS - 19] Markings	N/A
[LRS - 20] Points of Interest	N/A

B. System Evaluation Plan

Test Planning		
Component	**Equipement**	**Procedures**
Parachute	• Truck • Baggage weight scale	While driving at 25 mph deploy the chute and record the drag force shown on scale
Black powder	• Block powder • Ematch • Nose cone • Avionics bay • Blue Raven	Starting with 2 grams of black powder, initiate ground ignition of the charge to ensure sufficient force is provided for separation of the nose cone from the body. Place 1 lb of weight on nose cone to replicate expected wind resistance at terminal velocity.

Altimeter	• Blue raven • Ground station • Avionics bay	With the Blue raven on and ground station nearby, throw the avionics bay directly up to verify the ability of measuring altitude changes. Ensure the max altitude is recorded on device after completion of test.
Centering rings	• Centering rings • Motor casing • 80lb of force	Once the motor mount is completed and epoxied in the body tube, flip the rocket upside down so the tail end is facing up with the nose cone removed. Place 10 lbs as a time on top of the motor mount until 80 lbs of force is reached. This will recreate the expected force of the motor during launch.
Payload bay	• Eggs • Payload bay • Cardboard shipping tube • Plastic wrap	Place 12 eggs inside the payload bay and seal the individual components together with plastic wrap. Insert payload bay inside cardboard tube. Drop the tube at intervals of 10 ft with crack checks in between each drop to verify the payload's ability to protect the eggs.

C. User Manual

1. First, assemble the payload bay by gathering the necessary foam pucks to carry the desired amount of eggs up to 24 eggs.

2. Stack foam pucks with the eggs inside and wrap tightly with plastic wrap to make one solid structure.
3. Create a handle with duct tape on top of the payload for easy removal.
4. Slowly place the payload bay inside the body tube of the rocket until the payload reaches the base plate.
5. Next, ensure the Blue raven is turned on and tapped to prevent shutting off during launch.
6. Place the avionics bay on top of the payload and align the holes for the screws.
7. Secure the avionics bay with 4 screws and attached matches with black powder attached. (DO NOT TURN ARM YET)
8. Fold parachute with appropriate folding technique and attached to the top of the avionics bay.
9. Place the black powder at the base of the nose cone and make sure the parachute sits directly on top of the charge.
10. Once the rocket is placed on the launch rail, arm the system.
11. Place the igniter inside the motor.
12. Test for continuity.
13. Go for launch

D. Cost Analysis and Manufacturability Analysis

Labor Description	Hours	Cost	Subtotal

Laser cutting fins	1	$85.00	$85.00
Laser cutting center rings	1	$70.00	$70.00
3D Printing	1	$100.00	$100.00
Avionics Assembly	2	$30.00	$60.00
Rocket Assembly	4	$25.00	$100.00
Materials	**Quantity**	**Cost**	**Subtotal**
Blue Raven Altimeter	1	$175.00	$175.00
20 AWG wiring (prorated)	1	$2.50	$2.50
GPS Tracker	1	$165.00	$165.00
9V battery	1	$10.00	$10.00
Power Distribution Block	1	$13.00	$13.00
Balsa Wood (prorated)	1	$8.75	$8.75
Pine Wood (prorated)	1	$5.00	$5.00
Blue Tube	1	$58.00	$58.00
Motor Mount Tube	1	$8.25	$8.25
3D Filament	1	$25.00	$25.00
M3 Bolts	10	$0.02	$0.17
M3 Nuts	10	$0.02	$0.17
M5 Bolts	8	$0.03	$0.26
M5 Nuts	8	$0.03	$0.26
Super Glue (prorated)	1	$7.50	$7.50
Epoxy (prorated)	1	$15.00	$15.00
Yoga Blocks	6	$6.00	$36.00
	Labor Subtotal:	$415.00	
	Materials Subtotal:	$529.86	
	Manufacturing Estimate:	$944.86	

E. Expense Report

Item	Quantity	Cost	Total
Cesaroni I216	1	$116.74	$116.74
Blue Tube	1	$57.90	$57.90
Super Glue	1	$15.29	$15.29
Shrink Wrap	1	$18.95	$18.95
Motor Spacer	1	$15.00	$15.00
Motor Spacer Shipping	1	$50.00	$50.00
Polycarbonate Filament	1	24.99	24.99
Switch/Testing lights (avionics)	1	$8.99	$8.99
Wiring connectors (avionics)	1	$8.98	$8.98
Yoga Blocks	2	$12.99	$25.98
Power distribution board (avionics)	1	$12.99	$12.99
Balsa wood	1	$35.00	$35.00
Yoga blocks	2	$16.99	$33.98
Black paint	1	$12.08	$12.08
gold paint	1	$6.98	$6.98
9v battery	1	$9.99	$9.99
	Additional Shipping Cost Estimate		$100.00
	Total Spent		$553.84
	Total Budget		$600.00
	Remaining Budget		$46.16

Item	Checkout/Freebie	Value
Blue Raven Altimeter	Checkout	$175.00

Featherweight Tracker	Checkout	$165.00
Featherweight Ground station	Shared (in possession)	$190.00
58" parachute	Checkout	$33.00
"Dog Barf"	Checkout	$8.00
Cesaroni 38mm motor casing	Checkout	$122.00
E-matches	Checkout (one time use)	$30.00
Black powder	Checkout (one time use)	$5.00
2nd Cesaroni I216	Freebie - Kurt	$116.74
38 mm cardboard tube (motor mount)	Freebie - Kurt	$8.26
36" parachute	Freebie - Kurt	$100.00
Epoxy	Freebie	$40.00
Shock cord	Freebie	$10.00
Pine plywood	Freebie	$30.00
Masking tape	Freebie	$4.00
M3 nuts and bolts	Freebie	$12.00
M5 nuts and bolts	Freebie	$15.00
Eyebolt	Freebie	$0.50
Threadlock	Freebie	$6.00
20 AWG wires	Freebie	$15.00
Quick connectors	Freebie	$20.00
Aluminum tape	Freebie	$7.00
Eggs (approx. 60 organic)	Freebie	$27.00
	Total Value	$1,139.50

F. List of Manuals and Other Documents

- TECHNICAL WORKFORCE DEVELOPMENT PROGRAM STUDENT GUIDE
- Blue Raven User's Guide
- Pro-X® Rocket Motor Reload Kits & Fuel Grains

G. Design Competencies

Aerospace Engineering Design Competence Evaluation

Aeronautical	Critical/ Main contributor	Strong Contributor	Necessary but not a primary contributor	Necessary but only a minor contributor	Only a passing reference	Not included in this design project
Aerodynamics	X					
Aerospace Materials			X			
Flight Mechanics		X				
Propulsion	X					
Stability and Controls	X					
Structures		X				

Astronautical	Critical /Main contributor	Strong Contributor	Necessary but not a primary contributor	Necessary but only a minor contributor	Only a passing reference	Not included in this design project
Aerospace Materials			X			
Attitude Determination and Control						X
Orbital Mechanics						X
Rocket Propulsion	X					
Space Environment						X

Space Structures						X
Telecommunications					X	

Mechanical Engineering Design Competence Evaluation

ME Design Areas	Critical /Main contributor	Strong Contributor	Necessary but not a primary contributor	Necessary but only a minor contributor	Only a passing reference	Not included in this design project
Thermal-Fluid Energy Systems	X					
Machines and Mechanical Systems			X			
Controls and Mechatronics	X					
Material Selection	X					
Modeling and Measurement Systems					X	
Manufacturing			X			

Topic Competence Criticality Matrix

Project Title: 2K Rocket Launch **Semester:** Spring 2024

Aeronautical and/or Astronautical topics utilized in this senior design project:

Topic	**Criticality to Project**	**Section**	**Comments**
Aerodynamics	Critical/Main	2, 3	

Aerospace Materials	Necessary/Minor	3, 6	
Flight Mechanics	Strong	3, 5, 7	
Stability and Control	Critical/Main	3, 5, 7	
Structures	Strong	3, 5, 6	
Propulsion	Critical/Main	3, 5, 7	

Mechanical topics utilized in this senior design project:

Topic	Criticality to Project	Section	Comments
Thermal Fluid Energy Systems	Critical/Main	3, 5, 7	
Machines and Mechanical Systems	Strong	3, 6, 7	
Controls and Mechatronics	Strong	3, 6, 7	
Materials Selection	Necessary	3, 5, 6	
Manufacturing	Necessary	3, 6	

H. Aerodynamic Equations Mathematical Representation

$$q_\infty = \frac{1}{2}\rho_\infty V_R^2$$

$$C_L = \frac{L}{q_\infty S_{Fin}}$$

$$C_D = \frac{D}{q_\infty S_{ref}}$$

$$C_N = \frac{F_N}{q_\infty S_{ref}}$$

$$\overline{y}_i = CoM_{Body} - CoP_i$$

$$M_0 = \sum_{i=1} (F_{N,i} \cdot \overline{y}_i)$$

$$C_{mm} = \frac{M_0}{q_\infty d_{ref} S_{ref}}$$

$$C_{mqm} = \frac{\partial C_{mm}}{\partial\left(\frac{q_m d_{ref}}{2V_R}\right)}$$

$$C_{mmd} = \frac{q_m d_{ref}}{2V_R} \cdot C_{mqm}$$

$$M_Y = q_\infty d_{ref} S_{ref} (C_{mm} + C_{mmd})$$

I. Pressure Integration Code

```
clear all, clc, close all;

pkg load io

################################################

        %% Calvin Dahl 3/6/24 %%

################################################


%%%% DATA FORMAT INSTRUCTIONS %%%%

  %For NEW data, Check Excel DATA location size and update in code

  %Excel Data should be formatted { x/c | Cp }

  %Where x/c is from 0 to 1 for CpLower and 0 to 1 for CpUpper
```

%%%% DATA FORMAT INSTRUCTIONS %%%%

Read Data From Excel Sheets

%Station 1 Data

%cOne = xlsread('Cp1deg.xlsx','y1','E2'); %chord

yOne_l = xlsread('Cp1deg.xlsx','y1', 'A2:B64'); %Lower Cp Data

yOne_u = xlsread('Cp1deg.xlsx','y1', 'A66:B129'); %Upper Cp Data

%Station 2 Data

%cTwo = xlsread('Cp1deg.xlsx','y2','E2'); %chord

yTwo_l = xlsread('Cp1deg.xlsx','y2', 'A2:B87'); %Lower Cp Data

yTwo_u = xlsread('Cp1deg.xlsx','y2', 'A89:B175'); %Upper Cp Data

%Station 3 Data

%cThree = xlsread('Cp1deg.xlsx','y3','E2'); %chord

yThree_l = xlsread('Cp1deg.xlsx','y3', 'A2:B77'); %Lower Cp Data

yThree_u = xlsread('Cp1deg.xlsx','y3', 'A79:B157'); %Upper Cp Data

%Station 4 Data

%cFour = xlsread('Cp1deg.xlsx','y4','E2'); %chord

yFour_l = xlsread('Cp1deg.xlsx','y4', 'A2:B60'); %Lower Cp Data

yFour_u = xlsread('Cp1deg.xlsx','y4', 'A62:B127'); %Upper Cp Data

%Station 5 Data

%cFive = xlsread('Cp1deg.xlsx','y5','E2'); %chord

yFive_l = xlsread('Cp1deg.xlsx','y5', 'A2:B87'); %Lower Cp Data

yFive_u = xlsread('Cp1deg.xlsx','y5', 'A89:B180'); %Upper Cp Data


```
%Station 6 Data

%cSix = xlsread('Cp1deg.xlsx','y6','E2'); %chord

ySix_l = xlsread('Cp1deg.xlsx','y6', 'A2:B138'); %Lower Cp Data

ySix_u = xlsread('Cp1deg.xlsx','y6', 'A140:B277'); %Upper Cp Data


%Initialization

CL_y1 = 0;

CL_y2 = 0;

CL_y3 = 0;

CL_y4 = 0;

CL_y5 = 0;

CL_y6 = 0;


%Loop Thru Cp Data To Calculate Cl

## CL = SUM(Cp,l(i) - Cp,u(i))*c(i) ##

## Where c(i) is the chord length between data points ##


% Lower Surface Loop

for i=1:1:(size(yOne_l,1)-1) %Station y1

  CL_y1 -= (yOne_l(i,2))*(yOne_l(i+1,1) - yOne_l(i,1));

endfor

for i=1:1:(size(yTwo_l,1)-1) %Station y2

  CL_y2 -= (yTwo_l(i,2))*(yTwo_l(i+1,1) - yTwo_l(i,1));
```

```
endfor
for i=1:1:(size(yThree_l,1)-1) %Station y3
  CL_y3 -= (yThree_l(i,2))*(yThree_l(i+1,1) - yThree_l(i,1));
endfor
for i=1:1:(size(yFour_l,1)-1) %Station y4
  CL_y4 -= (yFour_l(i,2))*(yFour_l(i+1,1) - yFour_l(i,1));
endfor
for i=1:1:(size(yFive_l,1)-1) %Station y5
  CL_y5 -= (yFive_l(i,2))*(yFive_l(i+1,1) - yFive_l(i,1));
endfor
for i=1:1:(size(ySix_l,1)-1) %Station y6
  CL_y6 -= (ySix_l(i,2))*(ySix_l(i+1,1) - ySix_l(i,1));
endfor

% Upper Surface Loop
for i=1:1:(size(yOne_u,1)-1)
  CL_y1 -= (yOne_u(i,2))*(yOne_u(i+1,1) - yOne_u(i,1));
endfor
for i=1:1:(size(yTwo_u,1)-1) %Station y2
  CL_y2 -= (yTwo_u(i,2))*(yTwo_u(i+1,1) - yTwo_u(i,1));
endfor
for i=1:1:(size(yThree_u,1)-1) %Station y3
  CL_y3 -= (yThree_u(i,2))*(yThree_u(i+1,1) - yThree_u(i,1));
```

```
endfor
for i=1:1:(size(yFour_u,1)-1) %Station y4
  CL_y4 -= (yFour_u(i,2))*(yFour_u(i+1,1) - yFour_u(i,1));
endfor
for i=1:1:(size(yFive_u,1)-1) %Station y5
  CL_y5 -= (yFive_u(i,2))*(yFive_u(i+1,1) - yFive_u(i,1));
endfor
for i=1:1:(size(ySix_u,1)-1) %Station y6
  CL_y6 -= (ySix_u(i,2))*(ySix_u(i+1,1) - ySix_u(i,1));
endfor

%Combined CL for each section
CLtot = (CL_y1*0.2 + CL_y2*0.2 + CL_y3*0.2 + CL_y4*0.2 + CL_y5*0.15 +
    CL_y6*0.04);
fprintf('\n Rocket Fin averaged CLtotal  = %g', CLtot)

%Averaged Pressure to Pressure Coefficient
#{
Force = 2*(CLtot*101325)/(1.225*(137.166^2));
fprintf('\n Rocket Fin averaged Lift  = %g', Force)
#}
#Lift = 0.5*Force*1.225*(137.166^2)*0.01034397933
```

J. CurveFitting Code

```
##############################################
      %% Calvin Dahl 3/10/24 %%
##############################################
function[Y] = StabilityFunction(Stability,m)
  for(i=1:5)
    x = Stability(:,1);
    y = Stability(:,i);
    [coeffs] = LeastSquares(x,y,m);
    Y{i} = [coeffs];
  endfor
endfunction


##############################################
      %% Calvin Dahl 3/10/24 %%
##############################################
function[coeffs] = LeastSquares(x,y,M)
  % solving for coeffs a0, a1, a2 using sum of Sx, Sxx, Sxxx... Sy, Sxy, Sxxy...
  %memory allocation
  C = zeros(M,M);
  b = zeros(M,1);
```

```
  for i =1:1:M % looping through each rows
    for j = 1:1:M % looping through each column of the selected rows
      C(i,j) = sum(x.^(i-1).*x.^(j-1)); % recall: (row,column) so: i=row j=column
      b(i) = sum(y.*x.^(i-1));
    endfor
  endfor

  coeffs = transpose(C\b);
endfunction

##############################################
        %% Calvin Dahl 3/10/24 %%
##############################################
function[y] = evalFit(a,x)

  ##%exaluate the LS fit at x values
  % creating y functions
  i = 1:length(a);
  y = sum(a.*x.^(i-1),2);

endfunction
```

K. Rocket Performance Program

```
clear all, clc, close all;

pkg load io

pkg load statistics

##############################################

      %% Calvin Dahl 3/10/24 %%

##############################################


%%%%%%%%%%% INSTRUCTIONS FOR OPERATION %%%%%%%%%%%

 % - (Optional) Check Thrust Curve Data And

 %    Change Coordinates Appropriately In Code

 %    Format Is Time (Column 1) Thrust (Column 2)

 %    NOTE -> Include Time 0 Thrust 0

 % - (Optional) Include Stability File:

 %    Alpha | Cl | Cd | Fbody | Aero Center

 %    NOTE -> Comment out unused sections of code

 % - Change Rocket Specifications, Initial Conditions

 %    And Loop Parameters As Needed

%%%%%%%%%%% INSTRUCTIONS FOR OPERATION %%%%%%%%%%%


%%%%%%%%%%% ASSUMPTIONS %%%%%%%%%%%

 % - Non-Dimensional Coefficients  (Cm, Cd, Cl) at AoA constant

 %    with respect to velocity / changing Reynolds Number
```


```
% - Force acting on fins applied at quarter chord
% - Center of Pressure of nose applied at 33% length from base of nose
%%%%%%%%%% ASSUMPTIONS %%%%%%%%%%

%Rocket Specifications
Cd = 0.4001; % (N/A) Coefficient of Drag Total (At 0 Sideslip)
m = 4.153; % (kg) Initial Rocket Mass
Mp = 0.3125; % (kg) Propellant Mass
Tb = 2.94; % (s) Motor Burn Time
H_Rocket = 1.4033; % (m) Total Rocket Height
H_Nose = 0.1778; % (m) Rocket Nose Height
H_Motor = 0.367; % (m) Motor Height
d = 102; % (mm) Diameter of Rocket
A_Front = pi*(d/2000)^2; % (m^2) Frontal Rocket Area
I = 636; % (Ns) Rocket Total Impulse

%Average Thrust
Thrust = I/Tb; % (N) Rocket Thrust
%Thrust Curve Data Points Input
motor = xlsread('Cesaroni_636I216-14A.xlsx','Cesaroni_636I216-14A','A6:B22');

%Parachute Specifications
CdParachute = 1.5; %Parachute Drag Coefficient
```

```
dParachute = 1219.2; % (mm) Parachute Diameter


%Stability Specifications
Iy = 0.7395447; % (kg*m^2) Inital Moment Of Inertia measured in longitudinal
   direction
CoM = 0.78673955; % (m) Initial Center of Mass Measured From Base of Rocket
   (Do not Include Fin Distance)
RailHeight = 2.4384 + (H_Rocket - CoM); % (m) Rail Height + Location From Nose
   to CoM(initial)
Stability = xlsread('DragAndLiftData.xlsx','Sheet1','A2:E6'); % Data For Stability
Order = 4; %Spline Order of CurveFit function (1 -> Linear fit, 2 -> Quadratic fit,
   etc...)
[Coeffs] = StabilityFunction(Stability,Order+1); % Function to curvefit Data Points
%Fin Specifications
Cr = 0.13462; % (m) root chord length
Ct = 0.117602; % (m) tip chord length
b = 0.047244; % (m) fin span
Theta = 35.54; % (deg) Sweep Angle at Leading Edge
%Aerodynamic Center Approximations
Sw = 0.5*(Ct + Cr)*b; % (m^2) fin area
FinY_AC = (b/3)*(Cr+2*Ct)/(Cr+Ct); % (m) y Aero Center
C_crit = Cr - (FinY_AC/b)*(Cr-Ct); % (m) Chord at Aero Center
```

```
FinX_AC = Cr - 0.25*C_crit - FinY_AC*tan(Theta*pi/180); % (m) x Aero Center
   measured from base of rocket
Nose_AC = H_Rocket - H_Nose*0.66666; % (m) Aero Center of Nose measured
   from base of rocket


%Initial Conditions
rho = 1.225; % (kg/m^3) Density of Air
g = 9.81; % (m/s^2) Earth Gravity
Wspeed(1) = 3.048; % (m/s) Constant Wind Speed (in x-coord only)
Sigma = 0; % Standard Deviation to Wind Speed'
t_Wind = 0.1; % (s) time to change wind randomness


%Loop Parameters and Initialization
h = 0.1; % (m) Rocket Height
v = 0.1; % (m/s) Rocket Velocity
acc = 0; % (m/s^2) Rocket Acceleration
x = 0; % (m) Rocket Initital x Coordinate
OmegaDot = 0; % (rad/s^2) Rocket Angular Acceleration
Omega = 0; % (rad/s) Rocket Angular Rotation Rate
Gamma = 0*pi/180; % (rad) Rocket Flight Path Angle
Alpha = 0; % (rad) Wind SideSlip Angle
Cm = 0; % Initial Moment Coefficient
dt = 0.001; % (s) Time Step
```

```
 tmax = 300; % (s) Max Time till loop ends
 TimeToApogee = tmax; % (s) Time once Apogee Achieved
 i = 1; % Counter to store Height & Velocity Values
 k = 0; % Counter to store Gamma Values

%MAIN() LOOP FUNCTION
for t=dt:dt:tmax

    if(v < 0 && TimeToApogee > t) % Once max height achieved deploy parachute
   TimeToApogee = t;
            A_Front = 3.14159*(dParachute/2000)^2; %Reference Area change to
    Parachute Reference Area
   Cd = -CdParachute; %Change Drag Coefficient And Direction
 endif

 if(h < 0) % Once touchdown occurs break loop
   tmax = t;
   break
 endif

 if(t < Tb) %Thrust = 0 once burn time ends
   m -= (Mp*dt/Tb); %Update Rocket Mass
   CoM += (Mp*dt/(Tb*m))*(CoM - H_Motor/2); %Update Center of Mass
```

```
  Iy -= (dt/Tb)*Mp*(CoM - (H_Motor/2))^2; %Update Longitudinal Moment of Inertia
endif

%Thrust Calculation
if(t < motor(size(motor,1),1))
  for j=1:1:(size(motor,1)-1)
    if(t < motor(j+1,1)) %Linear Interpolation Between Data Points
      Thrust = motor(j,2) + ((t - motor(j,1))/(motor(j+1,1) - motor(j,1)))*(motor(j+1,2) -
    motor(j,2));
      break
    endif
  endfor
endif


%Rocket Stability Loop
if(v > 0 && h > RailHeight) %Vertical Ascent Stage

  %Rocket Flight Path Angle Calculations
  Alpha = atan(Wspeed(i-1)/v) - Gamma; %Angle of Attack (SideSlip Angle
    Calculation - Flight Path Angle)

  %Rocket Coefficients Found Through CFD / Wind Tunnel Testing
```

```
  %evalFit evaluates the curvefit
Cl_Fin = evalFit(Coeffs{2},abs(Alpha)*180/pi);
Cd = evalFit(Coeffs{3},abs(Alpha)*180/pi);
CN_Nose = evalFit(Coeffs{4},abs(Alpha)*180/pi);
Cm_Body = evalFit(Coeffs{5},abs(Alpha)*180/pi);
if(Alpha*180/pi > 15) %Cutoff Values After Alpha > 15 (IF STALLING VALUES
 NOT MEASURED)
  Cl_Fin = evalFit(Coeffs{2},abs(15));
  Cd = evalFit(Coeffs{3},abs(15));
  CN_Nose = evalFit(Coeffs{4},abs(15));
  Cm_Body = evalFit(Coeffs{5},abs(15));
endif

%Moment Generated By Forces (From Rocket Coefficients) (Nm)
Moment = 0.5*rho*(v^2)*(Cl_Fin*(2*Sw)*(CoM-FinX_AC) -
 CN_Nose*A_Front*(CoM-Nose_AC) + Cm_Body*(d/2000)*A_Front);

%Moment Coefficients
Cm_0 = Cm; %Store Previous Moment Coefficient
Cm = (Moment)/(0.5*rho*(v^2)*(d/2000)*A_Front); %Moment Coefficient
 Calculation
```

```
Cmd =
 Omega*(d/2000)*(2.2*Cl_Fin*(2*Sw/A_Front)*((CoM-FinX_AC)/C_crit)^2)/(2*v);
 %Damping Moment Coefficient

if Alpha > 0 %If Alpha > 0 Correcting Positively
  OmegaDot += ((Cm-Cmd)*0.5*rho*(v^2)*(d/2000)*A_Front/Iy); %Rotational
 Acceleration Calculation (rad/s^2)
else %If Alpha < 0 Correcting Negatively
  Cmd = -Cmd;
  OmegaDot -= ((Cm-Cmd)*0.5*rho*(v^2)*(d/2000)*A_Front/Iy); %Rotational
 Acceleration Calculation (rad/s^2)
endif
Omega = OmegaDot*dt; %Angular Rate Calculation (rad/s)
Gamma += Omega*dt; %Update Flight Path Angle (rad)

%STORE LONGITUDINAL STABILITY COEFFICIENTS AND VALUES%
CMD(i-k) = Cmd; %Moment Damping Coefficient
CM(i-k) = (Cm); %Moment Coefficient
CoeffLift(i - k) = Cl_Fin; %Lift Coefficient
CoeffDrag(i - k) = Cd; %Drag Coefficient
Alp(i - k) = Alpha*180/pi; %SideSlip Angle
G(i - k) = Gamma*180/pi; %Flight Path Angle
OMEGA(i - k) = Omega; %Flight Path Angle
```

```
  %STORE LONGITUDINAL STABILITY COEFFICIENTS AND VALUES%
elseif(v > 0 && h < RailHeight) %Time rocket is on rail
  k++; %Parameter to store stability values
  T_Rail = t;
else
  Gamma = abs(atan(Wspeed(i-1)/v));
endif

if(rem(t,t_Wind) == 0)
  Wspeed(i) = normrnd(Wspeed(1),Sigma); % Wind Randomness Calculation
elseif(i>2)
  Wspeed(i) = Wspeed(i-1);
else
  Wspeed(i) = Wspeed(1);
endif

   Drag = 0.5*rho*(v^2)*Cd*A_Front; % Drag Calculation
   v += (Thrust - Drag - g*m)*dt/m; % Velocity Calculation
acc = (Thrust - Drag - g*m)/m; % Acceleration Calculation
   h = h + (v*cos(Gamma)*dt); % Height Calculation
x = x - (v*sin(Gamma)*dt); % Rocket Drift Calculation

%CONVERSION FROM METRIC TO IMPERIAL UNITS%
```

```
  H(i) = h*3.2808399;
  V(i) = v*3.2808399;
  X(i) = x*3.2808399;
  M(i) = m*2.20462262;
  Acc(i) = acc*3.2808399;
  Th(i) = Thrust*0.224808943;
  %CONVERSION FROM METRIC TO IMPERIAL UNITS%
  i++;
endfor

##############################################
      %% Data Plots And Values %%
##############################################

%Print Values
fprintf(' ########## Rocket Data ##########')
fprintf('\n Rocket Max Altitude = %g ft', max(H))
fprintf('\n Rocket Max Velocity = %g ft/s', max(V))
fprintf('\n Rocket Max Acceleration = %g ft/s^2', max(Acc))
fprintf('\n Rocket Empty Mass = %g lbs', min(M))
fprintf('\n Rocket Time to Apogee = %g s', TimeToApogee)
fprintf('\n Rocket Average Drag Coefficient = %g', mean(CoeffDrag))
fprintf('\n\n ########## Rocket Recovery Data ##########')
```

```
fprintf('\n Rocket Descent Rate = %g ft/s', min(V))
fprintf('\n Rocket Drift = %g ft', max(X))
fprintf('\n Wind Speed = %g ft/s = %g mph', Wspeed(1)*3.2808399,
    Wspeed(1)*2.23693629)
fprintf('\n\n ######### Rail Conditions #########')
fprintf('\n SideSlip Angle Off Rail = %g deg', Alp(1))
fprintf('\n Rocket Velocity Off Rail = %g ft/s', V(k))

%Subplots For Velocity, Height, Acceleration
%%{
figure(1)
t=0:dt:tmax - (2*dt);
subplot(3,1,1)
plot(t,H,"linewidth", 1.5)
title('Rocket Altitude Vs Time','fontsize',14)
xlabel('time (s)','fontsize',12)
ylabel('Altitude (ft)','fontsize',12)
grid on

subplot(3,1,2)
plot(t,V,"linewidth", 1.5)
title('Rocket Velocity Vs Time','fontsize',14)
xlabel('time (s)','fontsize',12)
```

```
ylabel('Velocity (ft/s)','fontsize',12)
grid on

subplot(3,1,3)
plot(t,Acc,"linewidth", 1.5)
title('Rocket Acceleration Vs Time','fontsize',14)
xlabel('time (s)','fontsize',12)
ylabel('Acceleration (ft/s^2)','fontsize',12)
grid on

%Thrust Curve
figure(2)
plot(t,Th, 'r')
title('Rocket Thrust Vs Time','fontsize',14)
xlabel('time (s)','fontsize',12)
ylabel('Thrust (lbf)','fontsize',12)
xlim([-Inf, Tb])
grid on

%Rocket X and Y Position Across Time
figure(3)
plot(X,H,'g',"linewidth", 2)
title('Rocket Position Tracking','fontsize',14)
```

```
xlabel('Drift (ft)','fontsize',12)
ylabel('Altitude (ft)','fontsize',12)
ylim([0, Inf])
grid on

%Flight Path Angle & SideSlip Angle
t=0:dt:TimeToApogee-((2+k)*dt);
figure(4)
plot(t,Alp, 'r')
hold on
plot(t,G, 'g')
title('Rocket Flight Path Angle & SideSlip Angle','fontsize',16)
xlabel('time (s)','fontsize',14)
ylabel('Flight Path Angle (deg)','fontsize',14)
line("xdata",[(Tb - ((k+2)*dt)),(Tb - ((k+2)*dt))],
    "ydata",[-10,90],"linewidth",1,"linestyle","--")
line("xdata",[(TimeToApogee - ((k+2)*dt)),(TimeToApogee - ((k+2)*dt))],
    "ydata",[-10,90],"linewidth", 1)
h = legend('SideSlip Angle','Flight Path Angle','t burnout (s)','t apogee (s)');
set(h,"fontsize",14)
grid on

%Drag & Lift Coefficients
```

```
figure(5)
plot(t,CoeffLift)
hold on
plot(t,CoeffDrag)
title('Lift And Drag Coefficients During Flight','fontsize',16)
xlabel('time (s)','fontsize',14)
ylabel('CL & CD','fontsize',14)
h = legend('CL(Fins)','CD(System)');
set(h,"fontsize",16)
grid on
%}

%View CurveFit
%{
for(i=2:1:length(Stability(:,1)))
  figure(i-1)
  y_LS = evalFit(Coeffs{i}, Stability(:,1));
  plot(Stability(:,1), y_LS);
  hold on
  scatter(Stability(:,1),Stability(:,i));
  xlabel('Angle of Attack (Degrees)','fontsize',18)
  Name = {'CL Fin','CD Sys','CN Nose','CM Body'};
  ylabel(Name{i-1},'fontsize',18)
```

```
 title('CurveFitting Graphs','fontsize',20)
 h = legend('CurveFit','CFD');
 set(h,"fontsize",14)
 grid on

 % sum of squares of errors
 SSE = sum((Stability(:,i)-y_LS).^2);
 % standard error
 std_error = sqrt(SSE/(length(Stability(:,1)-(Order+1))));
 y_mean = mean(Stability(:,i));
 So = sum((Stability(:,i)-y_mean).^2);
 % R squared
 r2 = (So-SSE)/So;

 printf('\n\n ########## Curve Fit Values (%s) ##########\n',Name{i-1})
 printf(' Sum of Squares of Errors (SSE) = %12.5e \n', SSE)
 printf(' Mean = %12.5e \n', y_mean)
 printf(' R squared = %.6f \n', r2)
 printf(' Standard error = %12.5e', std_error)
endfor
%}
```